1

No Polar Coordinates

Lectures by Richard Cushman

Text prepared by Konstantinos Efstathiou and Dmitrií Sadovskií

From the lecturer

R.C. would like to thank the organizer Dr. James Montaldi of the MASIE summer school which was held in Peyresq, France in September 2–16, 2000 for inviting him to give several lectures on integrable Hamiltonian systems. This work was partially supported by the EU project MASIE contract HPCFCT-1999-00067.

R.C. declines to take any responsibility for the contents of these notes even though he helped write and typeset them, contributed his scratchy notes to the preparers, and wrote up his homework (sec. 1.D).

The principal printed source which should be read along with these notes is the "blue book" [5].

Avant propos

It is a great pleasure for me to introduce these lecture notes. In the last few years after our first meeting in 1997 I have been constantly learning from Richard Cushman and am glad to be one of his co-workers. What I appreciate the most in Richard's lectures and in his work is that he presents and studies modern mathematics based on examples of concrete dynamical systems which he considers in great detail. As such his approach is very accessible to physicists and practitioners.

The five lectures are presented in the way they were given, except for interchanging Lecture IV and V back to their intended logical order. Some comments and discussion are added separately at the end of each lecture. The idea of these lecture notes is to give a very informal introduction to Richard's work. We even tried to preserve some of the style of Richard's presentation peppered with such phrases as "don't be caught dead in the water", "you will eat crow", "sneaky gadget", "dirty trick", "this is deep", etc. We feel that this personalization is inseparable from the imprint his lectures left in our heads. We therefore attempted to take full advantage of the lecture note format, especially since a more conventional and detailed presentation of the subject can be found in [5] (known to connoisseurs as "the blue book").

The title of these lectures originates from a comment of Hans Duistermaat on the blue book [5]. He remarked that Lagrange was proud to have stated in the front matter to *Mécanique Analytique* (Paris, 1788) that his book had no pictures. Hans suggested that in the dedication to the blue book should appear the statement: "This book uses no polar coordinates".

Initially the number of volunteers to do the write up was larger and each could choose which lecture was closest to his work and interests. In the end, Konstantinos worked on the harmonic oscillator and I was left with practically everything else. Fortunately, Richard himself came to my rescue. He wrote up the Euler top (I should confess that he used this as an occasion to further polish his presentation which deviates a bit from the original lecture) and an appendix which contains his solution of his "homework" problem. I concentrated on the spherical pendulum (one of Richard's favorites) and on the editorial work. Richard Morrison volunteered as a technical editor and I like to end by citing him :

> I have to confess that my understanding of Cushman's lectures was not maximal, and indeed I volunteered for this project to motivate my working through his notes at a more steady pace than had I been doing it purely for fun. ... given the speed that Cushman lectures and my unfamiliarity with the mathematics at the time, I don't really have what could be described as a complete set of accurate figures in my notes from the lectures. On the bright side, my (somewhat nominal) involvement with this project has meant I have been motivated to work a little on the notes and increase my understanding (no doubt they would have been relegated to gathering dust along with many other things that I have little time for academically).

It seems to me that much of this applies equally to the rest of us.

D. Sadovskií, Boulogne-sur-Mer, October 29, 2001

1.1 Lectures I and II. The two-dimensional harmonic oscillator

We will be dealing with 'simple' integrable systems: 2D harmonic oscillator, Euler top, and spherical pendulum. People often ask why Cushman still works on these examples. He replies: because they are tricky.

1.1.1 The harmonic oscillator

1.1.1.1 Preliminaries

Configuration space. The configuration space of the two-dimensional harmonic oscillator is $\mathbf{R}^2$ with coordinates $x = (x_1, x_2)$.

Phase space. The phase space is $T^*\mathbf{R}^2 \cong \mathbf{R}^4$ with coordinates $(x, y) = (x_1, x_2, y_1, y_2)$.

Canonical 1-form. On $T^*\mathbf{R}^2$ the canonical 1-form is

$$\Theta = y_1 \, \mathrm{d}x_1 + y_2 \, \mathrm{d}x_2 = \langle y, \mathrm{d}x \rangle.$$

Symplectic form. The symplectic form on $T^*\mathbf{R}^2$ is the closed nondegenerate 2-form

$$\omega = -\,\mathrm{d}\Theta = \mathrm{d}x_1 \wedge \mathrm{d}y_1 + \mathrm{d}x_2 \wedge \mathrm{d}y_2 \tag{1.1.1}$$

with the matrix representation

$$\omega = \begin{pmatrix} \mathrm{d}x \\ \mathrm{d}y \end{pmatrix}^t \begin{pmatrix} 0 & I_2 \\ -I_2 & 0 \end{pmatrix} \begin{pmatrix} \mathrm{d}x \\ \mathrm{d}y \end{pmatrix}. \tag{1.1.2}$$

Hamiltonian function. The Hamiltonian function of the two dimensional harmonic oscillator is

$$H : T^*\mathbf{R}^2 \to \mathbf{R} : (x, y) \mapsto \tfrac{1}{2}\,(x_1^2 + y_1^2) + \tfrac{1}{2}\,(x_2^2 + y_2^2). \tag{1.1.3}$$

Vector field. The corresponding Hamiltonian vector field

$$X_H = \langle X_1, \frac{\partial}{\partial x} \rangle + \langle X_2, \frac{\partial}{\partial y} \rangle$$

is computed using $X_H \;\lrcorner\; \omega = \mathrm{d}H = -X_2 \, \mathrm{d}x + X_1 \, \mathrm{d}y$. We get

$$X_1 = \frac{\partial H}{\partial y} \quad \text{and} \quad X_2 = -\frac{\partial H}{\partial x}. \tag{1.1.4}$$

Therefore the equations of motion of the harmonic oscillator are

$$\dot{x} = y \quad \text{and} \quad \dot{y} = -x. \tag{1.1.5}$$

Flow. The solution to the above equations is the one parameter family of transformations

$$\phi_t^H(x,y) = A(t) \;=\; \begin{pmatrix} (\cos t)\, I_2 & -(\sin t)\, I_2 \\ (\sin t)\, I_2 & (\cos t)\, I_2 \end{pmatrix} \begin{pmatrix} x \\ y \end{pmatrix} \tag{1.1.6}$$

This defines an S^1 action on $T^*\mathbf{R}^2$, which is a map from $\mathbf{R}$ to $\mathrm{Sp}(4,\mathbf{R})$ that sends t to the 4×4 symplectic matrix $A(t)$, which is periodic of period 2π.

As Poincaré liked to say, formulae are not the answer. This means that we have not solved our problem yet.

Symplectic group. A real $2n \times 2n$ matrix is symplectic if it satisfies the relation

$$A^t J A = J. \tag{1.1.7}$$

These matrices form a Lie group denoted by $\mathrm{Sp}(2n,\mathbf{R})$. The Lie algebra $\mathfrak{sp}(2n,\mathbf{R})$ of the symplectic group $\mathrm{Sp}(2n,\mathbf{R})$ consists of the *Hamiltonian* matrices X that satisfy $X^t J + JX = 0$.

Conservation of energy. We calculate

$$L_{X_H} H = \langle y, \frac{\partial H}{\partial x}\rangle - \langle x, \frac{\partial H}{\partial y}\rangle = \langle y, x\rangle - \langle x, y\rangle = 0 \tag{1.1.8}$$

This shows that H is constant along the integral curves of X_H.

Invariant manifold. Therefore the manifold

$$H^{-1}(h) = \{(x,y) \in \mathbf{R}^4 \big| x^2 + y^2 = 2h, h > 0\} \cong \mathbf{S}^3_{\sqrt{2h}} \tag{1.1.9}$$

is invariant under the flow of X_H.

1.1.1.2 S^1 symmetry.

S^1 action on $\mathbf{R}^2$. The configuration space $\mathbf{R}^2$ is invariant under the S^1 action

$$S^1 \times \mathbf{R}^2 \to \mathbf{R}^2 : (t,x) \mapsto R_t x,$$

where R_t is the matrix $\begin{pmatrix} \cos t & -\sin t \\ \sin t & \cos t \end{pmatrix}$.

Lift. This map lifts to a symplectic action Φ_t of S^1 on phase space $T^*\mathbf{R}^2$ that sends (x,y) to $\Phi_t(x,y) = (R_t x, R_t y)$.

Generator. This infinitesimal generator of this action is

$$Y(x, y) = \left.\frac{d}{dt}\right|_{t=0} \Phi_t(x, y) = (-x_2, x_1, -y_2, y_1). \tag{1.1.10}$$

Conservation of angular momentum. The vector field Y is Hamiltonian corresponding to the Hamiltonian function

$$L(x, y) = \langle y, (x_2, -x_1)\rangle = x_1 y_2 - x_2 y_1,$$

that is, $Y = X_L$. L is readily recognized as the angular momentum. The hamiltonian of the harmonic oscillator is an integral of X_L.

Check. Since $H(\Phi_t(x, y)) = H(x, y)$, we find that

$$0 = L_{X_L} H = \{H, L\} = -\{L, H\} = -L_{X_H} L. \tag{1.1.11}$$

Invariant manifold. Since both H and L are integrals of X_H, the manifold

$$\mathcal{M}_{h,\ell} = H^{-1}(h) \cap L^{-1}(\ell) \tag{1.1.12}$$

is invariant.

What is it? I claim that in most cases it is a 2-torus. How do we derive this?

We have to diagonalize the flow.

1.1.1.3 The geometry of $\mathcal{M}_{h,\ell}$.

Diagonalize L. In order to understand the geometry of the set $\mathcal{M}_{h,\ell}$, we want to find a transformation in $\mathrm{Sp}(4, \mathbf{R}) \cap \mathrm{O}(4, \mathbf{R})$ that diagonalizes L. Such a transformation P is given by

$$\begin{pmatrix} x \\ y \end{pmatrix} = \begin{pmatrix} A & -B \\ B & A \end{pmatrix} \begin{pmatrix} \xi \\ \eta \end{pmatrix}, \tag{1.1.13}$$

where $A = \left(\begin{smallmatrix} 0 & 0 \\ 1 & -1 \end{smallmatrix}\right)$ and $B = \left(\begin{smallmatrix} -1 & -1 \\ 0 & 0 \end{smallmatrix}\right)$.

Transform. In the new coordinates (ξ, η) the functions H and L become

$$\widetilde{H}(\xi, \eta) = (H \circ P)(\xi, \eta) = \tfrac{1}{2}\,(\eta_1^2 + \xi_1^2 + \eta_2^2 + \xi_2^2) \tag{1.1.14}$$

and

$$\widetilde{L}(\xi, \eta) = (L \circ P)(\xi, \eta) = \tfrac{1}{2}\,(-\eta_1^2 - \xi_1^2 + \eta_2^2 + \xi_2^2), \tag{1.1.15}$$

respectively.

Level sets. We have

$$\mathcal{M}_{h,\ell} = H^{-1}(h) \cap L^{-1}(\ell) = \widetilde{H}^{-1}(h) \cap \widetilde{L}^{-1}(\ell). \tag{1.1.16}$$

The level set $\mathcal{M}_{h,\ell}$ is determined by

$$\begin{aligned} \eta_2^2 + \xi_2^2 &= h + \ell \\ \eta_1^2 + \xi_1^2 &= h - \ell. \end{aligned}$$

Therefore

$$\mathcal{M}_{h,\ell} = \begin{cases} \emptyset, & \text{if } |\ell| > h \\ 0, & \text{if } h = \ell = 0 \\ \mathbf{S}^1, & \text{if } |\ell| = h,\ h > 0 \\ \mathbf{T}^2, & \text{if } |\ell| < h. \end{cases} \tag{1.1.17}$$

Energy-momentum mapping. Define

$$\mathcal{EM} : \mathbf{R}^4 \to \mathbf{R}^2 : (x, y) \mapsto (H(x, y), L(x, y)). \tag{1.1.18}$$

Obviously $\mathcal{EM}^{-1}(h, \ell) = \mathcal{M}_{h,\ell}$.

Bifurcation diagram. We summarize the preceding discussion of the level sets of the energy-momentum mapping in the *bifurcation diagram* that shows the change of topological type of $\mathcal{EM}^{-1}(h, \ell)$ as (h, ℓ) changes, see figure 1.1.1.

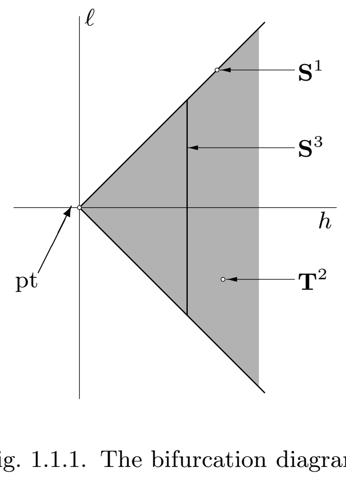

Fig. 1.1.1. The bifurcation diagram.

Regular values of $\mathcal{EM}$. $\mathcal{R} = \{(h,\ell) \in \mathbf{R}^2 \big| |\ell| < h, h > 0\}$ is the set of regular values of the energy-momentum map. For $(h,\ell) \in \mathcal{R}$ the fibers $\mathcal{EM}^{-1}(h,\ell)$ are 2-tori. This is a consequence of the *Arnol'd-Liouville* theorem, since $\mathrm{d}H$ and $\mathrm{d}L$ are linearly independent on $\mathcal{EM}^{-1}(\mathcal{R})$, X_H and X_L are complete, and $\mathcal{EM}^{-1}(\mathcal{R})$ is an open dense subset of $T^*\mathbf{R}^2$.

The Arnol'd-Liouville theorem. *(A very powerful result, Avez and others are somewhere in here too.)* We consider a symplectic manifold (M^{2n},ω) and a Hamiltonian function $H : M^{2n} \to \mathbf{R}$. Consider a collection of n functions $F_1 = H, F_2, \ldots, F_n$ such that

1. $F_1, \ldots, F_n$ are integrals of X_H and the corresponding vector fields X_{F_i} have flows which are defined for all time.
2. $\{F_i, F_j\} = 0$ for all i, j.
3. $dF_1 \wedge \cdots \wedge dF_n \neq 0$ on an open dense subset of M^{2n}.

Define the momentum map $\mathcal{EM} : M^{2n} \to \mathbf{R}^n : x \to (F_1(x), \ldots, F_n(x))$. If

4. the set of regular values $\mathcal{R}$ of $\mathcal{EM}$ is a nonempty open subset of $\mathbf{R}^n$, and
5. for $c \in \mathcal{R}$, the set $\mathcal{EM}^{-1}(c)$ is compact[1] and connected,

then $\mathcal{EM}^{-1}(c)$ is an n-torus.

The Arnol'd-Liouville theorem is boring, because it tells us everything there is to know about connected components of fibers of the energy momentum mapping corresponding to regular values. But what about the singular values? Knowing all individual fibers is not going to finish the problem either. We should also understand how these fibers fit together.

At this point we know the topological type of each fiber of the energy-momentum mapping of the harmonic oscillator, but we can not say anything about the way that $\mathbf{S}^3$ is made up from 2 circles and a bunch of 2-tori. This is the question that we study next.

1.1.2 U(2) momentum map

Quadratic integrals. We now find all the quadratic integrals of X_H. Any quadratic function on $\mathbf{R}^4$ can be expressed as

$$F(x,y) = \tfrac{1}{2} \begin{pmatrix} x \\ y \end{pmatrix}^t \begin{pmatrix} -B & A^t \\ A & C \end{pmatrix} \begin{pmatrix} x \\ y \end{pmatrix} \qquad (1.1.19)$$

[1] Compactness is needed to make sure that near a given torus we should find other tori on which the motion is also quasi-periodic.

where A, B and C are 2×2 matrices with $B = B^t$ and $C = C^t$.

Hamiltonian vector field. The corresponding hamiltonian vector field is

$$X_F(x,y) = \begin{pmatrix} A & B \\ C & -A^t \end{pmatrix} \begin{pmatrix} x \\ y \end{pmatrix} \tag{1.1.20}$$

where $X_F \in \mathfrak{sp}(4, \mathbf{R})$.

Statement. For any two quadratic functions F and H

$$0 = L_{X_H} F = \{F, H\} \Leftrightarrow [X_H, X_F] = 0. \tag{1.1.21}$$

Application. When $X_H = \begin{pmatrix} 0 & -I \\ I & 0 \end{pmatrix}$, $X_F = \begin{pmatrix} A & C \\ B & -A^t \end{pmatrix}$ and $0 = [X_H, X_F]$, then

$$X_F = \begin{pmatrix} A & -B \\ B & A \end{pmatrix}, \tag{1.1.22}$$

where A, B are 2×2 real matrices such that $A = -A^t$ and $B = B^t$.

The Lie algebra $\mathfrak{u}(2)$. By definition

$$\mathfrak{u}(2) = \{\mathcal{A} \in \mathrm{gl}(2, \mathbf{C}) \big| \bar{\mathcal{A}}^t + \mathcal{A} = 0\} \tag{1.1.23}$$

Setting $\mathcal{A} = A + \mathrm{i}B$ we see that the set of solutions (1.1.22) is isomorphic to $\mathfrak{u}(2)$ (the Lie algebra of $\mathrm{U}(2)$).

Hamiltonian. Consider the linear vector field $X_v(z) = v(z)$ with $v \in \mathfrak{sp}(4, \mathbf{R})$, then X_v is hamiltonian with hamiltonian function

$$F_v(z) = \tfrac{1}{2}\, \omega(v(z), z) \tag{1.1.24}$$

Therefore if v is of the form (1.1.22), then F_v is an integral of X_H. Let Q be the set of quadratic integrals of X_H.

A basis for Q. Since Q is isomorphic to $\mathfrak{u}(2)$ we can find a basis for Q by taking a basis of $\mathfrak{u}(2)$ and then tranforming it. We select the following basis for $\mathfrak{u}(2)$:

$$\epsilon_1 = \begin{pmatrix} 0 & \mathrm{i} \\ \mathrm{i} & 0 \end{pmatrix} \quad \epsilon_2 = \begin{pmatrix} 0 & -1 \\ 1 & 0 \end{pmatrix} \quad \epsilon_3 = \begin{pmatrix} \mathrm{i} & 0 \\ 0 & -\mathrm{i} \end{pmatrix} \quad \epsilon_4 = \begin{pmatrix} \mathrm{i} & 0 \\ 0 & \mathrm{i} \end{pmatrix}. \tag{1.1.25}$$

and then take the corresponding Hamiltonian matrices in $\mathfrak{sp}(4, \mathbf{R})$ and their Hamiltonian functions. This way we get the basis

$$\begin{aligned} w_1(x,y) &= x_1x_2 + y_1y_2 \\ w_2(x,y) &= x_1y_2 - x_2y_1 \\ w_3(x,y) &= 1/2(x_1^2 + y_1^2 - x_2^2 - y_2^2) \\ w_4(x,y) &= 1/2(x_1^2 + x_2^2 + y_1^2 + y_2^2), \end{aligned} \tag{1.1.26}$$

for Q. We see that Q with the usual Poisson bracket is a Lie algebra isomorphic to $\mathfrak{u}(2)$. The commutation relations between the four basis functions w_i are given in the following table

$\{w_i, w_j\}$	w_1	w_2	w_3	w_4
w_1	0	$2w_3$	$-2w_1$	0
w_2	$-2w_3$	0	$2w_2$	0
w_3	$2w_1$	$-2w_2$	0	0
w_4	0	0	0	0

The Lie group U(2)**.** By definition

$$\begin{aligned} \mathrm{U}(2) &= \{u \in \mathrm{GL}(2,\mathbf{C}) \big| \bar{u}^t u = I\} \\ &= \{\left(\begin{smallmatrix} a & -b \\ b & a \end{smallmatrix}\right) \in \mathrm{GL}(4,\mathbf{R}) \big| a^t a + b^t b = I,\ a^t b = b^t a, a, b \in \mathrm{GL}(2,\mathbf{R})\} \\ &\cong \mathrm{Sp}(4,\mathbf{R}) \cap \mathrm{O}(4,\mathbf{R}) \end{aligned} \tag{1.1.27}$$

Consider the linear action $\Phi : \mathrm{U}(2) \times \mathbf{R}^4 \to \mathbf{R}^4 : (u, z = (x,y)) \mapsto u(z)$. Φ_u is a linear symplectic map on $(\mathbf{R}^4, \omega)$.

Flow. If $u \in \mathfrak{u}(2)$, then $\Phi_{\exp tu}$ is the flow of the linear hamiltonian vector field

$$X^u(z) = \left.\frac{d}{dt}\right|_{t=0} \Phi_{\exp tu} z \;=\; u(z). \tag{1.1.28}$$

Associated to X^u is the hamiltonian function

$$J^u(z) = \tfrac{1}{2}\, \omega(u(z), z). \tag{1.1.29}$$

The function J^u depends *linearly* on u.

Momentum map. We define the U(2) momentum map $J : \mathbf{R}^4 \to \mathfrak{u}(2)^*$ of the U(2) action Φ to be $J(x,y)(u) = J^u(x,y)$. If E_j^* is the dual basis of $\mathfrak{u}(2)^*$ then

$$J(x,y) = \sum_j w_j(x,y) E_j^*. \tag{1.1.30}$$

J intertwines the linear action of U(2) on $\mathbf{R}^4$ with the coadjoint action of U(2) on $\mathfrak{u}(2)^*$, that is,

$$J(Uz) = \mathrm{Ad}^t_{U^{-1}} J(z). \tag{1.1.31}$$

Some people call the coadjoint action the dual action. Actually it is the contragradient action.

Check.

$$\begin{aligned} J(Uz)u &= J^u(Uz) = \tfrac{1}{2}\,\omega(u(Uz), Uz) \\ &= \omega(U^{-1}uUz, z) = J^{U^{-1}uU}(z) = J(z)(U^{-1}uU) \\ &= J(z)(\mathrm{Ad}_{U^{-1}}u) = \mathrm{Ad}^t_{U^{-1}}(J(z)u). \qquad \square \end{aligned}$$

In the original problem we saw only S^1 symmetry which acted on the configuration space. Now we found a larger symmetry which acts on phase space.

Killing form. By definition the Killing form on $\mathfrak{u}(2)$ is

$$\mathrm{k} : \mathfrak{u}(2) \times \mathfrak{u}(2) \to \mathbf{C} : (u,v) \mapsto -\tfrac{1}{2}\ \mathrm{trace}(u\overline{v}^t). \tag{1.1.32}$$

Let $\widetilde{J} : \mathbf{R}^4 \to \mathfrak{u}(2) : z \mapsto \mathrm{k}^\flat \circ J(z)$. Then

$$\widetilde{J}(z) = (w_1(z), w_2(z), w_3(z), w_4(z))$$

because the ϵ_j's form an orthonormal basis with respect to k.

1.1.3 Hopf fibration

Hopf map. Define the *Hopf map* (formerly known as $\widetilde{J}$) by

$$\mathcal{H} : \mathbf{R}^4 \to \mathbf{R}^4 : z = (x,y) \mapsto (w_1(z), w_2(z), w_3(z), w_4(z)). \tag{1.1.33}$$

Obviously

$$w_1^2 + w_2^2 + w_3^2 = w_4^2. \tag{1.1.34}$$

Hopf fibration. Restricting $\mathcal{H}$ to the sphere

$$\mathbf{S}^3_{\sqrt{2h}} = \{(x, y) \in \mathbf{R}^4 \big| x_1^2 + x_2^2 + y_1^2 + y_2^2 = 2h\} \tag{1.1.35}$$

we get the *Hopf fibration*

$$\mathcal{F} : \mathbf{S}^3_{\sqrt{2h}} \to \mathbf{S}^2_h : z = (x, y) \mapsto w = (w_1(z), w_2(z), w_3(z)) \tag{1.1.36}$$

where

$$\mathbf{S}^2_h = \{(w_1, w_2, w_3) \in \mathbf{R}^3 \big| w_1^2 + w_2^2 + w_3^2 = h^2\}. \tag{1.1.37}$$

1.1.3.1 Properties of the Hopf fibration

Property 1. Let $w \in \mathbf{S}^2_h$. Then $\mathcal{F}^{-1}(w)$ is a great circle on $\mathbf{S}^3_{\sqrt{2h}}$.

Proof.
Case 1. $w \in \mathbf{S}^2_h - \{(0, 0, -h)\}$. Suppose $(x, y) \in \mathcal{F}^{-1}(w)$. Since $x_1^2 + y_1^2 + x_2^2 + y_2^2 = 2h$ and $x_1^2 + y_1^2 - x_2^2 - y_2^2 = 2w_3$ it follows that $x_1^2 + y_1^2 = h + w_3 > 0$. Therefore we may solve the linear equations

$$\begin{pmatrix} x_1 & y_1 \\ -y_1 & x_1 \end{pmatrix} \begin{pmatrix} x_2 \\ y_2 \end{pmatrix} = \begin{pmatrix} w_1 \\ w_2 \end{pmatrix} \tag{1.1.38}$$

to obtain

$$\begin{aligned} w_1x_1 - w_2y_1 + (h + w_3)x_2 &= 0 \\ w_2x_1 + w_1y_1 + (h + w_3)y_2 &= 0. \end{aligned}$$

The above equations define a 2-plane Π^w in $\mathbf{R}^4$, since $\left(\begin{smallmatrix} w_1 & -w_2 & h+w_3 & 0 \\ w_2 & w_1 & 0 & h+w_3 \end{smallmatrix}\right)$ has rank 2. Hence $\mathcal{F}^{-1}(w) \subseteq \Pi^w \cap \mathbf{S}^3_{\sqrt{2h}}$. Reversing the argument shows that $\Pi^w \cap \mathbf{S}^3_{\sqrt{2h}} \subseteq \mathcal{F}^{-1}(w)$.
Case 2. $w = (0, 0, -h)$. Then $x_1^2 + y_1^2 = 0$ which implies $x_1 = y_1 = 0$. Thus

$$\mathcal{F}^{-1}(w) = \{(0, x_2, 0, y_2) \in \mathbf{R}^4 \big| x_2^2 + y_2^2 = 2h\}, \tag{1.1.39}$$

which is a great circle and it is $\mathbf{S}^3_{\sqrt{2h}} \cap \{x_1 = y_1 = 0\}$. □

Consequence 1. Each fiber of the Hopf fibration is a single orbit of the harmonic oscillator of energy h. In other words, the orbit space $H^{-1}(h)/S^1$ of the harmonic oscillator of energy h is $\mathbf{S}^2_h$.

Property 2. Let $w, v \in \mathbf{S}^2_h$ with $w \neq v$. Then $\mathcal{F}^{-1}(w)$ and $\mathcal{F}^{-1}(v)$ are linked once in $\mathbf{S}^3_{\sqrt{2h}}$.

Proof. Since $v \neq w$, the 2-planes Π^v and Π^w are transverse, that is, $\Pi^v \cap \Pi^w = \{0\}$. Let Π be any 3-plane containing Π^w. Then $\Pi^v \not\subseteq \Pi$, so $\Pi^v \cap \Pi = \ell^v$ which is a line through the origin. $\Pi \cap \mathbf{S}^3_{\sqrt{2h}}$ is a great 2-sphere $\mathbf{S}^2_{\sqrt{2h}}$ with equator $\Pi^w \cap \mathbf{S}^3_{\sqrt{2h}}$. Let H^+ be an open hemisphere of $\mathbf{S}^2_{\sqrt{2h}}$ whose closure has boundary $\Pi^w \cap \mathbf{S}^3_{\sqrt{2h}}$. Since $\ell^v \cap \Pi^w = \{0\}$, ℓ^v intersects H^+ at one point p. Hence the great circle $\Pi^v \cap \mathbf{S}^3_{\sqrt{2h}}$ intersects H^+ only at p. Thus the fibers $\mathcal{F}^{-1}(v)$ and $\mathcal{F}^{-1}(w)$ are linked once in $\mathbf{S}^3_{\sqrt{2h}}$. □

Consequence 2. There is *no global* Poincaré section for the flow of X_H on $H^{-1}(h)$.

Proof. Suppose that a 2-disc $\mathbf{D}^2 \subseteq \mathbf{S}^3_{\sqrt{2h}}$ is a global cross section. Since every orbit of X_H on $\mathbf{S}^3_{\sqrt{2h}}$ is a circle, it would follow that $\mathbf{S}^3_{\sqrt{2h}}$ is homeomorphic to $\mathbf{D}^2 \times \mathbf{S}^1$. But two distinct orbits of X_H, are two distinct fibers of the Hopf fibration. Therefore they are linked in $\mathbf{S}^3_{\sqrt{2h}}$ but they would be unlinked in $\mathbf{D}^2 \times \mathbf{S}^1$. This is impossible if these sets are topologically the same. The same argument works for any topological 2-manifold in $\mathbf{S}^3_{\sqrt{2h}}$. □

Consequence 3. The orbit space $H^{-1}(h)/S^1$ is *not* a submanifold of $H^{-1}(h)$.

Proof. See the last sentence of the proof of consequence 2. □

Consequence 4. We need at least two local Poincaré sections. (In fact, two are enough. We will see that the orbit space is a 2-sphere. Any $\mathbf{S}^2$ requires two charts.)

Visualization. We visualize $\mathbf{S}^3$ using stereographic projection. In figure 1.1.2 we have drawn the level sets of w_1 (the angular momentum). Each level set is a 2-torus. The two critical points of the energy-momentum map correspond to the two thick black curves in figure 1.1.2, given by $(0, 0, t)$ and $(\cos t, \sin t, 0)$. Both curves are circles, thinking of $\mathbf{S}^3$ as $\mathbf{R}^3$ together with a point at infinity.

Proof of consequence 4. Select any level set ℓ of w_1 with $|\ell| < h$ and consider the two open disks A and B in figure 1.1.3. Each open disk is a local Poincaré section, since any orbit that begins on one of the disks crosses the same disk again. □

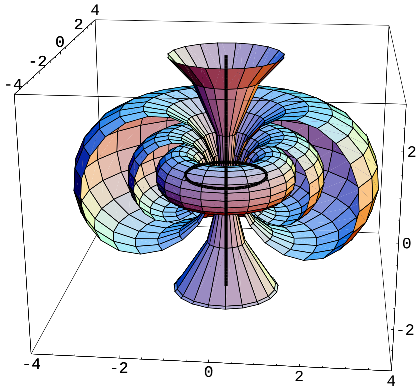

Fig. 1.1.2. Visualization of $\mathbf{S}^3$

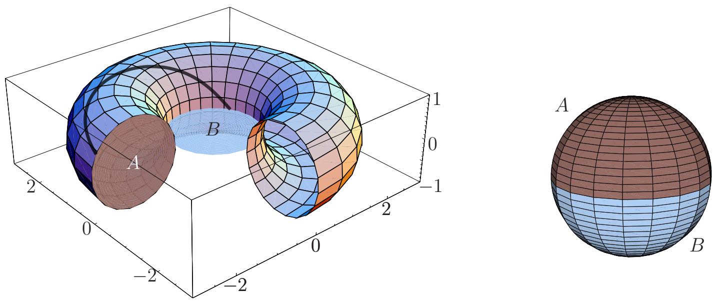

Fig. 1.1.3. Poincaré disks used to construct the orbit space (left). The orbit space $H^{-1}(h)/S^1 = \mathbf{S}^2_h$ (right).

The orbit space. *(For all except Boris Zhilinskií: an orbifold is an orbit space of a locally free action.)* Our local Poincaré sections (figure 1.1.3, left) are charts of the orbit space. every orbit intersects at least once one of the two disks. We glue them together and obtain a 2-sphere. Indeed, as shown in figure 1.1.3, left, an orbit that begins on a point $q \in \partial A$ will cross ∂B at a point p exactly once before returning to its initial point. Identifying q and p gives a 2-sphere, which is the orbit space $H^{-1}(h)/S^1$, see figure 1.1.3. The orbit space $\mathbf{S}^2$ is *not* sitting in the energy level $\mathbf{S}^3$ (shown in figure 1.1.2); thus $\mathbf{S}^2$ is an *abstract* manifold (as Hopf showed in 1935). Indeed, every orbit intersects the orbit space $\mathbf{S}^2$ transversally. So if our $\mathbf{S}^2$ *were* a submanifold of $\mathbf{S}^3$ then $\mathbf{S}^3$ would decompose as $\mathbf{S}^1 \times \mathbf{S}^2$. But it does not. Thus $\mathbf{S}^3$ is a nontrivial $\mathbf{S}^1$ bundle over $\mathbf{S}^2$.

We have completed regular reduction (= Marsden-Weinstein reduction).

1.1.4 Normalization

1.1.4.1 Dynamics on the orbit space

Harmonic oscillator symmetry. Consider a map $K : T^*\mathbf{R}^2 \to \mathbf{R}$ that factors through the $\mathfrak{u}(2)$ momentum map $\widetilde{\mathcal{J}} : T^*\mathbf{R}^2 \to \mathbf{R}^4$, that is, there is a smooth function $\widetilde{K} : \mathbf{R}^4 \to \mathbf{R}$ such that $K(x,y) = \widetilde{\mathcal{J}}^*\widetilde{K}(x,y)$. In other words

$$K(x,y) = \widetilde{K}(w_1(x,y), w_2(x,y), w_3(x,y), w_4(x,y)) \tag{1.1.40}$$

Integral. K is an integral of X_H, that is, $L_{X_H}K = 0$.

Induced equations of motion on $\mathbf{R}^4$. Since $\{w_j, w_4\} = 0$ for $j = 1, \ldots, 4$, we obtain

$$\begin{aligned} \dot{w}_j &= \{w_j, \widetilde{K}\} = \sum_{k=1}^{3} \{w_j, w_k\} \frac{\partial \widetilde{K}}{\partial w_k} \\ &= \sum_{k=1}^{3}\sum_{l=1}^{3} 2\varepsilon_{jkl} w_l \frac{\partial \widetilde{K}}{\partial w_k} = 2(\nabla \widetilde{K} \times w)_j \end{aligned}$$

for $j = 1, 2, 3$ and $\dot{w}_4 = 0$.

Restrict to $H^{-1}(h)$. Restricting $\widetilde{K}$ to $H^{-1}(h)$ gives

$$\widetilde{K}_h(w_1, w_2, w_3) = \widetilde{K}(w_1, w_2, w_3, h). \tag{1.1.41}$$

Induced equations of motion on $\mathbf{R}^3$. Set $w = (w_1, w_2, w_3)$. Then

$$\dot{w} = 2(\nabla \widetilde{K}_h \times w) \tag{1.1.42}$$

is satisfied by integral curves of a vector field X on $\mathbf{R}^3$.

Invariant manifold. The sphere $\mathbf{S}^2_h$ is invariant under the flow of the vector field X.

Check.

$$L_X\langle w, w\rangle = 2\langle w, \dot{w}\rangle = 4\langle w, \nabla\widetilde{K}_h(w) \times w\rangle = 0. \tag{1.1.43}$$

X **is hamiltonian.** Consider the matrix of the Poisson structure

$$W(w) = (\{w_j, w_k\}) = 2\begin{pmatrix} 0 & -w_3 & w_2 \\ w_3 & 0 & -w_1 \\ -w_2 & w_1 & 0 \end{pmatrix} \tag{1.1.44}$$

Since $\ker W(w) = \operatorname{span}\{w\}$ and $T_w\mathbf{S}^2_h = \operatorname{span}\{w\}^{\perp}$, the matrix $W(w)\big|_{T_w\mathbf{S}^2_h}$ is invertible. On $\mathbf{S}^2_h$ define the symplectic form

$$\omega(w)_h(u,v) = \langle W^t(w)^{-1}u, v\rangle.$$

Since $W^t(w)y = -2w \times y = z$ we have

$$\begin{aligned} w \times z = w \times (-2w \times y) &= -2w \times (w \times y) = -2(w\,\langle w, y\rangle - y\,\langle w, w\rangle) \\ &= 2y\,\langle w, w\rangle = 2h^2\,y, \end{aligned}$$

which implies $y = \frac{1}{2h^2} w \times z$. Therefore

$$\omega_h(w)(u,v) = \frac{1}{2h^2}\,\langle w \times u, v\rangle = \frac{1}{2h^2}\,\langle w, u \times v\rangle. \tag{1.1.45}$$

The vector field X is hamiltonian with respect to ω_h with hamiltonian function $\widetilde{K}_h$, because

$$\begin{aligned} \omega_h(w)(X(w), u) &= \frac{1}{h^2}\,\langle w, (\nabla\widetilde{K}_h \times w) \times u\rangle = \frac{1}{h^2}\,\langle w \times (\nabla\widetilde{K}_h \times w), u\rangle \\ &= \frac{1}{h^2}\,\langle -w\,\langle \nabla\widetilde{K}_h, w\rangle + \nabla\widetilde{K}_h\,\langle w, w\rangle, u\rangle = \langle \nabla\widetilde{K}_h, u\rangle = \mathrm{d}\widetilde{K}_h(w)u, \end{aligned}$$

where $u, v \in T_w\mathbf{S}^2_h$.

Complex variables. On $\mathbf{R}^4$ introduce complex variables

$$z_j = x_j + \mathrm{i}y_j \quad \bar{z}_j = x_j - \mathrm{i}y_j.$$

Hamiltonian. The Hamiltonian of the harmonic oscillator becomes

$$\widetilde{H}(z_1, z_2) = \tfrac{1}{2}\,(z_1\bar{z}_1 + z_2\bar{z}_2).$$

Symplectic form. The symplectic form ω becomes

$$\Omega = \frac{1}{2\mathrm{i}}(dz_1 \wedge d\bar{z}_1 + dz_2 \wedge d\bar{z}_2).$$

Vector field. The hamiltonian vector field corresponding to $\widetilde{H}$ satisfies

$$X_{\widetilde{H}} \mathbin{\lrcorner} \Omega = \mathrm{d}\widetilde{H}, \tag{1.1.46}$$

where

$$\widetilde{H} = \tfrac{1}{2}\,(z_1\,\mathrm{d}\bar{z}_1 + z_2\,\mathrm{d}\bar{z}_2 + \bar{z}_1\,\mathrm{d}z_1 + \bar{z}_2\,\mathrm{d}z_2).$$

Using equation (1.1.46) a calculations shows that

$$X_{\widetilde{H}} = i\left(z_1\,\frac{\partial}{\partial z_1} + z_2\,\frac{\partial}{\partial z_2} - \bar{z}_1\,\frac{\partial}{\partial \bar{z}_1} - \bar{z}_2\,\frac{\partial}{\partial \bar{z}_2}\right).$$

whose flow is

$$\phi_t^{\widetilde{H}}(z_1, z_2, \bar{z}_1, \bar{z}_2) = (e^{\mathrm{i}t} z_1, e^{\mathrm{i}t} z_2, e^{-\mathrm{i}t} \bar{z}_1, e^{-\mathrm{i}t} \bar{z}_2).$$

Quadratic integrals. In complex coordinates

$$\begin{array}{llll} w_1 & = \operatorname{Im} z_1 \bar{z}_2 & w_2 & = \operatorname{Re} z_1 \bar{z}_2 \\ w_3 & = \tfrac{1}{2}\,(z_1\bar{z}_1 - z_2\bar{z}_2) & w_4 & = \tfrac{1}{2}\,(z_1\bar{z}_1 + z_2\bar{z}_2). \end{array} \tag{1.1.47}$$

Assertion. The integrals w_1, w_2, w_3, w_4 generate the algebra of polynomials invariant under the flow of the harmonic oscillator vector field X_H.

Proof. Consider a monomial $M = z_1^{j_1} z_2^{j_2} \bar{z}_1^{k_1} \bar{z}_2^{k_2}$ such that

$$0 = L_{X_{\widetilde{H}}} M = \mathrm{i}(j_1 + j_2 - k_1 - k_2)M.$$

Then M is invariant under the flow $\phi_t^{\widetilde{H}}$ if and only if $j_1 + j_2 = k_1 + k_2$. We write the factors of M in two lists

$$\begin{array}{c} \overbrace{z_1 \cdots\cdots z_1}^{j_1}\ \overbrace{z_2 \cdots z_2}^{j_2} \\ \underbrace{\bar{z}_1 \cdots \bar{z}_1}_{k_1}\ \underbrace{\bar{z}_2 \cdots\cdots \bar{z}_2}_{k_2} \end{array}$$

Since these lists have equal length, their entries can be paired off. This expresses M as a product of $z_1\bar{z}_1$, $z_1\bar{z}_2$, $z_2\bar{z}_1$ and $z_2\bar{z}_2$. □

Consequence. By a theorem of Schwarz (*a heavy theorem about smooth invariant functions on [37]*) every *smooth* integral of X_H factors through $\widetilde{J}$.

1.1.5 Normalization of the Hénon-Heiles hamiltonian

Hamiltonian. The Hénon-Heiles hamiltonian is

$$H : \mathbf{R}^4 \to \mathbf{R} : (x, y) \mapsto \tfrac{1}{2}\,(y_1^2 + y_2^2 + x_1^2 + x_2^2) + \frac{\varepsilon}{3}(x_1^3 - 3x_1x_2^2). \quad (1.1.48)$$

Normalization. Normalizing H means that we find a symplectic change of coordinates so that the new Hamiltonian has a two dimensional harmonic symmetry, that is, it commutes with w_4 up to a certain order, see [11] for more details.

Normalized Hénon-Heiles. The normalized Hénon-Heiles hamiltonian up to sixth order is

$$\mathcal{H} = \mathcal{H}^{(2)} + \varepsilon^2\mathcal{H}^{(4)} + \varepsilon^4\mathcal{H}^{(6)} + \cdots \quad (1.1.49)$$

where

$$\begin{aligned} \mathcal{H}^{(2)} &= \frac{1}{2}w_4 \\ \mathcal{H}^{(4)} &= \frac{1}{48}(7w_2^2 - 5w_4^2) \\ \mathcal{H}^{(6)} &= \frac{1}{64}\Big(-\frac{67}{54}w_4^3 - \frac{7}{8}w_2^2w_4 - \frac{28}{9}w_3^3 + \frac{28}{3}w_1^2w_3\Big). \end{aligned} \quad (1.1.50)$$

1.1.5.1 The Hénon-Heiles hamiltonian normalized up to 4th order

Restrict. We sit on the constant energy surface $w_4 = h$, that is, on the set $\mathbf{S}_h^2$. The fourth order normalized hamiltonian restricted to $\mathbf{S}_h^2$ is

$$\mathcal{H}_h = \mathcal{H}\big|_{\mathbf{S}_h^2} = \frac{h}{2} + \frac{\varepsilon^2}{48}(7w_2^2 - 5h^2). \quad (1.1.51)$$

Simplification. Simplify the hamiltonian $\mathcal{H}_h$ by removing the additive constants and rescaling time. We get

$$\mathcal{H}_h = w_2^2. \quad (1.1.52)$$

Critical points of $\mathcal{H}_h$ on $\mathbf{S}_h^2$. In order to find the critical points of $\mathcal{H}_h$ on the surface $\mathbf{S}_h^2$ we solve

$$(0,0,0) = D\mathcal{H}_h(w) + \lambda DG(w) \quad \text{and} \quad G(w) = 0, \quad (1.1.53)$$

where

$$G : \mathbf{R}^3 \to \mathbf{R} : (w_1, w_2, w_3) \mapsto w_1^2 + w_2^2 + w_3^2 - h^2.$$

Solutions. The system of equations for the critical points is

$$\begin{aligned} 2\lambda\, w_1 &= 0 \\ 2\, w_2 + 2\lambda\, w_2 &= 0 \\ 2\lambda\, w_3 &= 0 \end{aligned}$$

and the constraint $w_1^2 + w_2^2 + w_3^2 = h^2$. For $\lambda \neq 0$ the solutions of these equations are $w_1 = 0$, $w_3 = 0$, $w_2 = \pm h$, $\lambda = -1$. These correspond to two critical points $p_\pm = (0, \pm h, 0)$. For $\lambda = 0$ the solution is $w_2 = 0$, $w_1^2 + w_3^2 = h^2$. This is a critical submanifold of $\mathbf{S}_h^2$, which is the heavy darkened circle in figure 1.1.4.

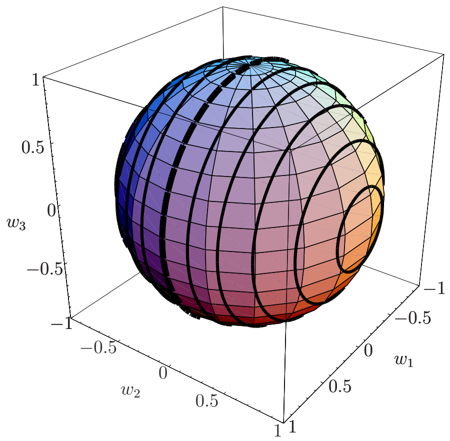

Fig. 1.1.4. Constant level sets of the reduced Hénon-Heiles Hamiltonian $\mathcal{H}_h$ of order 4 on the reduced phase space $\mathbf{S}_h^2$; heavy darkened circle is the critical set at $w_2 = 0$.

Hessian. The Hessian of $\mathcal{H}_h\big|_{\mathbf{S}_h^2}$ at the critical points $p_\pm$ is

$$D^2\mathcal{H}_h\big|_{S_h^2}(p_\pm) = (D^2\mathcal{H}_h - D^2G)\big|_{T_{p_\pm}\mathbf{S}_h^2}, \tag{1.1.54}$$

where $T_w\mathbf{S}_h^2 = \ker DG(w)$. Since $DG(p_\pm) = (0, \pm 2h, 0)$, we see that $\ker DG(w) = \operatorname{span}\{e_1, e_3\}$. Therefore

$$D^2\mathcal{H}\big|_{S_h^2}(p_\pm) = \left(\begin{pmatrix} 0 & & \\ & 2 & \\ & & 0 \end{pmatrix} - \begin{pmatrix} 2 & & \\ & 2 & \\ & & 2 \end{pmatrix} \right)\Big|_{\operatorname{span}\{e_1,e_3\}} = -2I_2 \tag{1.1.55}$$

and the critical points $p_\pm$ are maxima of $\mathcal{H}_h$ on $\mathbf{S}_h^2$.

Until 1982 physicists did not know how to carry on since the 4th order system remained degenerate.

Our function behaves like a Morse function at the two critical points with $w_2 = \pm 1$. These points remain in place and will remain stationary due to symmetry, a small perturbation will not destroy them. On the contrary, the critical circle is a nondegenerate Bott-Morse critical submanifold. It will nearly completely disappear due to the small perturbation of higher order.

1.1.5.2 The Hénon-Heiles hamiltonian normalized up to 6th order

Restrict We sit on the constant energy surface $\mathbf{S}^2_h$. The sixth order normalized hamiltonian restricted to $\mathbf{S}^2_h$ is

$$\begin{aligned}\mathcal{H}_h &= \mathcal{H}^{(2)} + \varepsilon^2 \mathcal{H}^{(4)} + \varepsilon^6 \mathcal{H}^{(6)} \\ &= \frac{7}{48} w_2^2 + \frac{\varepsilon^2}{64} \left(-\frac{7h}{8} w_2^2 - \frac{28}{9} w_3^3 + \frac{28}{3} w_1^2 w_3 \right)\end{aligned}$$

Critical points. To find the critical points of $\mathcal{H}_h | \mathbf{S}^2_h$ we solve

$$(0,0,0) = D\mathcal{H}_h(w) + \lambda DG(w) \quad \text{and} \quad G(w) = 0 \tag{1.1.56}$$

where

$$G : \mathbf{R}^3 \to \mathbf{R} : (w_1, w_2, w_3) \mapsto w_1^2 + w_2^2 + w_3^2 - h^2$$

as before.

Solutions. The system of equations for the critical points is

$$\begin{aligned}&\frac{7\varepsilon^2}{24} w_1 w_3 + 2\lambda w_1 = 0 \\ &\frac{7}{24} w_2 - \frac{7\varepsilon^2 h}{256} w_2 + 2\lambda w_2 = 0 \\ &\frac{7\varepsilon^2}{48} w_1^2 - \frac{7\varepsilon^2}{48} w_3^2 + 2\lambda w_3 = 0.\end{aligned}$$

together with the constraint $w_1^2 + w_2^2 + w_3^2 = h^2$. We search for solutions where $w_2 = 0$. Set $\lambda = 7\varepsilon^2 \mu / 24$. Then the above system of equations becomes

$$\begin{aligned}&w_1 w_2 + 2\mu w_1 = 0 \\ &w_1^2 - w_3^2 + 4\mu w_3 = 0 \\ &w_1^2 + w_3^2 = h^2\end{aligned}$$

The solutions of this system are $w_1 = 0$, $w_3 = \pm h$, $\mu = \pm \frac{1}{2} h$ and $w_1 = \pm \frac{1}{2}\sqrt{3} h$, $w_3 = \pm \frac{1}{2} h$, $\mu = \mp \frac{1}{2} h$.

Geometry. Because of the introduction of the sixth order term, the nondegenerate critical manifold that we had for the fourth-order hamiltonian breaks up into 6 critical points: three of them stable (elliptic) and three unstable (hyperbolic) that are connected by their stable and unstable manifolds (figure 1.1.5). For a geometric explanation of this bifurcation see [4]. This picture does not change qualitatively if we add higher order terms to the hamiltonian.

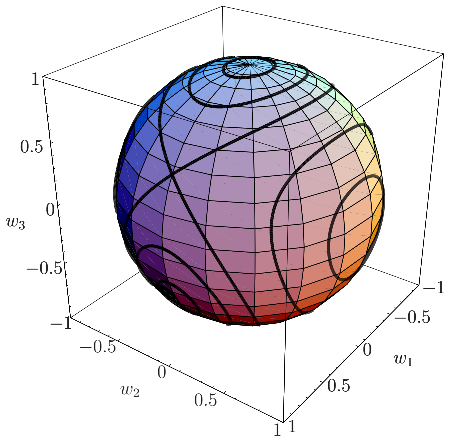

Fig. 1.1.5. Constant level sets of the reduced Hénon-Heiles hamiltonian $\mathcal{H}_h$ of order 6 on the reduced phase space $\mathbf{S}^2_h$.

Reconstruction. In the case of the 4th order normalized Hénon-Heiles hamiltonian, we found two critical points $p_{\pm} = (0, \pm h, 0)$ and a critical manifold $w_2 = 0$. After reconstruction, the critical points become periodic orbits in phase space, while the critical manifold becomes a 2-torus on which the flow of the normalized hamiltonian has rotation number 0.

In the case of the 6th order normalized Hénon-Heiles hamiltonian, we found eight critical points. Six of the critical points have $w_2 = 0$ while the other two are again $p_{\pm} = (0, \pm h, 0)$. Three of the critical points with $w_2 = 0$ are elliptic, while the other three are hyperbolic. The hyperbolic critical points are connected by their stable and unstable manifolds. After reconstruction these manifolds form a 2-torus in phase space that intersects itself three times cleanly along three circles.

1.A Comments on lecture I. Hénon-Heiles system

A great number of papers on this system has appeared since the first publication by Hénon and Heiles in 1964 [22], see [33] for a brief review. It has served both as a model of a nonintegrable (chaotic) system and as a test bed for various normalization techniques. Although originating in astronomy, the Hénon-Heiles system is quite popular in molecular physics where it has many analogues, such as doubly degenerate vibrations of a triatomic molecule A_3 (for example H_3^+ [18]) or of a tetrahedral molecule AB_4. Here we discuss aspects of the Hénon-Heiles system related to its finite symmetry which simplify significantly the analysis in [3]. Despite extensive work, this paper has been overlooked.

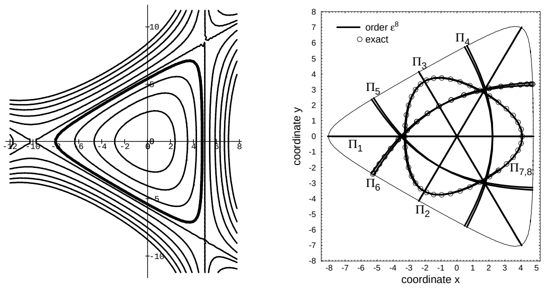

Fig. 1.A.1. Hénon-Heiles potential $V(x)$ calculated for $\epsilon = 0.1$ and $E/E_{\text{saddle}} = 0.2, 0.45, 0.7, \mathbf{0.9}, 1, 1.2, \ldots$ (left); Relative equilibria (nonlinear normal modes) of the Hénon-Heiles system reconstructed from the ϵ^8 normal form at the energy $E/E_{\text{saddle}} = 0.9$ (right).

The spatial symmetry group of (1.1.48) is a dihedral group D_3. The full symmetry group is $D_3 \times \mathcal{T}$ where $\mathcal{T}$ is a Z_2 symmetry of the kind $(q, p) \to (q, -p)$ or equivalently $z \to \bar{z}$, which is often called *time reversal* or *momentum reversal*. Operations of the spatial group D_3 commute with the oscillator symmetry S^1. Operations which involve $\mathcal{T}$ are antisymplectic and do not commute with S^1.

1.A.1 Invariants and integrity basis

Dynamical invariants. As in the lecture, we consider quadratic polynomial invariants of the oscillator symmetry. For obscure historical reasons[1], our definition differs by a factor 2, namely,

$$H_0 = 2J = \tfrac{1}{2}(z_2\bar{z}_2 + z_1\bar{z}_1) = w_4,$$
$$\mathbf{J} = \begin{pmatrix} J_1 \\ J_2 \\ J_3 \end{pmatrix} = \frac{1}{4}\begin{pmatrix} z_2\bar{z}_1 + z_1\bar{z}_2 \\ iz_2\bar{z}_1 - iz_1\bar{z}_2 \\ z_2\bar{z}_2 - z_1\bar{z}_1 \end{pmatrix} = \frac{1}{2}\begin{pmatrix} w_2 \\ w_1 \\ -w_3 \end{pmatrix}.$$

The Poisson algebra generated by the components of the 3-vector $\mathbf{J}$ is the standard so(3) with bracket $\{J_a, J_b\} = \epsilon_{abc} J_c$ and the Casimir $J = |\mathbf{J}|$ (or H_0).

Action of $D_3 \times \mathcal{T}$. The action of the symmetry group $D_3 \times \mathcal{T}$ on the components of $\mathbf{J}$ is equivalent to the action of the point group D_{3h} of transformations of $\mathbf{R}^3$ with coordinates (J_1, J_2, J_3) [20]. Since J_2 is invariant with respect to any rotation of the initial coordinate plane (x_1, x_2), it is convenient to choose J_2 along the vertical axis in $\mathbf{R}^3$. Then time reversal $\mathcal{T}$, which sends (J_1, J_2, J_3) to $(J_1, -J_2, J_3)$ (as can be verified directly), acts as the horizontal reflection plane of D_{3h}.

Integrity basis. Due to the relation

$$J_1^2 + J_2^2 + J_3^2 = J^2 = \tfrac{1}{4}\, h^2. \tag{1.A.1}$$

the ring $\mathcal{R}$ of invariant polynomials generated by J and (J_1, J_2, J_3) is not free. To analyze the normalized system we should have the way to express the normal form $H_{\rm nf}$ uniquely in terms of (J_1, J_2, J_3, J). The standard recipe for this is a Gröbner basis. We use a slightly more sophisticated integrity basis which (when it works) has certain advantages. An *integrity basis* consists of *principal* and *auxiliary* polynomials. The ring $\mathcal{R}$ decomposes as $\mathbf{R}[J, J_a, J_b] \oplus J_c\,\mathbf{R}[J, J_a, J_b]$ meaning that any member of $\mathcal{R}$ can be written uniquely as a real polynomial in the principal polynomials $\{J, J_a, J_b\}$ and J_c times another polynomial in $\{J, J_a, J_b\}$. Using (1.A.1) any power of J_3 can be represented this way.

In general, the number of principal polynomials equals the dimension of the reduced phase space (which is 2 for $\mathbf{S}^2_h$) plus the number of integrals of motion (we have one such integral J). Since the values of principal polynomials distinguish orbits of the action of the dynamical symmetry, they can serve as coordinates for charts of the reduced phase space, while auxiliary polynomials can be used to distinguish different charts. Thus for the reduced space $\mathbf{S}^2_J$ we need two charts $J_c > 0$ and $J_c < 0$ with coordinates (J_a, J_b).

[1] Our factors correspond to the quantum mechanical analogue of (1.A.1) called Schwinger [38] or boson representation of the angular momentum system.

Molien function. An explicit construction of an integrity basis is aided by knowing the Molien generating function. The generating function for the polynomials in four initial phase space variables $(z_1, z_2, \bar{z}_1, \bar{z}_2)$ invariant with respect to the S^1 oscillator symmetry is

$$g(\lambda) = (1+\lambda^2)/(1-\lambda^2)^3. \tag{1.A.2}$$

Here the formal variable λ represents one of $\{z, \bar{z}\}$. This function can be computed directly from Molien's theorem in representation theory. It indicates that there are three principal invariants represented by terms $1-\lambda^k$ in the denominator and one nontrivial auxiliary invariant represented by terms λ^k in the numerator. Since $k=2$, all invariants are of degree 2 in $\{z, \bar{z}\}$. This kind of information is invaluable in high dimensional situations.

Fully symmetrized integrity basis. Our polynomials $\{J_1, J_2, J_3\}$ are *not* symmetric with respect to $D_3 \times \mathcal{T}$. The group $D_3 \times \mathcal{T}$ acts on (J_3, J_1, J_2) in the same way as D_{3h} acts on (X, Y, Z) in 3-space, that is, (J_3, J_1, J_2) span the $E \oplus A_2$ representation of D_{3h}. The Molien generating function for the $D_3 \times \mathcal{T}$ invariant polynomials in (J_1, J_2, J_3) is

$$g(E \oplus A_2 \to A_1; \lambda) = \frac{1}{(1-\lambda^2)(1-\lambda^3)}.$$

This can be obtained straightforwardly from the action of the finite group $D_3 \times \mathcal{T}$ on (J_1, J_2, J_3). Note that here λ stands for any one of $\{J_1, J_2, J_3\}$. We conclude that the ring of all polynomial invariants of the combined action of $D_3 \times \mathcal{T}$ and oscillator symmetry S^1 is freely generated by (n, μ, ξ), where n is the main oscillator invariant (see (1.A.1)), and μ and ξ are polynomials in $\{J_1, J_2, J_3\}$ of degree 2 and 3 respectively. The invariants $\{n, \mu, \xi\}$ can be chosen explicitly as follows

$$n = 2J, \quad \mu = J_2^2, \quad \xi = \tfrac{1}{2}\, J_3(3J_1^2 - J_3^2). \tag{1.A.3}$$

This means that the normalized Hénon-Heiles Hamiltonian is a function $H_{\mathrm{nf}}(n, \mu,\ \xi)$ with n later relegated as a parameter. This basic result of invariant theory has not been appreciated in the numerous studies on the Hénon-Heiles system, including Cushman's early work in [7] and his lecture in Peyresq. Yet, this observation along with the rest of our comment is entirely in the spirit of Cushman's contemporary approach to the analysis of reduced systems [5].

1.A.2 Qualitative analysis of the reduced system

Most of the qualitative information on the Hénon-Heiles system presented in the lecture can be obtained simply from the $\mathbf{S}^2_h$ topology of the reduced phase space and the full use of the symmetry group action on it.

Table 1.A.1. *Critical orbits of the $D_3 \times \mathcal{T} \sim D_{3h}$ action on the reduced phase space $\mathbf{S}^2_h$ of the Hénon-Heiles system. The $C_3 \wedge \mathcal{T}_2$ subgroup of $D_3 \times \mathcal{T}$ is generated by C_3 and $\mathcal{T}_2 = C_2 \circ \mathcal{T}$; the groups $C_3 \wedge \mathcal{T}_2$, D_3, and C_{3v} are isomorphic as abstract groups. "Historic" labels Π_k were introduced for the nonlinear normal modes in [3, 29] and used in [18].*

orbit	stabilizer	ξ/J^3	μ/J^2	$(J_3, J_1, J_2), J$
$\Pi_{7,8}$	$C_3 \wedge \mathcal{T}_2$	0	1	$(0,0,\pm 1)$
$\Pi_{4,5,6}$	$C_2 \times \mathcal{T}$	$-1/2$	0	$(1,0,0)$, $(\cos\frac{2\pi}{3}, \pm\sin\frac{2\pi}{3}, 0)$
$\Pi_{1,2,3}$	$C_2' \times \mathcal{T}$	$1/2$	0	$(-1,0,0)$, $(\cos\frac{\pi}{3}, \pm\sin\frac{\pi}{3}, 0)$

Stratification of the reduced phase space. The action of the symmetry group $D_3 \times \mathcal{T}$ on $\mathbf{S}^2_h \subseteq \mathbf{R}^3$ follows from the action of the point group D_{3h} of transformations acting on $\mathbf{R}^3$ with coordinates $(X, Y, Z) = (J_3, J_1, J_2)$. This action has 8 fixed points which form three critical orbits characterized in table 1.A.1. Note the immediate advantage of fully symmetrized main invariants $\{\xi, \mu\}$ over the coordinates (J_3, J_1, J_2). The values of (ξ, μ) represent entire orbits of the group action. This amounts to introducing polar coordinates by the back door, which is a no no, according to Cushman.

Orbit space. As shown in figure 1.A.2, right, the orbit space $\mathcal{O}$ of the $D_3 \times \mathcal{T}$ action on $\mathbf{S}^2_h$ is the semialgebraic variety in $\mathbf{R}^3$ with coordinates (ξ, η, t) defined by

$$0 \le \frac{\mu}{J^2} \le 1 - t^2, \quad \frac{|\xi|}{J^3} \le \tfrac{1}{2}\, t^3, \quad t \in [0,1].$$

Each point in the interior of $\mathcal{O}$ represents a 12-point generic orbit of the $D_3 \times \mathcal{T}$ group action. Its three singular boundary points correspond to critical orbits in table A.1. The other boundary points represent 6-point orbits with nontrivial stabilizers $\mathcal{T}$ or $\mathcal{T}_s$. Knowing how D_{3h} acts on the

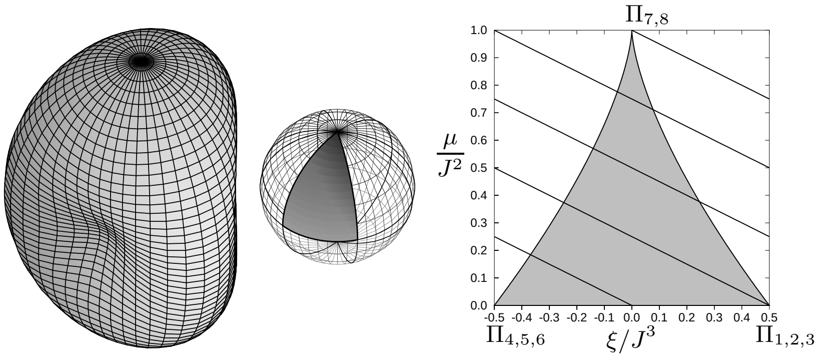

Fig. 1.A.2. Relative equilibria of the Hénon-Heiles system as stationary points of the reduced Hamiltonian H^J_{nf} on the reduced phase space $\mathbf{S}^2_J$. On the left we show H^J_{nf} as a function on $\mathbf{S}^2_J$. The shaded area on the right and central panel represents the orbit space (orbifold) $\mathcal{O}$ of the $D_3 \times \mathcal{T}$ action on $\mathbf{S}^2$; straight lines in the right panel are constant level sets of the simplest $D_3 \times \mathcal{T}$-invariant Morse Hamiltonian $\mathcal{H} = \mu + \epsilon\xi$.

$\mathbf{S}^2_h$ (figure 1.A.2, centre), we see that $\mathcal{O}$ is the image of the triangular petal on $\mathbf{S}^2_h$ cut out by the three symmetry planes: two vertical planes intersecting at the angle $\pi/3$ and the horizontal plane. Those who prefer using "pure algebra" (and avoid any scent of polar coordinates) would do better by considering

$$\mathcal{J} = \det\left[\frac{\partial(\mu,\xi,J)}{\partial(J_1,J_2,J_3)}\right] = -6J_1J_2(3J_3^2 - J_1^2) = 0$$

and observing that the boundary and singular points of $\mathcal{O}$, that is, its 1 and 0-dimensional strata on $\mathbf{S}^2_h$, correspond to simple and double zeroes of $\mathcal{J}$.

Symmetric Morse functions. We now ask the question: what is a typical $D_3 \times \mathcal{T}$ symmetric function $\mathcal{H}$ on $\mathbf{S}^2_h$? We characterize $\mathcal{H}$ primarily by finding its set of critical points which in our case correspond to *relative equilibria* of our system. Points on the critical orbits are isolated and *must* be critical points of $\mathcal{H}$. Points in the same orbit are *equivalent* and therefore have the same stability. Furthermore, the two equivalent points $\Pi_{7,8}$ must be elliptic (stable) because of their high local symmetry. If we further assume that $\mathcal{H}$ is a Morse function, that is, a function with only nondegenerate critical points, and remember that

Morse's relation for the Euler characteristic of the 2-sphere is

$$c_0 - c_1 + c_2 = 2,$$

where c_0, c_1, and c_2 are the number of maxima, saddle (hyperbolic), and minima of $\mathcal{H}$, we can conclude that a function $\mathcal{H}$ with minimum possible number of critical points has three equivalent elliptic points and three equivalent saddle points in addition to $\Pi_{7,8}$. One possible such simplest Morse function is drawn in figure 1.A.2, left.[1] It has maxima at $\Pi_{7,8}$, minima at $\Pi_{1,2,3}$ and saddle points at $\Pi_{4,5,6}$. The other possibility is to have an oblate shape with two minima at $\Pi_{7,8}$ and three maxima. Trajectories of the reduced system shown in figure 1.1.5 are constant level sets of $\mathcal{H}$ which can be obtained as intersections of the surface in figure 1.A.2 left, and spheres of different radii.[2]

Simplest polynomial Morse Hamiltonian. The most natural way to construct the simplest Morse Hamiltonian $\mathcal{H}$ explicitly is to consider $\mathcal{H}$ as a polynomial in (μ, ξ) defined on the orbit space $\mathcal{O}$. It can be seen that a linear function $\mathcal{H}(\mu, \xi) = a\mu + b\xi$ with nonzero a and b is generic. Indeed, while μ alone is too symmetric (it has axial symmetry S^1), together with the cubic invariant ξ it reproduces all symmetry properties of $D_3 \times \mathcal{T}$ correctly. The absence of auxiliary integrity basis invariants also indicates that we need no other terms in $\mathcal{H}$. In general, coefficients in $\mathcal{H}(\mu, \xi)$ are functions of the parameter J. Since ξ is of higher degree in $(z, \bar{z})$ than μ, the contribution $b(J)$ is likely to be smaller (at least for low values of J) than $a(J)$. Therefore, the reduced Hénon-Heiles system at low J should be qualitatively correctly represented by the level sets of $\mathcal{H} = \mu + \varepsilon\xi$ where $0 < \varepsilon \ll 1$. As shown in figure 1.A.2, right, the family of constant level sets of such $\mathcal{H}$ on the orbifold $\mathcal{O}$ has three exceptional (critical) levels which pass at $\Pi_{1,2,3}$, $\Pi_{4,5,6}$, and $\Pi_{7,8}$. The extremal levels correspond necessarily to stable relative equilibria, the critical level at the intermediate energy $\mathcal{H}_{\Pi_{4,5,6}}$ contains unstable relative equilibria and their stable/unstable manifold (separatrix).

[1] Plots of this kind are used in molecular physics to represent effective rotational energy of nonrigid molecules as function of the orientation of the total angular momentum **J** (orientation of the rotation axis), they are called *rotational energy surfaces* [21]

[2] Note that vertical axis in figure 1.A.2 corresponds to the horizontal axis w_2 in figure 1.1.5.

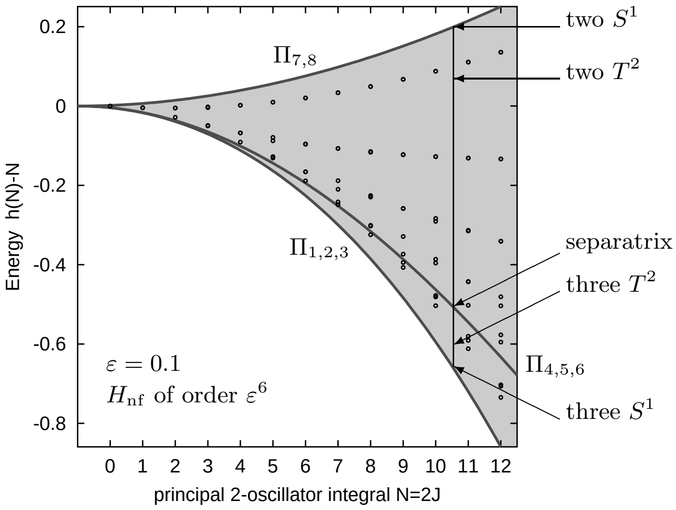

Fig. 1.A.3. Image of the energy-momentum map (shaded area), energies of relative equilibria (solid lines) and quantum energies (circles) of the Hénon-Heiles system with $\varepsilon = 0.1$ obtained using order ε^6 normal form $H_{\rm nf}$. The classical action (momentum) $2J = n$ equals $N + 1$ where N is the polyad quantum number.

1.A.3 Normal form and remarks on further analysis

Now, after the Hénon-Heiles system has been understood qualitatively, we compute the normal form

$$H_{\rm nf} = n - \varepsilon^2 \left(\tfrac{5}{12}n^2 - \tfrac{7}{3}\mu\right) - \varepsilon^4 \left(\tfrac{67}{432}n^3 + \tfrac{7}{36}\mu n - \tfrac{56}{9}\xi\right) + \ldots, \tag{1.A.4}$$

where the coefficients in the higher orders are listed below.

order	1	μn^{-2}	ξn^{-3}	$\mu^2 n^{-4}$	$\mu\xi n^{-5}$
$\varepsilon^6 n^4$	$-\frac{42229}{155520}$	$-\frac{76447}{6480}$	$\frac{2093}{135}$	$\frac{115171}{1944}$	
$\varepsilon^8 n^5$	$-\frac{15624833}{18662400}$	$-\frac{11656729}{2332800}$	$\frac{353843}{8100}$	$\frac{2217943}{233280}$	$\frac{6701639}{4050}$

It comes as little surprise that $H_{\rm nf}$ is a function of (μ, ξ) and parameter n. We can use table 1.A.1 to find the energy of $H_{\rm nf}$ at the critical points Π_k. The results plotted against n give the image of the energy-momentum map $\mathcal{EM}$ of the system, see figure 1.A.3. Note that the $\mathcal{EM}$ map of $\mathcal{H} = \mu + \varepsilon\xi$ has qualitatively the same image.

We now look at reconstruction. In other words, we lift constant energy sets of H_{nf} on the orbifold $\mathcal{O}$ first to the reduced phase space $\mathbf{S}^2_h$ and then all the way back to the initial phase space $\mathbf{R}^4$. This process is a good exercise for those who like to understand the role of the $D_3 \times \mathcal{T}$ symmetry of the system in detail. From the same point of view, it is helpful to compare the image of the $\mathcal{EM}$ map in figure 1.A.3 to that in figure 1.1.1 and to reconstruct $\mathcal{EM}^{-1}(h,n)$. In the simple case of relative equilibria Π_k, we can describe qualitatively the corresponding periodic orbits S^1 in $\mathbf{R}^4$ entirely on the basis of their local symmetry properties (stabilizers) listed in table 1.A.1. This reproduces the results of [3, 29]. Figure 1.A.1, right, demonstrates how these periodic orbits can be reconstructed analytically using the inverse normal form transformation. Finally we can consider quantum analogue of our system on the basis of the EBK torus quantization, see figure 1.A.3.

We conclude with one more remark. We have seen that much of the analysis of the normalized Hénon-Heiles system can be simplified, if not avoided entirely, after we take discrete symmetries into account. Of course this does not reflect the general situation. In certain cases, typically when symmetries are low and dimensions are high, the critical point analysis of the kind presented in the first two lectures becomes necessary. Rather the general conclusion should be that analyzing symmetries helps to distinguish specific properties of the system from more common dynamical behaviour.

1.2 Lectures III and V. The Euler top

Physically the Euler top is a rigid body which is spinning around its (fixed) center of mass with no other forces acting upon it.

1.2.1 Preliminaries on the rotation group

Rotation group. The group of rotations in $\mathbf{R}^3$ is

$$\mathrm{SO}(3) = \{A \in \mathrm{GL}(3,\mathbf{R}) \big| A^t A = I \text{ and } \det A = 1\}.$$

Lie algebra. The Lie algebra of SO(3) is

$$\mathrm{so}(3) = \{X \in \mathrm{gl}(3,\mathbf{R}) \big| X + X^t = 0\}$$

with Lie bracket $[X,Y] = XY - YX$.

Isomorphism. $(\mathbf{R}^3, \times) \simeq (\mathrm{so}(3), [\,,])$. The isomorphism is

$$x = \begin{pmatrix} x_1 \\ x_2 \\ x_3 \end{pmatrix} \rightarrow \widehat{x} = \begin{pmatrix} 0 & -x_3 & x_2 \\ x_3 & 0 & -x_1 \\ -x_2 & x_1 & 0 \end{pmatrix} = X.$$

Properties of this isomorphism. $\widehat{x}(y) = Xy = x \times y$, and $[\widehat{x}, \widehat{y}] = \widehat{x \times y}$; for $A \in \mathrm{SO}(3)$, $A\widehat{x}A^{-1} = \widehat{Ax}$.

Inner product on $\mathrm{so}(3)$**.** Define an inner product on $\mathrm{so}(3)$ as

$$\mathrm{k}(X, Y) = -\tfrac{1}{2}\,\mathrm{tr}XY^t \;=\; \langle \widehat{x}, \widehat{y} \rangle,$$

where $\langle\,,\,\rangle$ is the Euclidean inner product on $\mathbf{R}^3$.

1.2.2 Traditional derivation of the equations of motion

Here we derive the equations of motion of the Euler top in the traditional nonhamiltonian manner. We use Coriolis' theorem and the conservation of angular momentum.

1.2.2.1 Reference frames

Let V be a three dimensional real vector space with Euclidean inner product $\langle\,,\,\rangle$. A *frame of reference* $\mathcal{F}$ is a positively oriented orthonormal basis $\{f_1, f_2, f_3\}$ of V. A vector $v \in V$ *looks like* the vector $x \in \mathbf{R}^3$ *in the frame* $\mathcal{F}$ means $v = \sum_{i=1}^{3} x_i\, f_i$. Corresponding to the frame $\mathcal{F}$ is its *coframe* $\mathcal{F}^* = \{f_1^*, f_2^*, f_3^*\}$, where $f_i^*(f_j) = \delta_{ij}$. Suppose that $\mathcal{A} = \{a_1, a_2, a_3\}$ is another reference frame such that the vector $v \in V$ looks like the vector $X \in \mathbf{R}^3$, that is, $v = \sum_{i=1}^{3} X_i\, a_i$. Let A be the 3×3 matrix whose $\mathrm{ij}^{\mathrm{th}}$ entry is $f_i^*(a_j)$, that is, a_j looks like the j^{th} column of A in the frame $\mathcal{F}$. Then

$$x = AX, \tag{1.2.1}$$

because

$$x_i = f_i^*(\sum_{j=1}^{3} x_j\, f_j) \;=\; f_i^*(\sum_{j=1}^{3} X_j\, a_j) \;=\; \sum_{j=1}^{3} f_i^*(a_j) X_j.$$

In other words, the vector $v \in V$, which in the frame $\mathcal{F}$ looks like the vector $x \in \mathbf{R}^3$, in the frame $\mathcal{A}$ looks like the vector X.

1.2.2.2 Rotating frame

Let

$$A : \mathbf{R} \rightarrow \mathrm{SO}(3) : t \mapsto A(t) = \mathrm{col}(a_1(t), a_2(t), a_3(t)).$$

Then $\mathcal{A} = \{a_1(t), a_2(t), a_3(t)\}$ is a frame for V whose j^{th} member $a_j(t)$ looks like the j^{th} column of $A(t)$ with respect to the fixed frame $\mathcal{F}$. We say that $\mathcal{A}$ is a *frame which rotates with respect to the fixed frame* $\mathcal{F}$.

1.2.2.3 Coriolis' theorem

Before starting the derivation Richard points out that "Physicists don't know how to prove this theorem". Before a fight between the mathematicians and physicists in the audience has time to break out Daryl Holm replies "Don't mock the alligator until you've crossed the river safely." The lecture continues.

Let $x : \mathbf{R} \rightarrow \mathbf{R}^3 : t \mapsto x(t)$ be a differentiable function. Suppose that $\Xi : \mathbf{R} \rightarrow V : t \mapsto \Xi(t)$ is a motion in V so that its position $\Xi(t)$ at time t in the fixed frame $\mathcal{F}$ looks like $x(t)$, while its position in the rotating frame $\mathcal{A}$ looks like $X(t)$. Then from (1.2.1) we obtain

$$x(t) = A(t)X(t). \tag{1.2.2}$$

Differentiating (1.2.2) gives

$$\frac{dx}{dt} = A'(t)X + A(t)\frac{dX}{dt} \; = \; A'(t)A^{-1}(t)x + A(t)\frac{dX}{dt}. \tag{1.2.3}$$

The velocity of $t \mapsto \Xi(t)$ at time t with respect to the fixed frame $\mathcal{F}$ is a vector in V which looks like $\frac{dx}{dt}$, while with respect to the rotating frame $\mathcal{A}$ it is a vector in V which looks like $\frac{dX}{dt}$. The skew symmetric matrix $A'(t)A^{-1}(t)$ is an *infinitesimal motion* in the fixed frame. The corresponding vector $\omega(t) \in \mathbf{R}^3$, where

$$\widehat{\omega(t)} = A'(t)A^{-1}(t),$$

is the *angular velocity in the fixed frame at time t of the rotating frame.* We can rewrite (1.2.3) as

$$\frac{dx}{dt} - \omega(t) \times x(t) = A(t)\frac{dX}{dt}, \tag{1.2.4}$$

which is a form of Coriolis' theorem (in the fixed frame). Define $\Omega(t)$ to be the vector in $\mathbf{R}^3$ which looks like $\omega(t)$ in the rotating frame, that is,

$$\omega(t) = A(t)\Omega(t). \tag{1.2.5}$$

Using the definition of $\omega(t)$ we find that

$$\widehat{\omega(t)} = A'(t)A^{-1}(t) \; = \; A(t)(A^{-1}(t)A'(t))A^{-1}(t).$$

Taking the hat of both sides of (1.2.5) gives $\widehat{\omega(t)} = A(t)\widehat{\Omega(t)}A^{-1}(t)$. Thus

$$\widehat{\Omega(t)} = A^{-1}(t)A'(t).$$

Thus we may rewrite (1.2.3) as

$$\begin{aligned} \frac{dx}{dt} &= A(t)[A^{-1}(t)A'(t)X + \frac{dX}{dt}] = A(t)[\widehat{\Omega(t)}X + \frac{dX}{dt}] \\ &= A(t)[\Omega(t) \times X + \frac{dX}{dt}], \end{aligned} \tag{1.2.6}$$

which is another form of Coriolis' theorem (in the rotating frame).

Richard says that he has now crossed the river safely.

1.2.2.4 Constant angular momentum

Suppose we have a rigid body $\mathcal{B}$ in $\mathbf{R}^3$ made up of a finite number of point masses m_i at position r_i, not all on a single line through the origin. Suppose that the center of mass of $\mathcal{B}$ lies at the origin O of $\mathbf{R}^3$ and that $\mathcal{B}$ is subjected to no external forces.

Fix the frame $\mathcal{E} = \{e_1, e_2, e_3\}$ consisting of the standard basis vectors in $\mathbf{R}^3$. We call $\mathcal{E}$ the *space frame*. The angular momentum of $\mathcal{B}$ with respect to the space frame is given by

$$\ell = \sum_i m_i \, r_i \times v_i, \tag{1.2.7}$$

where $v_i = \frac{dr_i}{dt}$ is the velocity of the ith point mass in $\mathcal{B}$ with respect to the space frame. ℓ is constant throughout the motion of $\mathcal{B}$.

Proof. Differentiating (1.2.7) gives

$$\frac{d\ell}{dt} = \sum_i m_i \frac{dr_i}{dt} \times v_i + \sum_i m_i r_i \times \frac{dv_i}{dt} = \sum_i r_i \times \frac{d(m_i v_i)}{dt} = \sum_i r_i \times F_i.$$

F_i is the total force exerted on the i$^{\text{th}}$ point mass.

$$F_i = F_i^{\text{int}} + F_i^{\text{ext}},$$

where F_i^{int} and F_i^{ext} is the internal and external forces, respectively. $F_i^{\text{int}} = \sum_{j \neq i} F_{ij}^{\text{int}}$, where F_{ij}^{int} is the force exerted on the ith particle by the jth particle of the body. But action and reaction are equal and lie along a line joining the ith and jth particle, that is,

$$0 = r_i \times F_{ij}^{\text{int}} + r_j \times F_{ji}^{\text{int}} = (r_i - r_j) \times F_{ij}^{\text{int}}.$$

Consequently,

$$\begin{aligned}\sum_i r_i \times F_i^{\text{int}} &= \sum_{\substack{i,j\\ i\neq j}} r_i \times F_{ij}^{\text{int}} = \sum_{i<j} r_i \times F_{ij}^{\text{int}} + \sum_{j<i} r_i \times F_{ij}^{\text{int}} \\ &= \sum_{i<j} (r_i \times F_{ij}^{\text{int}} - r_j \times F_{ij}^{\text{int}}) = 0.\end{aligned}$$

Thus

$$\frac{d\ell}{dt} = \sum_i r_i \times F_i = \sum_i r_i \times (F_i^{\text{int}} + F_i^{\text{ext}}) = \sum_i r_i \times F_i^{\text{ext}} = 0. \quad \square$$

1.2.2.5 Euler's equations

Attach an orthonormal frame to $\mathcal{B}$ with origin at O in $\mathbf{R}^3$. As $\mathcal{B}$ rotates, the attached frame rotates with it and thus defines a differentiable curve $\mathbf{R} \to \mathrm{SO}(3) : t \mapsto A(t)$. The column vectors of $A(t)$ define the *body frame*. Let $L = A(t)^{-1}\ell$ be the *angular momentum in the body frame.* Coriolis' formula (1.2.6) applied to ℓ gives

$$\frac{d\ell}{dt} = A(t)[\Omega(t) \times L + \frac{dL}{dt}], \tag{1.2.8}$$

Since $\frac{d\ell}{dt} = 0$, we obtain

$$\frac{dL}{dt} = L \times \Omega, \tag{1.2.9}$$

where L is the angular momentum in the body frame and Ω is the angular velocity of the body in the body frame. Now

$$L = I(\Omega). \tag{1.2.10}$$

I is the *moment of inertia tensor* of $\mathcal{B}$ in the body frame. I does not depend on t as the body is rigid, which means that the positions and the magnitudes of the masses are constant in the body frame. Thus (1.2.9) can be written as

$$I(\dot{\Omega}) = I(\Omega) \times \Omega, \tag{1.2.11}$$

which are called *Euler's equations*. We may choose the body frame so that $\{e_1, e_2, e_3\}$ are the *principal axes* of $\mathcal{B}$, that is, $I(e_j) = I_j\, e_j$ for $j = 1, 2, 3$. From now on we assume that $0 < I_1 < I_2 < I_3$. In components (1.2.11) reads

$$\begin{aligned} I_1\, \dot{\Omega}_1 &= (I_2 - I_3)\, \Omega_2\Omega_3 \\ I_2\, \dot{\Omega}_2 &= (I_3 - I_1)\, \Omega_1\Omega_3 \\ I_3\, \dot{\Omega}_3 &= (I_1 - I_2)\, \Omega_1\Omega_2. \end{aligned} \tag{1.2.12}$$

Let $a = I_1^{-1}$, $b = I_2^{-1}$, $c = I_3^{-1}$ (so $0 < c < b < a$) and let $p_j = I_j \Omega_j$. Then (1.2.12) becomes

$$\begin{aligned} \dot{p}_1 &= -(b-c)\, p_2 p_3 \\ \dot{p}_2 &= (a-c)\, p_1 p_3 \\ \dot{p}_3 &= -(a-b)\, p_1 p_2. \end{aligned} \tag{1.2.13}$$

1.2.3 Qualitative behavior of solutions of Euler's equations

To describe the qualitative behavior of the solutions of Euler's equations (1.2.11), we note that the functions

$$E = \tfrac{1}{2} \langle I\Omega, \Omega \rangle = \tfrac{1}{2} \langle I^{-1}(p), p \rangle \tag{1.2.14}$$

$$L = \langle I\Omega, I\Omega \rangle = \langle p, p \rangle \tag{1.2.15}$$

are constant on the solutions of (1.2.11) and thus are constant on the solutions of (1.2.13).

Check.

$$\dot{E} = \langle I(\dot{\Omega}), \Omega \rangle = \langle I(\Omega) \times \Omega, \Omega \rangle = 0$$

and

$$\dot{L} = 2 \langle I(\dot{\Omega}), I(\Omega) \rangle = \langle I(\Omega) \times \Omega, I(\Omega) \rangle = 0. \qquad \square$$

The function E is a Morse function on the 2-sphere $\mathbf{S}^2_{|\ell|}$ defined by $\langle p, p \rangle = |\ell|^2$. It has six nondegenerate critical points: 2 of Morse index 0, 2 of index 1, and 2 of index 0.

Check. If p^0 is a critical point of E on $\mathbf{S}^2_{|\ell|}$, then

$$0 = \mathrm{d}E(p^0) - \lambda^0 \, \mathrm{d}L(p^0) = (I^{-1} - \lambda^0 \, \mathrm{id}) p^0 \quad \text{and} \quad \langle p^0, p^0 \rangle = |\ell|^2.$$

Then p^0 is an eigenvector of length $|\ell|$ of $I^{-1} = \mathrm{diag}(a, b, c)$ corresponding to the eigenvalue λ^0. Thus

$$p^0 = \begin{cases} \pm |\ell| e_1, & \text{when } \lambda^0 = a \\ \pm |\ell| e_2, & \text{when } \lambda^0 = b \\ \pm |\ell| e_3, & \text{when } \lambda^0 = c. \end{cases}$$

The Hessian of $E\big|_{\mathbf{S}^2_{|\ell|}}$ at the critical point p^0 is

$$\begin{aligned} D^2(E\big|_{\mathbf{S}^2_{|\ell|}})(p^0) &= (D^2E(p^0) - \lambda^0\, D^2L(p^0))\big|_{T_{p^0}\mathbf{S}^2_{|\ell|}} \\ &= (I^{-1} - \lambda^0\,\mathrm{id})\big|_{T_{p^0}\mathbf{S}^2_{|\ell|}} \\ &= \begin{cases} \mathrm{diag}(b-a, c-a), & p^0 = \pm|\ell|e_1 \\ \mathrm{diag}(a-b, c-b), & p^0 = \pm|\ell|e_2 \\ \mathrm{diag}(a-c, b-c), & p^0 = \pm|\ell|e_3. \end{cases} \end{aligned}$$

Its Morse index is 2, 1, 0, if p^0 is $\pm|\ell|e_1$, $\pm|\ell|e_2$, and $\pm|\ell|e_3$, respectively.
□

According to the Morse lemma, the level sets of $E\big|_{\mathbf{S}^2_{|\ell|}}$ near $p^0 = \pm|\ell|e_1$ or $\pm|\ell|e_3$ are circles, whereas those near $p^0 = \pm|\ell|e_2$ are hyperbolas. In fact the $\frac{1}{2}\,b|\ell|^2$-level set of $E\big|_{\mathbf{S}^2_{|\ell|}}$ is

$$\begin{aligned} \tfrac{1}{2}\,(a\,p_1^2 + b\,p_2^2 + c\,p_3^2) &= \tfrac{1}{2}\,b \\ p_1^2 + p_2^2 + p_3^2 &= |\ell|^2. \end{aligned}$$

Multiplying the first equation above by $|\ell|^2$ and subtracting $\frac{1}{2}\,b$ times the second equation gives

$$\begin{aligned} 0 &= \tfrac{1}{2}\,(a-b)p_1^2 - \tfrac{1}{2}\,(b-c)p_2^2 \\ &= \tfrac{1}{2}\,(\sqrt{a-b}\,p_1 + \sqrt{b-c}\,p_2)(\sqrt{a-b}\,p_1 - \sqrt{b-c}\,p_2). \end{aligned}$$

This means that the $\frac{1}{2}\,b|\ell|^2$-level set of E on $\mathbf{S}^2_{|\ell|}$ is the intersection of $\mathbf{S}^2_{|\ell|}$ with two transverse 2-planes (which intersect along the p_3-axis). Thus the $\frac{1}{2}\,b|\ell|^2$-level set of $E\big|_{\mathbf{S}^2_{|\ell|}}$ is the union of two great circles. All other level sets are diffeomorphic to *two* circles, except for $\frac{1}{2}\,a|\ell|^2$ and $\frac{1}{2}\,c|\ell|^2$, which are two distinct points.

1.2.4 Quantitative behavior of solutions of Euler's equations

1.2.4.1 A crash course in Jacobi elliptic functions

In order to solve Euler's equations quantitatively, we need Jacobi elliptic functions. Consider the system

$$\begin{aligned} \dot{x} &= yz \\ \dot{y} &= -xz \\ \dot{z} &= -k^2xy, \end{aligned} \tag{1.2.16}$$

on $\mathbf{R}^3$, where the parameter k lies in $(0,1)$. Define the *Jacobi elliptic functions* sn, cn, and dn as the solution

$$t \to (x(t), y(t), z(t)) = (\mathrm{sn}(t;k), \mathrm{cn}(t;k), \mathrm{dn}(t;k)) \tag{1.2.17}$$

of (1.2.16) with initial condition $(0,1,1)$. The functions

$$x^2 + y^2 \quad \text{and} \quad k^2x^2 + z^2$$

are integrals of (1.2.16). Hence

$$\begin{aligned} \mathrm{sn}^2(t;k) + \mathrm{cn}^2(t;k) &= 1 \\ k^2\mathrm{sn}^2(t;k) + \mathrm{dn}^2(t;k) &= 1, \end{aligned}$$

which implies that for all $t \in \mathbf{R}$

$$|\mathrm{sn}(t;k)| \leq 1, \;\; |\mathrm{cn}(t;k)| \leq 1 \text{ and } k' = \sqrt{1-k^2} \leq \mathrm{dn}(t;k) \leq 1. \tag{1.2.18}$$

Since $x^2 + y^2 = 1$ and $k^2x^2 + z^2 = 1$, we may drop the equations for $\frac{dy}{dt}$ and $\frac{dz}{dt}$ from (1.2.16) and obtain

$$\frac{dx}{dt} = \sqrt{(1-x^2)(1-k^2x^2)}. \tag{1.2.19}$$

Since the right hand side of (1.2.19) is positive when $x \in (-1,1)$, we find that

$$x \mapsto t(x) = \int_0^x \frac{dx}{\sqrt{(1-x^2)(1-k^2x^2)}} \tag{1.2.20}$$

is a smooth inverse to the function

$$x : \mathbf{R} \to (-1,1) : t \mapsto x(t) = \mathrm{sn}(t;k).$$

Because $t(\pm 1) = \pm K(k) = \pm K$ is finite, the function x is continuous on $[-1,1]$. Thus $\mathrm{sn}(K;k) = 1$, which implies that $\mathrm{cn}(K;k) = 0$ and $\mathrm{dn}(K;k) = k'$. From the definition of $t(x)$ it follows that for $k = 0$ and 1 the Jacobi elliptic functions degenerate to trigonometric functions. Explicitly, for $k = 0$ we have

$$\mathrm{sn}(t;0) = \sin t, \;\; \mathrm{cn}(t;0) = \cos t, \;\text{ and } \mathrm{dn}(t;0) = 1;$$

while for $k = 1$ we have

$$\mathrm{sn}(t;1) = \tanh t, \;\; \mathrm{cn}(t;1) = \mathrm{sech}\, t, \;\text{ and } \mathrm{dn}(t;1) = \mathrm{sech}\, t.$$

We now show that sn, cn, and dn are periodic. Let

$$\xi(t) = \frac{\mathrm{cn}(t;k)}{\mathrm{dn}(t;k)}, \;\; \eta(t) = -k'\frac{\mathrm{sn}(t;k)}{\mathrm{dn}(t;k)}, \;\text{ and }\; \zeta(t) = k'\frac{1}{\mathrm{dn}(t;k)}.$$

Then $t \to (\xi(t), \eta(t), \zeta(t))$ is an integral curve of (1.2.16) with initial condition $(1, 0, k')$. But so is $t \to (\mathrm{sn}(t+K;k), \mathrm{cn}(t+K;k), \mathrm{dn}(t+K;k))$. Hence

$$\begin{aligned}\mathrm{sn}(t+K;k) &= \frac{\mathrm{cn}(t;k)}{\mathrm{dn}(t;k)}\\ \mathrm{cn}(t+K;k) &= -k'\frac{\mathrm{sn}(t;k)}{\mathrm{dn}(t;k)}\\ \mathrm{dn}(t+K;k) &= k'\frac{1}{\mathrm{dn}(t;k)}.\end{aligned}$$

This implies that $\mathrm{sn}(t;k)$ and $\mathrm{cn}(t;k)$ are periodic of period $4K(k)$, while $\mathrm{dn}(t;k)$ is periodic of period $2K(k)$.

1.2.4.2 Explicit solutions of Euler's equations

Using Jacobi elliptic functions we find explicit solutions of Euler's equations. There are two cases which correspond to the two types of stable relative equilibria, see figure 1.2.5. This is a bit messy.

CASE 1. $|\ell|^2 b \geq 2h \geq |\ell|^2 c$.

Solving

$$\begin{aligned} a\,p_1^2 + b\,p_2^2 + c\,p_3^2 &= 2h\\ p_1^2 + p_2^2 + p_3^2 &= |\ell|^2\end{aligned}$$

for p_1^2 and p_3^2 we obtain

$$\begin{aligned} p_1^2 &= \frac{1}{a-c}(2h - |\ell|^2 c - (b-c)p_2^2)\\ p_3^2 &= \frac{1}{a-c}(-2h + |\ell|^2 a - (a-b)p_2^2).\end{aligned} \tag{1.2.21}$$

Thus the equation $\dot{p}_2 = (a-c)\,p_1 p_3$ becomes

$$\frac{dp_2}{dt} = \sqrt{(2h - |\ell|^2 c - (b-c)p_2^2)(-2h + |\ell|^2 a - (a-b)p_2^2)}. \tag{1.2.22}$$

We now transform (1.2.22) into (1.2.19). Let

$$\begin{aligned}\tau &= t\,n, \quad \text{where } n = \sqrt{(b-c)(a|\ell|^2 - 2h)}\\ x &= p_2\sqrt{\frac{b-c}{2h - |\ell|^2 c}},\end{aligned}$$

and

$$k^2 = \frac{(a-b)(2h - |\ell|^2 c)}{(b-c)(|\ell|^2 a - 2h)}.$$

Then

$$\begin{aligned}\frac{d\tau}{dx} =& \frac{d\tau}{dt} \Big/ \left(\frac{dx}{dp_2} \frac{dp_2}{dt} \right) \\ =& \frac{\sqrt{(b-c)(|\ell|^2 a - 2h)}}{\sqrt{\frac{b-c}{2h-|\ell|^2 c}} \sqrt{2h - |\ell|^2 c - (b-c)p_2^2)(|\ell|^2 a - 2h - (a-b)p_2^2)}} \\ =& \frac{1}{\sqrt{(1-x^2)(1-k^2x^2)}}. \qquad (1.2.23)\end{aligned}$$

Consequently, $x(\tau) = \mathrm{sn}(\tau; k) = \mathrm{sn}(nt; k)$. From (1.2.23) and (1.2.21) we obtain

$$\begin{aligned} p_1(t) &= A\,\mathrm{cn}(nt; k) \\ p_2(t) &= B\,\mathrm{sn}(nt; k) \\ p_3(t) &= C\,\mathrm{dn}(nt; k), \end{aligned}$$

where

$$A^2 = \frac{2h - |\ell|^2 c}{a-c}, \quad B^2 = \frac{2h - |\ell|^2 c}{b-c}, \quad \text{and} \quad C^2 = \frac{|\ell|^2 a - 2h}{a-c}.$$

The signs of the square roots are chosen so that $t \mapsto (p_1(t), p_2(t), p_3(t))$ sweeps out a connected component of $E^{-1}(h) \cap L^{-1}(|\ell|^2)$.

Case 2. $|\ell|^2 a \geq 2h \geq |\ell|^2 b$.

A similar argument gives

$$\begin{aligned} p_1(t) &= A\,\mathrm{dn}(nt; k) \\ p_2(t) &= B\,\mathrm{sn}(nt; k) \\ p_3(t) &= C\,\mathrm{cn}(nt; k), \end{aligned}$$

where

$$n = \sqrt{(a-b)(2h - c|\ell|^2)}, \quad k^2 = \frac{(b-c)(a|\ell|^2 - 2h)}{(a-b)(2h - |\ell|^2 c)},$$

and

$$A^2 = \frac{2h - |\ell|^2 c}{a-c}, \quad B^2 = \frac{a|\ell|^2 - 2h}{a-b}, \quad C^2 = \frac{a|\ell|^2 - 2h}{a-c}.$$

EXERCISE: if two of the moments of inertia are equal you get the case of precession, which can be integrated with sines and cosines.

1.2.5 The Euler-Arnol'd equations

We know all the solutions of Euler's equations and seem to know everything, yet we still have to integrate $\dot{A}(t)$ to obtain the motion of the top in space.

To find the motion of the Euler top $\mathcal{B}$ in the *space frame*, assuming we know the solution $t \mapsto \Omega(t) = I^{-1}(p(t))$ of Euler's equations (1.2.12), we first convert the curve $\Omega : \mathbf{R} \to \mathbf{R}^3 : t \mapsto \Omega(t)$ of angular velocities into a curve $\xi : \mathbf{R} \to \mathrm{so}(3) : t \mapsto \xi(t)$ of infinitesimal motions. To do this we choose $\xi(t)$ so that $\xi(t) = \widehat{\Omega(t)}$. Since $\xi(t) = A(t)^{-1} \frac{dA}{dt}$ we have

$$\frac{dA}{dt} = A(t)\,\xi(t), \tag{1.2.24}$$

which is a system of linear differential equations with time dependent coefficients. Here $A : \mathbf{R} \to \mathrm{SO}(3) : t \mapsto A(t)$ is the curve we would like to find, as it describes the motion of the body in the space frame. Equations (1.2.24) and (1.2.16) are the *Euler-Arnol'd* equations of a rigid body with respect to the space frame. To find a particular solution of the Euler-Arnol'd equations of course initial conditions need to be imposed. Note that if $t \mapsto (\xi(t), A(t))$ is a solution of the Euler-Arnol'd equations and if A_0 is a fixed rotation, then $t \mapsto (\xi(t), A_0(A(t)))$ is also a solution of the Euler-Arnol'd equations.

Euler's equations (1.2.13) only describe the motion of the angular velocity vector $\Omega(t)$ (or the angular momentum vector $L(t) = I(\Omega(t))$) in a frame corotating with the body. Note that this corotating frame is *not* an inertial frame. With respect to the space frame the angular momentum vector ℓ is actually constant through out the motion of the body. The center of mass of the body is fixed at the origin. The body does not necessarily come back to the same position even if the motion of the angular momentum vector L in the body frame is periodic. If the angular momentum vector has returned after time t to the same position in the body frame, all one can conclude is that the body frame has rotated in space around the angular momentum vector ℓ. To describe the motion of $\mathcal{B}$ in space we have to determine how much the body frame has rotated about the angular momentum vector ℓ after time t. First we choose a better space frame, namely a frame $\widetilde{\mathcal{F}} = \{\widetilde{f}_1, \widetilde{f}_2, \widetilde{f}_3\}$ so that the angular momentum of the body lies along the positive $\widetilde{f}_3$-axis. Let A_0 be the matrix whose j^{th} column looks like e_j in the new space frame. Then the angular momentum vector looks like $\widetilde{\ell} = A_0\ell = |\ell|\widetilde{f}_3$ in the new space frame $\{\widetilde{f}_1, \widetilde{f}_2, \widetilde{f}_3\}$. Write $\widetilde{A}(t) = (A_0\, A)(t)$. The j^{th} column of $\widetilde{A}(t)$ describes the j^{th} member of the body frame in the new space frame.

Physicists are a tough bunch of people. They like the old stuff. They still think that Poinsot solves everything, even though Poincaré did not. Now you think that Cushman's going to fall on his nose — but he didn't!

1.2.5.1 Qualitative Poinsot description

Since

$$I^{-1}(L(t)) = \Omega(t) = (\widetilde{A}(t))^{-1}\omega(t),$$

in order to describe the motion of the body in space it suffices to know the angular velocity vector $\omega(t)$ in the new space frame. We now give a geometric interpretation, due to Poinsot [31], of the curve $t \mapsto -\omega(t)$, see figure 1.2.1.

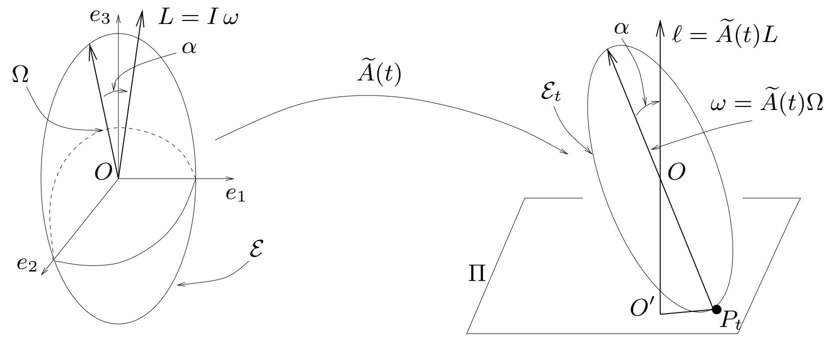

Fig. 1.2.1. Poinsot description of Euler top, the reference ellipsoid is on the left and the moving one is on the right.

I had a lot of trouble reading Goldstein [19] about all this, and usually this means that he is wrong *(at least in my experience). Your best reference remains Whittaker [42].*

Recall $\Omega(t)$ lies on the reference ellipsoid $\mathcal{E} = \{\Omega \in \mathbf{R}^3 \,\big|\, \langle I\Omega, \Omega\rangle = 2h\}$. Since $\omega(t) = \widetilde{A}(t)\Omega(t)$, the vector $\omega(t)$ lies on the ellipsoid $\mathcal{E}_t$ which is obtained by applying the rotation $\widetilde{A}(t)$ to the reference ellipsoid.

That is what rotating coordinates is all about guys!

We give more details. If $\widetilde{I}(t) = \widetilde{A}(t)\, I(\widetilde{A}(t))^{-1}$ denotes the matrix of the moment of inertia tensor with respect to the space frame $\{\widetilde{f}_1, \widetilde{f}_2, \widetilde{f}_3\}$, then $\mathcal{E}_t = \{\omega \in \mathbf{R}^3 \big| \langle \widetilde{I}(t)\omega, \omega\rangle = 2h\}$. We may think of $\mathcal{E}_t$ as an ellipsoid, which moves with respect to the space frame $\{\widetilde{f}_1, \widetilde{f}_2, \widetilde{f}_3\}$, with center of mass fixed at O. The inner product between the angular momentum vector $\widetilde{\ell} = \widetilde{I}(t)\omega(t)$ in the space frame and the angular velocity vector $\omega(t)$ in the space frame is $2h$ and $\widetilde{\ell}$ is constant. Hence $-\omega(t)$ lies on a fixed affine plane Π, which is perpendicular to $\widetilde{\ell}$ and consists of those vectors whose inner product with $-\widetilde{\ell}$ is $2h$. Let $-\omega(t)$ be the vector $\overrightarrow{OP_t}$. The point P_t lies on the plane Π as well as on the moving ellipsoid $\mathcal{E}_t$.

Fix $t = t_0$. Since the normal to $\mathcal{E}_t$ at P_t is

$$\mathrm{grad}_{-\omega}\langle I(t)\omega, \omega\rangle = -2\, I(t)\omega \;=\; -2\,\widetilde{\ell},$$

which is parallel to $\widetilde{\ell}$, the plane Π is tangent to $\mathcal{E}_t$ at P_t. Thus P_t is the point of contact of the ellipsoid $\mathcal{E}_t$ with Π. Consider the point P_0 on the reference ellipsoid whose image under $\widetilde{A}(t_0)$ is P_{t_0}. The velocity of the image of P_0 under $\widetilde{A}(t)$ with respect to the space frame at $t = t_0$ is

$$\omega \times \overrightarrow{OP_t} = \omega \times (-\omega) \;=\; 0.$$

This means that the moving ellipsoid $\mathcal{E}_t$ rolls without slipping on the plane Π. Its center of mass is fixed at O, which is a constant height $\frac{2h}{|\ell|}$ above Π. Thus $t \to -\omega(t)$ is the curve traced out on the invariant plane Π by the point of contact P_t of the rolling ellipsoid $\mathcal{E}_t$.

Many people – including Arnol'd – stop here without showing how to find the point of contact P_t. Thus Poinsot is not a quantitative solution as it should be. We have to find P_t and show what the body is doing.

1.2.5.2 Integration of the Euler-Arnol'd equations

Given a solution $t \mapsto \Omega(t)$ of Euler's equations, we now find a formula for the position $\widetilde{A}(t)$ of the body frame with respect to the space frame $\{\widetilde{f}_1, \widetilde{f}_2, \widetilde{f}_3\}$.

Now, what is the <u>most friendly</u> parametrization of the rotation group? Some people will say Euler angles — without even thinking. I use a different one, namely, two orthonormal vectors.

Write $x(t)$ for the first column of $\widetilde{A}(t)$ and $y(t)$ for the second. Then

$$\widetilde{A}(t) = (A_0\, A)(t) \;=\; \mathrm{col}(x(t), y(t), x(t) \times y(t)), \tag{1.2.25}$$

with

$$\langle x(t), x(t) \rangle = 1, \quad \langle y(t), y(t) \rangle \ = \ 1, \ \text{ and } \langle x(t), y(t) \rangle = 0. \qquad (1.2.26)$$

Note that $\dfrac{d\widetilde{A}}{dt} = \widetilde{A}(t)\xi(t)$, so equation (1.2.24) takes the form

$$\operatorname{col}\big(\dot{x}(t), \dot{y}(t), (x \overset{\cdot}{\times} y)(t)\big) = \operatorname{col}\big(x(t), y(t), (x \times y)(t)\big) \begin{pmatrix} 0 & -\Omega_3 & \Omega_2 \\ \Omega_3 & 0 & -\Omega_1 \\ -\Omega_2 & \Omega_1 & 0 \end{pmatrix}.$$

Because the third column in the above equation is redudant, we see that the Euler-Arnol'd equations (1.2.24) and (1.2.16) are equivalent to the following vector equations

$$\begin{aligned} \dot{x} \ &= \ \Omega_3\, y - \Omega_2(x \times y), && (1.2.27\text{a}) \\ \dot{y} \ &= \ -\Omega_3\, x + \Omega_1(x \times y), && (1.2.27\text{b}) \\ I(\dot{\Omega}) \ &= \ I(\Omega) \times \Omega. && (1.2.27\text{c}) \end{aligned}$$

subject to the constraints (which follow from (1.2.26))

$$\begin{aligned} x_1^2 + x_2^2 + x_3^2 \ &= \ 1, && (1.2.28\text{a}) \\ y_1^2 + y_2^2 + y_3^2 \ &= \ 1, && (1.2.28\text{b}) \\ x_1y_1 + x_2y_2 + x_3y_3 \ &= \ 0. && (1.2.28\text{c}) \end{aligned}$$

With no choice of chart of any kind we have reduced the motion of the Euler top in space to six equations (plus restrictions). These equations are Hamiltonian even though the symplectic form is a mess. This is in the blue book [5]. There is no other reference. Numerically these equations are incredibly stable near the unstable manifold where the motion of Euler's top is the most interesting.

Since we have chosen the body frame so that the matrix of the moment of inertia tensor I is $\operatorname{diag}(I_1, I_2, I_3)$ and since

$$\begin{aligned} I(\Omega) =& L = (\widetilde{A}(t))^{-1}\widetilde{\ell} = \widetilde{A}(t)^t\widetilde{\ell} = |\ell|\, \widetilde{A}(t)^t\, \widetilde{f}_3 \\ &= |\ell| \operatorname{row}(x(t), y(t), (x \times y)(t))\widetilde{f}_3, \qquad (1.2.29) \end{aligned}$$

we obtain

$$\begin{aligned} x_3 \ &= \ |\ell|^{-1} I_1\, \Omega_1 \ = \ M_1 && (1.2.30\text{a}) \\ y_3 \ &= \ |\ell|^{-1} I_2\, \Omega_2 \ = \ M_2 && (1.2.30\text{b}) \\ x_1y_2 - x_2y_1 \ &= \ |\ell|^{-1}\, I_3\Omega_3 \ = \ M_3. && (1.2.30\text{c}) \end{aligned}$$

Suppose that we know a solution $t \mapsto \Omega(t) = (\Omega_1(t), \Omega_2(t), \Omega_3(t))$ of Euler's equations (1.2.16) whose energy is h and whose angular momentum has magnitude $|\ell|$. The rotating frame $\{x, y, x \times y\}$ gives the position of the body with respect to the space frame $\{\widetilde{f}_1, \widetilde{f}_2, \widetilde{f}_3\}$. We want to find how much the $\widetilde{f}_1$-$\widetilde{f}_2$-component of the vector x has rotated about the $\widetilde{f}_3$-axis after time t. More precisely, we seek a differential equation for the angle θ that the projection of x on the $\widetilde{f}_1$-$\widetilde{f}_2$-plane makes with the $\widetilde{f}_1$-axis.

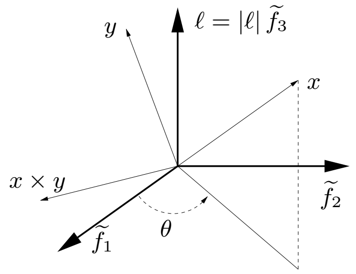

Fig. 1.2.2. Definition of the angle θ.

Because $\Omega = (\Omega_1, \Omega_2, \Omega_3)$ are assumed to be known functions of time, from (1.2.30a) and (1.2.30b) we see that x_3 and y_3 are also known. Eliminating x_3 and y_3 from (1.2.27a), (1.2.27b), (1.2.28a), (1.2.28b), (1.2.28c) and using (1.2.30a) and (1.2.30b) gives

$$\begin{aligned}
\frac{d}{dt}\begin{pmatrix} x_1 \\ x_2 \end{pmatrix} &= |\ell| I_3^{-1} M_3 \begin{pmatrix} y_1 \\ y_2 \end{pmatrix} - |\ell| I_2^{-1} M_2 \begin{pmatrix} -M_1\,y_2 + M_2\,x_2 \\ M_1\,y_1 - M_2\,x_1 \end{pmatrix} \\
\frac{d}{dt}\begin{pmatrix} y_1 \\ y_2 \end{pmatrix} &= -|\ell| I_3^{-1} M_3 \begin{pmatrix} x_1 \\ x_2 \end{pmatrix} + |\ell| I_1^{-1} M_1 \begin{pmatrix} -M_1\,y_2 + M_2\,x_2 \\ M_1\,y_1 - M_2\,x_1 \end{pmatrix}
\end{aligned}$$

$$\begin{aligned}
x_1^2 + x_2^2 &= 1 - |\ell|^{-2} I_1^2\,\Omega_1^2 \;=\; 1 - M_1^2 && (1.2.31a) \\
y_1^2 + y_2^2 &= 1 - |\ell|^{-2} I_2^2\,\Omega_2^2 \;=\; 1 - M_2^2 && (1.2.31b) \\
x_1 y_1 + x_2 y_2 &= -|\ell|^{-2} I_1 I_2\,\Omega_1 \Omega_2 \;= -M_1 M_2. && (1.2.31c)
\end{aligned}$$

Suppose that $\Omega \neq \left(\pm\frac{|\ell|}{I_1}, 0, 0\right)$. This is equivalent to assuming that the solution $t \to \Omega(t)$ of Euler's equations of energy h and magnitude of the angular momentum $|\ell|$ does not correspond to either one of the equilibrium points $\pm\frac{1}{I_1}e_1$. Consequently, the right hand side of (1.2.31a) is never zero. Writing (1.2.31c) and (1.2.30c) as

$$\begin{pmatrix} x_1 & x_2 \\ -x_2 & x_1 \end{pmatrix} \begin{pmatrix} y_1 \\ y_2 \end{pmatrix} = \begin{pmatrix} -M_1 M_2 \\ M_3 \end{pmatrix}$$

We may solve this equation for y_1 and y_2 obtaining

$$y_1 = \frac{-1}{1-M_1^2}\Big(M_1M_2\,x_1 + M_3\,x_2\Big) \tag{1.2.32a}$$

$$y_2 = \frac{1}{1-M_1^2}\Big(M_3\,x_1 - M_1M_2\,x_2\Big). \tag{1.2.32b}$$

In studying the Hopf fibration in the 2-dimensional harmonic oscillator (section 1.1.3), we have had to solve similar linear *equations.*

We now obtain the world's simplest differential equation (linear with time dependent coefficients)! Substituting (1.2.32a) and (1.2.32b) into the second equation above (1.2.31a) gives

$$\begin{aligned}\frac{dx_1}{dt} &= \alpha\,x_1 - \beta\,x_2\\ \frac{dx_2}{dt} &= \beta\,x_1 + \alpha\,x_2,\end{aligned} \tag{1.2.33}$$

where

$$\begin{aligned}\alpha &= |\ell|(I_2^{-1} - I_3^{-1})\,\frac{M_1M_2M_3}{1-M_1^2} = I_1(I_3-I_2)\,\frac{\Omega_1(t)\Omega_2(t)\Omega_3(t)}{|\ell|^2 - I_1^2\Omega_1^2(t)}\\ \beta &= |\ell|\,\frac{I_2^{-1}M_2^2 + I_3^{-1}M_3^2}{1-M_1^2} = |\ell|\,\frac{I_2\Omega_2^2(t) + I_3\Omega_3^2(t)}{|\ell|^2 - I_1^2\Omega_1^2(t)}.\end{aligned} \tag{1.2.34}$$

It cannot be that ridiculously simple — but it is. After all we are on a circle.

The angle θ that the projection of the vector x on the $\widetilde{f}_1$-$\widetilde{f}_2$ plane makes with the $\widetilde{f}_1$ axis is $\tan^{-1}(x_2/x_1)$. Therefore, using (1.2.33),

$$\dot{\theta} = \frac{x_1\dot{x}_2 - x_2\dot{x}_1}{x_1^2 + x_2^2} = \beta. \tag{1.2.35}$$

Oops, polar coordinates are trying to stick their ugly puss in here — but θ is an angle parametrizing a circle, so we are OK.

Integrating (1.2.35) gives

$$\theta(t) = \theta(0) + |\ell|\int_0^t \frac{I_2\,\Omega_2^2(s) + I_3\,\Omega_3^2(s)}{|\ell|^2 - I_1^2\,\Omega_1^2(s)}\,ds. \tag{1.2.36}$$

I am not a master of Weierstrass' theory of elliptic functions, so I won't do this integral. But Whittaker [42] is and he does it. See also [1].

θ is the rotation angle (a physical parameter) of the flow of the Euler-Arnol'd equations on a connected component of $E^{-1}(h)\cap L^{-1}(\ell)$, which is a 2-dimensional torus.

Montgomery [28] has found the rotation angle by hard *work.*

Knowing $t \mapsto \theta(t)$ and the $t \mapsto \Omega_i(t)$ we will now find the curve of rotations

$$t \mapsto \widetilde{A}(t) = \mathrm{col}(x(t), y(t), (x \times y)(t)),$$

which determines the position of the body with respect to the space frame $\{\widetilde{f}_1, \widetilde{f}_2, \widetilde{f}_3\}$. From the definition of θ and (1.2.31a) we find that

$$\begin{aligned} x_1(t) &= \sqrt{x_1^2 + x_2^2}\,\cos\theta = \sqrt{1 - M_1^2}\,\cos\theta && (1.2.37a)\\ x_2(t) &= \sqrt{1 - M_1^2}\,\sin\theta && (1.2.37b)\\ x_3(t) &= M_1, \quad \text{using (1.2.30a).} \end{aligned}$$

Substituting (1.2.37a) and (1.2.37b) into (1.2.32a) and (1.2.32b) gives

$$\begin{aligned} y_1(t) &= \frac{-1}{\sqrt{1 - M_1^2}}\Big[M_1 M_2\,\cos\theta + M_3 \sin\theta\Big] && (1.2.38a)\\ y_2(t) &= \frac{1}{\sqrt{1 - M_1^2}}\Big[M_3 \cos\theta - M_1 M_2\,\sin\theta\Big] && (1.2.38b)\\ y_3(t) &= M_2, \quad \text{using (1.2.30b).} && (1.2.38c) \end{aligned}$$

Therefore

$$\begin{aligned} (x \times y)_1(t) &= \frac{-1}{\sqrt{1 - M_1^2}}\Big[M_1 M_3\,\cos\theta - M_2 \sin\theta\Big]\\ (x \times y)_2(t) &= \frac{-1}{\sqrt{1 - M_1^2}}\Big[M_2 \cos\theta + M_1 M_3\,\sin\theta\Big]\\ (x \times y)_3(t) &= M_3, \quad \text{using (1.2.30c).} \end{aligned}$$

Thus we have found the curve $t \to \widetilde{A}(t)$ of motion of the body in space under the assumption that we know $t \to \Omega(t)$ and $t \to \theta(t)$.

So this is the solution of the Euler-Arnol'd equations – complete, straightforward, explicit, except for one quadrature. You can grumble, but not very much.

1.2.5.3 Quantitative Poinsot description

Using the curve $t \mapsto \widetilde{A}(t)$, which describes the motion of the body in space, we give an explicit parametrization of the curve $t \mapsto -\omega(t)$ traced out by the point of contact of the rolling moment of inertia ellipsoid on the invariant plane Π. This makes Poinsot's description of the motion of the Euler top in space *quantitative*.

We now find the instantaneous angular velocity $\omega(t)$ of the body $\mathcal{B}$

at time t with respect to the new space frame. By definition $\omega(t) = \widetilde{A}(t)\,\Omega(t)$. We compute the components of $\omega(t)$ as follows. From the construction of $\widetilde{A}(t)$ we have

$$\begin{aligned}
\omega_1(t) &= x_1\,\Omega_1 + y_1\,\Omega_2 + (x\times y)_1\Omega_3 \\
&= \frac{1}{\sqrt{1-M_1^2}}\Big\{\Big[\Omega_1 - M_1(M_1\Omega_1 + M_2\Omega_2 + M_3\Omega_3)\Big]\cos\theta + \\
&\qquad\qquad + \Big[\Omega_3 M_2 - \Omega_2 M_3\Big]\sin\theta\Big\} \\
&= \frac{1}{\sqrt{1-M_1^2}}\Big\{\Big[\Omega_1 - 2|\ell|^{-1}h\,M_1\Big]\cos\theta - \Big[\Omega_2 M_3 - \Omega_3 M_2\Big]\sin\theta\Big\}.
\end{aligned}$$

A similar argument gives

$$\omega_2(t) = \frac{1}{\sqrt{1-M_1^2}}\Big\{\Big[\Omega_2 M_3 - \Omega_3 M_2\Big]\cos\theta + \Big[\Omega_1 - 2|\ell|^{-1}h\,M_1\Big]\sin\theta\Big\}.$$

Also

$$\omega_3(t) = M_1\Omega_1 + M_2\Omega_2 + M_3\Omega_3 \;=\; 2|\ell|^{-1}h.$$

Note that this confirms that the inner product of the angular velocity vector with the angular momentum vector $|\ell|\widetilde{f}_3$ is constant. The above results may be written in matrix form as

$$\begin{aligned}
\begin{pmatrix}\omega_1\\ \omega_2\\ \omega_3\end{pmatrix} &= \begin{pmatrix}\Omega_1 - 2|\ell|^{-1}h\,M_1 & -(\Omega_2 M_3 - \Omega_3 M_2) & 0\\ \Omega_2 M_3 - \Omega_3 M_2 & \Omega_1 - 2|\ell|^{-1}h\,M_1 & 0\\ 0 & 0 & 1\end{pmatrix}\begin{pmatrix}\frac{\cos\theta}{\sqrt{1-M_1^2}}\\ \frac{\sin\theta}{\sqrt{1-M_1^2}}\\ 2|\ell|^{-1}h\end{pmatrix} \\
&= \begin{pmatrix}\cos u & -\sin u & 0\\ \sin u & \cos u & 0\\ 0 & 0 & 1\end{pmatrix}\begin{pmatrix}R\cos\theta\\ R\sin\theta\\ 2|\ell|^{-1}h\end{pmatrix},
\end{aligned}$$

where

$$\tan u(t) = \frac{\Omega_2 M_3 - \Omega_3 M_2}{\Omega_1 - 2|\ell|^{-1}h\,M_1} \;=\; \frac{|\ell|(I_3 - I_2)\Omega_2(t)\Omega_3(t)}{(|\ell|^2 - 2I_1 h)\Omega_1(t)} \qquad (1.2.39a)$$

and

$$\begin{aligned}
R(t) &= \sqrt{\frac{(\Omega_1 - 2|\ell|^{-1}h\,M_1)^2 + (\Omega_2 M_3 - \Omega_3 M_2)^2}{1-M_1^2}} \\
&= \frac{1}{|\ell|}\sqrt{\frac{(|\ell|^2 - 2I_1 h)^2\,\Omega_1^2(t) + |\ell|^2(I_3 - I_2)\,\Omega_2^2(t)\Omega_3^2(t)}{|\ell|^2 - I_1^2\Omega_1^2(t)}}.
\end{aligned} \qquad (1.2.39b)$$

Therefore we obtain

$$t \to \omega(t) = \begin{pmatrix} R(t)\cos(\theta(t)+u(t)) \\ R(t)\sin(\theta(t)+u(t)) \\ 2|\ell|^{-1}h \end{pmatrix}. \tag{1.2.40}$$

Remember that $u(t)$ is obtained from our solution to the Euler's equations. For the curve Γ traced out on the invariant plane Π by the point of contact P_t of the rolling ellipsoid $\mathcal{E}_t$ we get

$$t \to -\omega(t) = \begin{pmatrix} R(t)\cos(\theta(t)+u(t)+\pi) \\ R(t)\sin(\theta(t)+u(t)+\pi) \\ -2|\ell|^{-1}h \end{pmatrix}. \tag{1.2.41}$$

So we have parameterized Γ at no additional cost. Γ lies in an annulus

$$\mathcal{A} = \{(\varphi, R) \in \Pi \,\big|\, 0 < R_{\min} \le R(t) \le R_{\max}\}$$

and is alternately tangent to a different component of the boundary of $\mathcal{A}$. The rotation angle θ of the flow of the Euler-Arnol'd equations on a connected component of $E^{-1}(h) \cap L^{-1}(\ell)$ is the angle between every *second* (and not every) point of tangency on the same boundary component, if $a\ell^2 > 2h > b\ell^2$ and this angle *plus* 2π, if $c\ell^2 < 2h < b\ell^2$. For more details see [1] and [5].

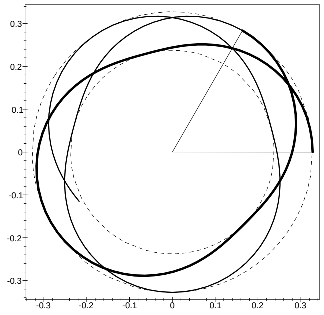

Fig. 1.2.3. The rotation angle of the flow of the Euler-Arnol'd equations on a 2-torus in $E^{-1}(h) \cap L^{-1}(\ell)$ as determined by the Poinsot description. The moments of inertia in this example are $I_1 = 1$, $I_2 = 2$, and $I_3 = 2.9$; $|\ell|$ is set equal to 1, initial point $(x, y) = \left(\frac{1}{\sqrt{2}}, 0, \frac{1}{\sqrt{2}}, 0, 1, 0\right)$, the initial point for Euler's equations is $(\Omega_1, \Omega_2, \Omega_3) = \left(\frac{1}{\sqrt{2}}, 0, \frac{1}{2.9\sqrt{2}}\right)$ with Euler energy $h = .344$, the Euler period is 17, and rotation number equals 1.1666.

1.2.6 Abstract derivation of equations of motion

In this section we give a Hamiltonian derivation of the Euler–Arnol'd equations.

1.2.6.1 Geodesic equations on a Lie group

Let G be a Lie group with the algebra $\mathfrak{g}$. On phase space T^*G with its canonical symplectic form $\widetilde{\omega}$ suppose that we have a hamiltonian $\widetilde{\mathcal{H}} : T^*G \to \mathbf{R}$. Consider the map *left translation* by $g \in G$, namely,

$$L_g : G \to G : h \to g \cdot h.$$

We have the *left trivialization*

$$\widetilde{\lambda} : G \times \mathfrak{g}^* \to T^*G : (g, \alpha) \mapsto (T_g L_{g^{-1}})^t \alpha = \alpha_g.$$

Warning. This trivialization does *not* give coordinates, because for $\xi \in \mathfrak{g}$ the coordinate vector fields $X^{\xi}(g) = \left.\frac{d}{dt}\right|_{t=0} L_{\exp t\xi}(g)$ on G, which are dual to the 1-forms α^{ξ}, do *not* commute.

1.2.6.2 Hamilton's equations on a Lie group

On $G \times \mathfrak{g}^*$ we have the 2-form $\widetilde{\Omega}$, which is the pull back by $\widetilde{\lambda}$ of the canonical 2-form $\widetilde{\omega}$. Thus

$$\widetilde{\Omega}(g, \alpha)\big((T_e L_g \xi, \beta), (T_e L_g \eta, \gamma)\big) = -\beta(\eta) + \gamma(\xi) + \alpha([\xi, \eta]),$$

where $\xi, \eta \in \mathfrak{g}$ and $\alpha, \beta, \gamma \in \mathfrak{g}^*$, see [5]appendix A. Pulling $\widetilde{\mathcal{H}}$ back by $\widetilde{\lambda}$ gives the Hamiltonian

$$\widetilde{H} = \widetilde{\lambda}^* \widetilde{\mathcal{H}} : G \times \mathfrak{g}^* \to \mathbf{R} : (g, \alpha) \mapsto \widetilde{H}(g, \alpha).$$

By definition, the hamiltonian vector field $X_{\widetilde{H}}$ satisfies $X_{\widetilde{H}} \,\lrcorner\, \widetilde{\Omega} = \mathrm{d}\widetilde{H}$. The integral curves of $X_{\widetilde{H}}$ are the solutions of the Euler-Arnol'd equations

$$\begin{aligned} \dot{g} &= T_e L_g D_2 \widetilde{H}(g, \alpha) \\ \dot{\alpha} &= -(T_e L_g)^t D_1 \widetilde{H}(g, \alpha) + \mathrm{ad}^t_{D_2 \widetilde{H}} \alpha \end{aligned} \tag{1.2.42}$$

These are *Hamilton's equations* on the Lie group G.

Suppose that $\mathcal{H}$ is *left invariant*, that is, $\widetilde{\mathcal{H}}(\alpha_{gh}) = \widetilde{\mathcal{H}}(\alpha_h)$, Then

$$\widetilde{H}(g \cdot h, \alpha) = \widetilde{H}(h, \alpha).$$

Since $D_1\widetilde{H} = 0$, the Euler–Arnol'd equations become

$$\begin{aligned} \dot{g} &= T_eL_gD_2\widetilde{H}(g,\alpha) \\ \dot{\alpha} &= \mathrm{ad}^t_{D_2\widetilde{H}}\alpha. \end{aligned} \tag{1.2.43}$$

1.2.6.3 Special case

Let $\mathcal{H}^*(\alpha_g) = \frac{1}{2}\,k^*(g)(\alpha_g,\alpha_g)$ be a hamiltonian on T^*G, where k^* is a left invariant dual metric on G. In other words,

$$k(g)(v_g,w_g) = k^*(g)\big(k^*(g)^\flat(v_g), k^*(g)^\flat(w_g)\big)$$

is a left invariant metric on G. The hamiltonian $\mathcal{H}^*$ is purely kinetic. We now show that the solutions of the Euler-Arnol'd equations (1.2.43) for $\mathcal{H}^*$ give the geodesic flow on the Lie group G.

Pull back the Hamiltonian system $(\mathcal{H}^*, T^*G, \widetilde{\omega})$ by the map $k^\sharp : TG \to T^*G$. The resulting Hamiltonian on $(TG, \omega = k^\flat\widetilde{\omega})$ is

$$\mathcal{H}(v_g) = \tfrac{1}{2}\,k(g)(v_g,v_g)$$

. Pulling the symplectic form ω back by the left trivialization of TG

$$\lambda : G\times\mathfrak{g} \to TG : (g,v) \mapsto v_g = T_eL_gv$$

gives a 2-form Ω on $G\times\mathfrak{g}$ on TG. Explicitly,

$$\Omega(g,v)((T_eL_g\xi,v),(T_eL_g\eta,w)) = -\mathrm{k}(v,\eta) + \mathrm{k}(w,\xi) + \mathrm{k}(v,[\xi,\eta]), \tag{1.2.44}$$

where $\mathrm{k} = \lambda^*k(e)$. The Hamiltonian $\mathcal{H}$ becomes

$$H = \lambda^*\mathcal{H} : G\times\mathfrak{g} \to \mathbf{R} : (g,v) \to \tfrac{1}{2}\,\mathrm{k}(v,v),$$

which is a left invariant metric on $G\times\mathfrak{g}$. By definition the hamiltonian vector field $X_H(g,v) = (T_eL_gX_1, X_2)$ satisfies

$$X_H \;\lrcorner\; \Omega = \mathrm{d}H. \tag{1.2.45}$$

We compute X_H as follows. From (1.2.45) and (1.2.44) we obtain

$$\begin{aligned} -\mathrm{k}(X_2,\eta)+\mathrm{k}(X_1,w) + \mathrm{k}(v,[X_1,\eta]) &= \Omega(g,v)((T_eL_gX_1,X_2),(T_eL_g\eta,w)) \\ &= \mathrm{d}H(g,v)(T_eL_g\eta,w) = D_1H(g,v)T_eL_g\eta + D_2H(g,v)w \\ &= \mathrm{k}(v,w), \end{aligned} \tag{1.2.46}$$

for every $(w,\eta) \in \mathfrak{g}$. In (1.2.46) set $\eta = 0$. Then $\mathrm{k}(X_1,w) = \mathrm{k}(v,w)$ for every $w \in \mathfrak{g}$. Since k is nondegenerate, we have $X_1 = v$. In (1.2.46) set $w = 0$. Then

$$\mathrm{k}(X_2,\eta) = \mathrm{k}(v,[v,\eta]) = \mathrm{k}(B(v),\eta),$$

for every $\eta \in g$. This implies $X_2 = B(v)$. Consequently, the Euler-Arnol'd equations are

$$\begin{aligned} \dot{g} &= T_e L_g v \\ \dot{v} &= B(v). \end{aligned} \tag{1.2.47}$$

These are equations for geodesics on G of the left invariant metric k.

1.2.6.4 An even more special case

Now we restrict ourselves to the case when G is semisimple. Then $\mathfrak{g}$ has an Ad-invariant nondegenerate inner product k called the Killing metric.

Using a k-symmetric invertible linear mapping $I : \mathfrak{g} \to \mathfrak{g}$, called the *generalized moment of inertia tensor*, we can write every metric k on $\mathfrak{g}$ as

$$k(v, w) = \mathrm{k}(I(v), w).$$

Thus for every $\eta \in g$

$$k(I(B(v)), \eta) = \mathrm{k}(B(v), \eta) = \mathrm{k}(v, [v, \eta]) = \mathrm{k}(I(v), [v, \eta]) = k([I(v), v], \eta),$$

since k is Ad-invariant. Consequently, $B(v) = I^{-1}([I(v), v])$. Hence the Euler-Arnol'd equations for geodesics of a left invariant metric on a semisimple Lie group are

$$\begin{aligned} \dot{g} &= T_e L_g v \\ \dot{v} &= I^{-1}[I(v), v]. \end{aligned} \tag{1.2.48}$$

Now suppose that $G = \mathrm{SO}(3)$ and $\mathfrak{g} = \mathrm{so}(3) \simeq (\mathbf{R}^3, \times)$. In addition, suppose that k is the Euclidean inner product on $\mathbf{R}^3$ and that the moment of inertia tensor I is $\mathrm{diag}(I_1, I_2, I_3)$. Then the solutions of the Euler-Arnol'd equations (1.2.48) give integral curves of a vector field V on $\mathrm{SO}(3) \times \mathbf{R}^3$ which satisfy

$$\begin{aligned} \dot{A} &= A\widehat{\Omega} \\ I(\dot{\Omega}) &= I(\Omega) \times \Omega, \end{aligned} \tag{1.2.49}$$

The above equations are the Euler-Arnol'd equations for the Euler top. They are *geodesic equations* and are Hamiltonian even though they do not look like it.

1.2.6.5 Integrals and reduction

The vector field V on $\mathrm{SO}(3) \times \mathbf{R}^3$ has two integrals:

Energy. $E(A, \Omega) = \frac{1}{2} \langle I(\Omega), \Omega \rangle$.

Check.

$$\dot{E} = \langle I(\dot{\Omega}), \Omega \rangle \ = \ \langle I(\Omega) \times \Omega, \Omega \rangle \ = \ 0.$$

and

Angular momentum. $L(A, \Omega) = AI\Omega$.

Check.

$$\begin{aligned} \dot{L} &= \dot{A}I(\Omega) + AI(\dot{\Omega}) = A\big(\widehat{\Omega}(I(\Omega))\big) + A(I(\Omega) \times \Omega) \\ &= A(\Omega \times I(\Omega) + I(\Omega) \times \Omega) = 0. \quad \square \end{aligned}$$

Angular momentum L comes from the lift of the action of left translation of SO(3) on itself to $T\,\mathrm{SO}(3)$. This action is Hamiltonian and commutes with the Hamiltonian H, which is a left invariant metric on SO(3). We have arranged that on $\mathrm{SO}(3) \times \mathbf{R}^3$ we have $L(A, \Omega) = \ell = |\ell|\, e_3$. Thus L is constant on the integral curves of V. Consequently,

$$L^{-1}(\ell) = \{(A, I^{-1}A^{-1}\ell) \in \mathrm{SO}(3) \times \mathbf{R}^3 \,\big|\, A \in \mathrm{SO}(3)\}$$

is an invariant manifold of the vector field V, which is diffeomorphic to SO(3).

Solid ball model of SO(3)**.** Consider an open ball $\mathbf{B}^3_\pi \subseteq \mathbf{R}^3$, whose closure has boundary which is a 2-sphere $\mathbf{S}^2_\pi$ of radius π (see fig. 1.2.4). Every point in $\mathbf{B}^3_\pi$ is a vector ℓ of length less than π and defines a unique rotation about axis ℓ by angle $|\ell| < \pi$. The vectors $\pm\ell$ define rotation about $\pm\ell$ by angle $\pm|\ell|$. We should be more careful with the points on $\mathbf{S}^2_\pi$ where $|\ell| = \pi$. In this case, $\pm\ell$ define the *same* rotation. Therefore, we should identify diametrically opposite points of $\mathbf{S}^2_\pi$, so that it becomes real projective 2-space $\mathbf{RP}^2$. To obtain all of SO(3) we add $\mathbf{B}^3_\pi$ and obtain real projective 3-space $\mathbf{RP}^3$.[1] We obtain the same picture of

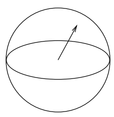

Fig. 1.2.4. Solid ball model of SO(3).

SO(3) ([5], p. 95) when we define the covering map $\mathbf{S}^3 \to \mathrm{SO}(3) \simeq \mathbf{RP}^3$.

[1] We have already seen that $\mathrm{so}(3) \simeq \mathbf{R}^3$. Correspondingly, SO(3) is locally an $\mathbf{R}^3$. Globally it is an $\mathbf{RP}^3$.

The 3-sphere $\mathbf{S}^3$ of unit radius is the space of all quaternions[2] q of unit length, $q\bar{q} = 1$. There is a one to one correspondence between these q s and the matrices

$$\begin{pmatrix} \alpha & \beta \\ -\overline{\beta} & \overline{\alpha} \end{pmatrix} \in \mathrm{SU}(2), \quad \alpha, \beta \in \mathbf{C}, \quad |\alpha|^2 + |\beta|^2 = 1,$$

which in turn correspond to rotations.[1] The exact correspondence is given by the two to one covering map $\rho : \mathrm{SU}(2) \to \mathrm{SO}(3); q \mapsto R_q$, where R_q is a real linear map

$$R_q : \mathbf{R}^3 \subseteq \mathbf{H} \to \mathbf{R}^3 \subseteq \mathbf{H} : x \to q \cdot x \cdot \bar{q},$$

and $x = x_1 i + x_2 j + x_3 k \in \mathbf{R}^3 \subseteq \mathbf{H}$. It can be shown that R_q is a rotation of $\mathbf{R}^3$ with its standard Euclidean inner product. It it is easy to see that q and $-q$ correspond to the same rotation R_q. Thus $\ker \rho = \mathbf{Z}_2$. Geometrically, this means that if we identify antipodal points q and $-q$ on the 3-sphere $\mathbf{S}^3 \subseteq \mathbf{R}^4$ we obtain real projective 3-space $\mathbf{RP}^3$. (This is similar to identifiying antipodal points on $\mathbf{S}^2$, which produces $\mathbf{RP}^2$.) After identifying antipodal points, the covering map ρ is a diffeomorphism. Hence SO(3) is $\mathbf{RP}^3$.

1.2.6.6 Reduction

Reduction on the ℓ level set of L. Consider the isotropy group

$$\mathrm{SO}(3)_\ell = \{B \in \mathrm{SO}(3) \big| B\ell = \ell\} \simeq S^1$$

of the action

$$\mathrm{SO}(3) \times (\mathrm{SO}(3) \times \mathrm{so}(3)) \to \mathrm{SO}(3) \times \mathrm{so}(3) : (B, (A, \widehat{\Omega}) \to (BA, B\widehat{\Omega}B^{-1}),$$

which comes from the lift of the action of inverse of *right* multiplication by SO(3) on itself to the left trivialization of the tangent bundle $T\,\mathrm{SO}(3)$ of SO(3). We have an action of $\mathrm{SO}(3)_\ell$ on $L^{-1}(\ell)$ defined by

$$\Phi : \mathrm{SO}(3)_\ell \times L^{-1}(\ell) \to L^{-1}(\ell) : (B, (A, \Omega)) \mapsto (BA, \Omega),$$

Check.

$$L(BA, \Omega) = B(AI\Omega) = BL(A, \Omega) = B\ell = \ell.$$

We now show that Φ is a proper free action with the orbit space $\mathbf{S}^2_{|\ell|}$.

[2] Recall that quaternions $\mathbf{H}$ are real linear combinations of $(1, i, j, k)$, where $i^2 = j^2 = k^2 = -1$ and $ij = k$ together with its cyclic permutations.

[1] Recall that $\mathrm{SU}(2) \to \mathrm{SO}(3)$ is a two to one homomorphism of groups. The variables α and β are known as Caley–Klein parameters for SU(2).

Proof. If $(A, \Omega) \in L^{-1}(\ell)$ and $B \in \mathrm{SO}(3)_\ell$ then $\Phi_B(A, \Omega) = (A, \Omega)$ implies that $BA = A$. Thus $B = e$, the identity element of SO(3). Hence the action Φ is free. Furthermore, since $\mathrm{SO}(3)_\ell$ is compact, Φ is a proper action. Consequently, the orbit space $L^{-1}(\ell)/\,\mathrm{SO}(3)_\ell$ is a smooth manifold.

Reduction map. Recall that $\ell = |\ell| e_3$. The reduction map removing the $\mathrm{SO}(3)_\ell$ symmetry on $L^{-1}(\ell)$ is

$$\pi_\ell : L^{-1}(\ell) \to \mathbf{S}^2_{|\ell|} : (A, I^{-1}A^{-1}\ell) \mapsto z = A^{-1}\ell = |\ell|\, A^{-1}e_3.$$

Check. If $\pi_\ell(A, \Omega) = \pi_\ell(A', \Omega')$, then $A^{-1}\ell = (A')^{-1}\ell$ implies $A'A^{-1} = B \in \mathrm{SO}(3)_\ell$. Thus

$$\begin{aligned} (A', \Omega') &= \big(A', I^{-1}(A')^{-1}\ell\big) = \big(BA, I^{-1}(A^{-1}B^{-1}\ell)\big) \\ &= (BA, I^{-1}A^{-1}\ell) = \Phi_B(A, \Omega). \end{aligned}$$

Therefore, π_ℓ^{-1} is a *unique* Φ-orbit in $L^{-1}(\ell)$ and the orbit space $L^{-1}(\ell)/\mathrm{SO}(3)_\ell$ is $\mathbf{S}^2_{|\ell|}$. □

Precomposing the reduction map π_ℓ with the two to one covering map $\mathbf{S}^3 \to \mathrm{SO}(3)$ gives the Hopf fibration. In other words, the double covering of the reduction map π_ℓ is the Hopf fibration.

Note that $\mathrm{SO}(3) \simeq \mathbf{RP}^3$ is not simply connected. Consequently, linking numbers *cannot* be defined for two closed curves in SO(3). That is why we need S^3. The double cover of the integral curves of the Euler top on a level set of angular momentum lie in S^3 and have linking number 1.

Reduced equations on $\mathbf{S}^2$. From $\ell = AI(\Omega)$ and $z = A^{-1}\ell$ it follows that $z = I(\Omega)$. Thus the reduced equations of motion are Euler's equations on $\mathbf{S}^2_{|\ell|}$, namely,

$$\dot{z} = I(\dot{\Omega}) = I(\Omega) \times \Omega = z \times I^{-1}(z).$$

Euler's equations are Hamilton's equations with respect to the symplectic form

$$\omega_{|\ell|}(z)(u, v) = \frac{1}{2|\ell|^2}\langle z, u \times v\rangle$$

and correspond to the reduced Hamiltonian

$$H_{|\ell|}(z) = \tfrac{1}{2}\,\langle I^{-1}(z), z\rangle.$$

$H_{|\ell|}$ is a Morse function on $\mathbf{S}^2_{|\ell|}$. $H_{|\ell|}$ is a *Morse function* with 6 nondegenerate critical points: 2 of index 0, 2 of index 1, and 2 of index 2 which are maxima, hyperbolic, and minima, respectively (see figure 1.2.5).[1] For each regular value $|\ell|$ the level set of $H_{|\ell|}$ on $\mathbf{S}^2_{|\ell|}$ consists of two equivalent disconnected circles. The nontrivial level set where $H_{|\ell|} = h_s = \frac{1}{2}\, b|\ell|^2$ is a heteroclinic connection and consists of two unstable relative equilibria connected by two great circles – their stable and unstable manifolds.

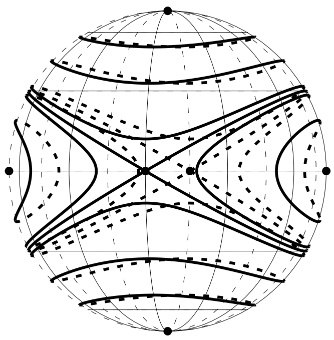

Fig. 1.2.5. Trajectories of the reduced Euler top on $\mathbf{S}^2_{|\ell|}$.

Qualitative reconstruction. We now reconstruct the geometry of the level sets of the reduced Hamiltonian $H_{|\ell|}$ on $\mathbf{S}^2_{|\ell|}$. This will describe how the level sets of the energy foliate a level set of angular momentum. Because the reduced Hamiltonian $H_{|\ell|}$ is a Morse function on $\mathbf{S}^2_{|\ell|}$ and because the Hamiltonian

$$H\big|_{L^{-1}(\ell)} : L^{-1}(\ell) \to \mathbf{R}$$

is $\mathrm{SO}(3)_\ell$ invariant, it follows that $H\big|_{L^{-1}(\ell)}$ is a *Bott-Morse function* on SO(3) with 6 nondegenerate critical circles: two of index 0, two of index 1 and two of index 2. Each critical point of $H_{|\ell|}$ lifts under the reduction map π_ℓ to a critical circle of $H\big|_{L^{-1}(\ell)}$ on $L^{-1}(\ell)$. A regular level set of $H_{|\ell|}$ lifts to two smooth 2-tori $\mathbf{T}^2$. The singular level set of $H^{-1}_{|\ell|}(h_s)$ corresponding to the hyperbolic critical points and their heteroclinic stable and unstable manifolds lifts to two 2-tori which intersect cleanly along two circles.

[1] Each pair of critical points with the same index lie on the same orbit of a nontrivial finite symmetry group $D_2 \times Z_2$ of the Euler top. They are said to be *equivalent*.

We now show how these level sets of $H_{|\ell|}$ fit together to form $L^{-1}(\ell)$. Remove a small open 2-disk $\mathbf{D}$ about the north pole of $\mathbf{S}^2_{|\ell|}$ and use stereographic projection to map $\mathbf{S}^2_{|\ell|} - \mathbf{D}$ onto a region $\mathcal{E} \subseteq \mathbf{R}^2$. The relative equilibria (except the one at the north pole) and the stable and unstable manifold are mapped into three points corresponding to elliptic relative equilibria and two circles which intersect transversely at point corresponding to the hyperbolic relative equilibria, respectively. The three elliptic points each lie in a compact region $\mathcal{D}_1 \cup \mathcal{D}_2$ bounded by the circles, see figure 1.2.6.

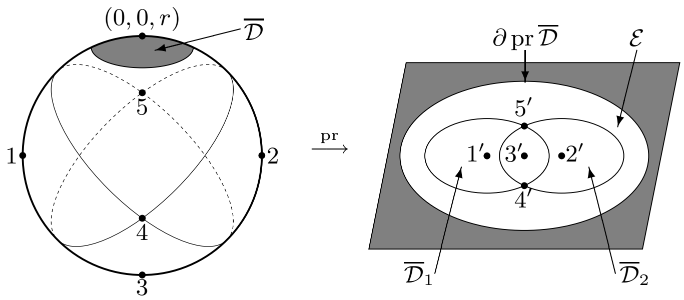

Fig. 1.2.6. The level sets of the reduced Hamiltonian flattened out. Stereographic projection of $\mathbf{S}^2$ without the north pole $(0,0,r)$.

Remove the solid torus $\mathcal{E}\times\mathbf{S}^1$ from SO(3). We have to replace $(\mathcal{D}_1\cup\mathcal{D}_2)\times \mathbf{S}^1$ (which is homeomorphic to $\mathcal{E}\times\mathbf{S}^1$) in the cored apple $\mathrm{SO}(3)-(\mathcal{E}\times\mathbf{S}^1)$, see figure 1.2.7.

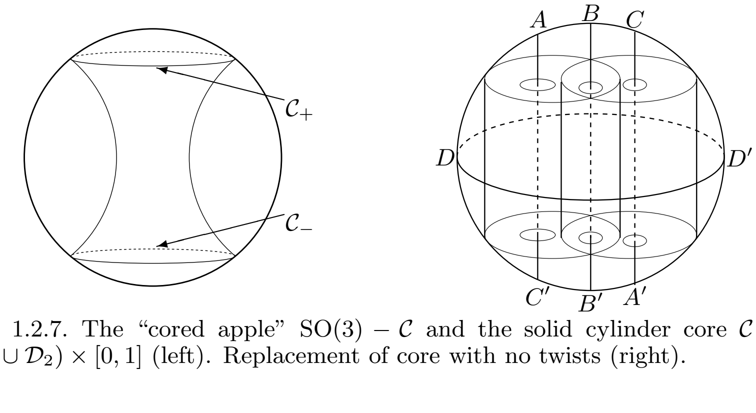

Fig. 1.2.7. The "cored apple" $\mathrm{SO}(3) - \mathcal{C}$ and the solid cylinder core $\mathcal{C} = (\mathcal{D}_1 \cup \mathcal{D}_2) \times [0,1]$ (left). Replacement of core with no twists (right).

The problem is: how many twists do we give the core, which is the solid cylinder $\mathcal{C} = (\mathcal{D}_1 \cup \mathcal{D}_2) \times [0,1]$, (whose ends are identified antipodally in the solid ball model of SO(3) and give $(\mathcal{D}_1 \cup \mathcal{D}_2) \times \mathbf{S}^1$) before replacing it in the cored apple $\mathrm{SO}(3) - (\mathcal{E} \times \mathbf{S}^1)$? No twists does not work, because then $H\big|_{L^{-1}(\ell)}$ would have two critical circles of elliptic type instead of three, see figure 1.2.7. One and one half twists do not work either,

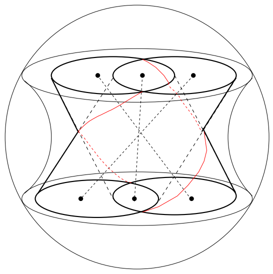

Fig. 1.2.8. Foliation of $L^{-1}(\ell)$ by the level sets of $H|L^{-1}(\ell)$.

because then $H\big|_{L^{-1}(\ell)}$ would have three critical circles of elliptic type whose two fold cover would have linking number more than one in $\mathbf{S}^3$. Generalizing this shows that placing the core $\mathcal{C}$ back in the cored apple with *one half a twist* is the only one possible. Thus we have obtained a *global* qualitatively accurate picture of how the level sets of $H\big|_{L^{-1}(\ell)}$ fit together to form $L^{-1}(\ell)$, see figure 1.2.8.

1.B Comments on lecture III.

1.B.1 The herpolhode

The curve traced out by the point P_t of contact of the moment of inertia ellipsoid rolling on the invariant plane was called the *herpolhode* by Poinsot [31]. It comes from the Greek word *herpes* meaning snake. Poinsot drew a picture of a snakelike herpolhode. On §9 page 472 Routh [34] gives a proof that the herpolhode has no inflection points for a physically realizable Euler top, that is, one in which the principal moments of inertia satisfy the inequalities

$$I_1 \le I_2 + I_3, \;\; I_2 \le I_1 + I_3 \text{ and } I_3 \le I_1 + I_2.$$

Thus the herpolhode is not snakelike at all. Routh says that Darboux [14] was the first to show this. Whittaker [42] leaves this as an exercise (# 29 on page 174) and refers to Lecornu [24] for a short proof.

In figure 1.B.1 below we see that the herpolhode can indeed be snakelike for nonphysical Euler tops.

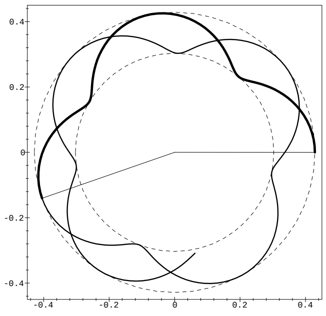

Fig. 1.B.1. The herpolhode for an unphysical Euler top with moments of inertia $I_1 = 1$, $I_2 = 2.8$, and $I_3 = 7$. Angular momentum has magnitude equal to 1; the Euler period is 13.21, and rotation number equals 0.5532.

1.B.2 Finite symmetries of the reduced Euler top

We saw in the lectures III and V that there is a great deal of similarity between the harmonic oscillator and the Euler top. The obvious difference between these systems is the remaining finite symmetry group.

For the Hénon-Heiles system (section 1.A) this group is $D_3 \times \mathcal{T}$. From its action on the reduced phase space $\mathbf{S}^2_h$ we found all critical points (relative equilibria) of the simplest reduced Hamiltonian for low energies. What is the symmetry of the rigid rotor? The reduced Hamiltonian

$$H_{|\ell|} = \tfrac{1}{2}\,(I_1^{-1}L_1^2 + I_2^{-1}L_2^2 + I_3^{-1}L_3^2)$$

is invariant with respect to any changes of the signs of L_1, L_2, and L_3. These operations form the group of order 8 with the structure $D_2 \times \mathbf{Z}_2$. Taking into account that $\mathbf{L} = (L_1, L_2, L_3)$ is an axial 3-vector which changes sign under time reversal $\mathcal{T} \sim \mathbf{Z}_2 : \mathbf{L} \mapsto -\mathbf{L}$, we can readily come up with the physical realization of this group in terms of transformations of the 3-space $\mathbf{R}^3$ with coordinates (L_1, L_2, L_3). Rotations $C_2^{(a)}$ by angle π about any of the principal axes of inertia 1, 2, or 3 constitute the abelian group D_2, which is extended by time reversal $\mathcal{T}$. Since the latter is equivalent to an inversion of $\mathbf{R}^3$, the group $D_2 \times \mathcal{T}$ corresponds to the Schoenflies point group D_{2h}; the three mutually orthogonal reflection planes of D_{2h} correspond, of course, to combinations $C_2 \circ \mathcal{T}$. The action of $D_2 \times \mathcal{T}$ on $\mathbf{S}^2$ is the action of the spatial group D_{2h} on a sphere in $\mathbf{R}^3$ (see figure 1.B.2). It has *six* fixed points, which are grouped into three pairs of equivalent points (two-point orbits) with stabilizers $C_2^{(a)}$,

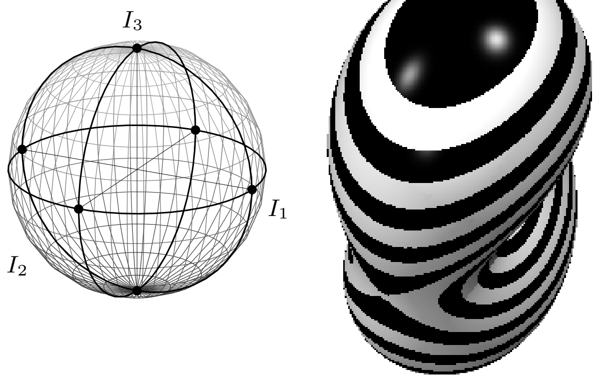

Fig. 1.B.2. Action of the $D_2 \times \mathcal{T}$ group on the sphere $\mathbf{S}^2$ (left). Reduced rigid body Hamiltonian $H_{|\ell|}$ for $|\ell| = 1$, $\frac{1}{2} I_1^{-1} = 0.4$, $\frac{1}{2} I_2^{-1} = 0.8$, and $\frac{1}{2} I_3^{-1} = 1.25$ as a simplest $D_2 \times \mathcal{T}$-invariant Morse function on $\mathbf{S}^2$ (right). Black and white stripes on the surface correspond to constant h (energy) levels drawn equidistantly, the width is ≈ 0.05.

$a = 1, 2, 3$. The two equivalent points are mapped into each other by operations $C_2^{(b)}$, $b \neq a$ and correspond to a rotation about a stationary axis a in two opposite directions ($\langle \mathbf{L}, \mathbf{e}_a \rangle = \pm|\ell|$).

A generic Morse function on $\mathbf{S}^2$ is required by the topology of this space to have two stationary points, a maximum and a minimum. In the presence of symmetry all critical points of the group action are necessarily stationary. The simplest $D_2 \times \mathcal{T}$-symmetric Morse function on $\mathbf{S}^2$ has *six* points situated on the critical orbits of the $D_2 \times \mathcal{T}$ action. Two points are minima, two are maxima, and two are hyperbolic (saddles), so that Euler's equation for the sphere remains satisfied. If $I_1 > I_2 > I_3$ then the values of $H_{|\ell|}$ lie in the interval $\frac{1}{2} I_1^{-1} \leq h \leq \frac{1}{2} I_3^{-1}$, and the value at the hyperbolic critical point (= unstable relative equilibrium) equals $\frac{1}{2} I_2^{-1}$. The Hamiltonian $H_{|\ell|}$ is the simplest $D_2 \times \mathcal{T}$ symmetric Morse function on $\mathbf{S}^2$. We have plotted $H_{|\ell|}$ in figure 1.B.2, right, as a surface function defined over the sphere $\mathbf{S}^2$. This representation is a familiar sight to many molecular physicists, who call it a "rotational energy surface" [21]. The constant energy levels painted on this surface show the trajectories of the reduced system. Many *asymmetric top* molecules, such as H_2O, O_3, have the zero-order rotational Hamiltonian of the type $H_{|\ell|}$. Higher order molecular terms emerge because the molecule is not rigid, that is, because there are interactions with vibrations.

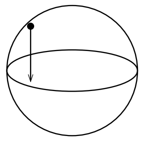

Fig. 1.2.3. Spherical pendulum.

1.3 Lecture IV. The spherical pendulum and monodromy

Spherical pendulum was discovered by Dutchman Christiaan Huygens about twenty years before Newton's *Principia*.[1]

This is immediately followed by confusion concerning the correct Dutch pronunciation of the name Huygens. A heated exchange with a Dutch grad student Bob Rink follows. The lecture continues.

1.3.1 The unconstrained system

Phase space. Give $T\mathbf{R}^3$ coordinates (x, y). We can confuse it with $T^*\mathbf{R}^3$ because we have the standard Euclidean inner product $\langle\, ,\, \rangle$ on $\mathbf{R}^3$. In fact $T\mathbf{R}^3 \simeq \mathbf{R}^3 \times \mathbf{R}^3$.

Symplectic form. The standard symplectic form on $T\mathbf{R}^3$ is

$$\widetilde{\omega} = \sum \mathrm{d}x_j \wedge \mathrm{d}y_j .$$

The unconstrained hamiltonian on $T\mathbf{R}^3$ is

$$\widetilde{H}(x, y) = \tfrac{1}{2}\,\langle y, y\rangle + \langle x, e_3\rangle .$$

S^1 **symmetry.** The unconstrained system $(\widetilde{H}, T\,\mathbf{R}^3, \widetilde{\omega})$ has an S^1 symmetry given by

$$S^1 \times T\mathbf{R}^3 \to T\mathbf{R}^3 : (t, (x, y)) \mapsto (R_t x, R_t y), \tag{1.3.1}$$

where $R_t = \begin{pmatrix} \cos t & -\sin t & 0 \\ \sin t & \cos t & 0 \\ 0 & 0 & 1 \end{pmatrix}$ is the matrix of rotation about axis e_3 by angle t.

[1] The work by Huygens (1629–1695) appeared in 1673, thirty years after Newton was born (1642). There are indications that Huygens understood this system earlier, see more in [5] on p. 402 and [40]. *Principia* [30] was published in 1687.

The unconstrained S^1-momentum map associated to the S^1-action (1.3.1) is

$$\widetilde{L}(x,y) = x_1 y_2 - x_2 y_1.$$

1.3.2 Constrained system

Constrained phase space. The phase space of the constrained system (= the spherical pendulum) is

$$T\mathbf{S}^2 = \{(x,y) \in T\mathbf{R}^3 \,\big|\, \langle x,x\rangle - 1 = 0, \quad \langle x,y\rangle = 0\}.$$

The constrained symplectic form on $T\mathbf{S}^2$ is $\omega = \widetilde{\omega}\big|_{T\mathbf{S}^2}$.

Hamiltonian. On $(T\mathbf{S}^2, \omega)$ the spherical pendulum hamiltonian is

$$H(x,y) = \widetilde{H}(x,y)\big|_{T\mathbf{S}^2}.$$

The equations of motion of the spherical pendulum are

$$\begin{aligned} \dot{x} &= y \\ \dot{y} &= -e_3 + \big(\langle x,e_3\rangle - \langle y,y\rangle\big)\, x. \end{aligned} \tag{1.3.2}$$

They determine the integral curves of the Hamiltonain vector field X_H on $(T\mathbf{S}^2, \omega)$, see p. 148 and 296 in [5]. Actually, equations (1.3.2) define a vector field on $T\,\mathbf{R}^3$ whose restriction to $T\mathbf{S}^2$ is X_H. To see this we need to verify that $T\mathbf{S}^2$ is an invariant manifold of (1.3.2).

Check.

$$\begin{aligned} \frac{d}{dt}\langle x,x\rangle &= 2\langle x,\dot{x}\rangle = 2\langle x,y\rangle = 0, \\ \frac{d}{dt}\langle x,y\rangle &= \langle \dot{x},y\rangle + \langle x,\dot{y}\rangle = \langle y,y\rangle - \langle x,e_3\rangle + \big(\langle x,e_3\rangle - \langle y,y\rangle\big)\langle x,x\rangle \\ &= 0 \end{aligned}$$

on $T\mathbf{S}^2$. □

Now, those people who use polar coordinates will give you only one system of equations for the spherical pendulum. In fact, they need at least two, *since $T\mathbf{S}^2$ requires at least two charts.*

S^1 symmetry. The S^1 symmetry of the spherical pendulum is

$$S^1 \times T\mathbf{S}^2 \to T\mathbf{S}^2 : \big(t,(x,y)\big) \mapsto (R_t x, R_t y). \tag{1.3.3}$$

The S^1-momentum map of the spherical pendulum is $L = \widetilde{L}\big|_{T\mathbf{S}^2}$.

Conserved quantity. Since S^1 action (1.3.3) preserves the constrained Hamiltonian H, we find that the Lie derivative of the momentum L with respect to the Hamiltonian vector field X_H of the spherical pendulum vanishes identically. Thus the spherical pendulum is Liouville integrable.

1.3.3 Reduction of S^1 symmetry

To remove the S^1 symmetry of the spherical pendulum we use invariants, because the S^1-action (1.3.3) is *not* free.

When you have compact group actions, invariant theory is the way to go. For general proper actions the situation is more complicated.

Algebra of invariants. The algebra of polynomials on $T\mathbf{R}^3$ which are *invariant* under the S^1 action (1.3.1) is generated by

$$\begin{array}{lll} \sigma_1 = x_3 & \sigma_3 = y_1^2 + y_2^2 + y_3^2 & \sigma_5 = x_1 y_1 + x_2 y_2 \\ \sigma_2 = y_3 & \sigma_4 = x_1^2 + x_2^2 & \sigma_6 = x_1 y_2 - x_2 y_1. \end{array}$$

Relation. The above invariants satisfy the relation

$$\sigma_5^2 + \sigma_6^2 = \sigma_4(\sigma_3 - \sigma_2^2), \text{ where } \sigma_4 \geq 0,\ \sigma_3 \geq \sigma_2^2. \tag{1.3.4}$$

This relation defines the orbit space $T\mathbf{R}^3/S^1$, which is a connected, *irreducible* semialgebraic variety in $\mathbf{R}^6$.

Orbit map. The orbit map is

$$\pi : T\mathbf{R}^3 \to \mathbf{R}^6 : (x, y) \mapsto \big(\sigma_1(x, y), \ldots, \sigma_6(x, y)\big).$$

In other words, each of the fibers of π is a unique S^1 orbit of the action (1.3.1). The orbit space $T\mathbf{R}^3/S^1$ is *singular*, because the S^1 action on $T\mathbf{R}^3$ leaves the points $(0, 0, x_3, 0, 0, y_3)$ fixed.

Another orbit space. What we really want is the orbit space of the S^1 action (1.3.1) restricted to $T\mathbf{S}^2$. This is the orbit space $T\mathbf{S}^2/S^1$ of the S^1 action (1.3.3). We obtain the defining equations of $T\mathbf{S}^2/S^1$ if we add two more relations to (1.3.4) (which come from the equations defining $T\mathbf{S}^2$), namely,

$$\sigma_4 + \sigma_1^2 = 1 \quad \text{and} \quad \sigma_5 + \sigma_1\sigma_2 = 0. \tag{1.3.5}$$

The gadget defined by (1.3.4) and (1.3.5) has *no chance* to be smooth because the action is *not free*. Singularities of $T\mathbf{S}^2/S^1$ contain dynamical information. We can use (1.3.5) to get rid of σ_4 and σ_5 in (1.3.4). We obtain

$$\sigma_1^2\sigma_2^2 + \sigma_6^2 = (\sigma_3 - \sigma_2^2)(1 - \sigma_1^2) = \sigma_3(1 - \sigma_1^2) - \sigma_2^2 + \sigma_1^2\sigma_2^2.$$

Simplifying gives the following description of $T\mathbf{S}^2/S^1$ as a semialgebraic variety in $\mathbf{R}^4$ (with coordinates $(\sigma_1, \sigma_2, \sigma_3, \sigma_6)$).

$$\sigma_2^2 + \sigma_6^2 = \sigma_3(1 - \sigma_1^2), \quad \text{where} \quad |\sigma_1| \le 1 \text{ and } \sigma_3 \ge 0. \tag{1.3.6}$$

The reduced phase space. The (singular) reduced phase space P_ℓ of the spherical pendulum is the orbit space $L^{-1}(\ell)/S^1$, where ℓ is the value of the momentum L. In terms of invariants L is σ_6. Thus P_ℓ is defined by adding the relation $\sigma_6 = \ell$ to equation (1.3.6). Thus as a subvariety of $\mathbf{R}^3$ (with coordinates $(\sigma_1, \sigma_2, \sigma_3)$), the singular reduced space P_ℓ is defined by

$$\sigma_2^2 + \ell^2 = \sigma_3(1 - \sigma_1^2), \quad |\sigma_1| \le 1, \quad \sigma_3 \ge 0.$$

In other words, P_ℓ is a $\sigma_6 = \ell$ *slice* of the orbit space $T\mathbf{S}^2/S^1$. When $\ell \ne 0$, P_ℓ is

$$\sigma_3 = \frac{\sigma_2^2 + \ell^2}{1 - \sigma_1^2} \quad \text{and} \quad |\sigma_1| < 1,$$

which is smooth and is diffeomorphic to $\mathbf{R}^2$. When $\ell = 0$ we have a "canoe" (see figure 1.3.1), whose two singular points $(\pm 1, 0, 0)$ are the fixed points of the S^1 action on $T\mathbf{S}^2$.

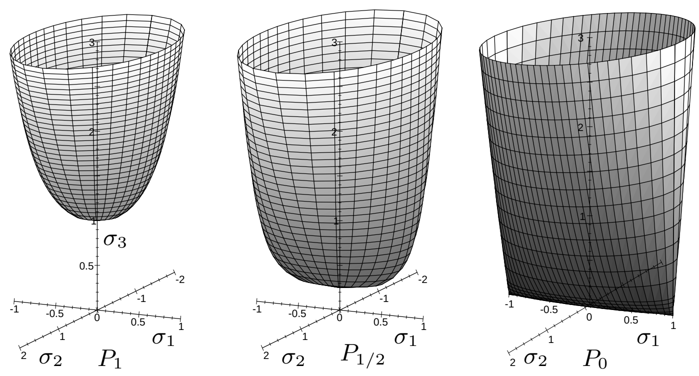

Fig. 1.3.1. Reduced phase spaces P_ℓ.

Note that all these guys P_ℓ have Poisson structure and there is reduced dynamics but I am not going to talk about it. The map $(x, y) \mapsto (\sigma_1, \sigma_2, \sigma_3)$ looks very much like a Hopf fibration but it is not and I will not discuss this either. I have completed reduction for the spherical pendulum.

1.3.4 Analysis of the reduced system

Reduced Hamiltonian. On the singular reduced space P_ℓ we have the reduced Hamiltonian

$$H_\ell : P_\ell \subseteq \mathbf{R}^3 \to \mathbf{R} : (\sigma_1, \sigma_2, \sigma_3) \mapsto \tfrac{1}{2}\,\sigma_3 + \sigma_1.$$

Critical values of H_ℓ on P_ℓ. How does $H_\ell = h$ intersect P_ℓ?

Calculus is difficult to use when P_ℓ has singularities. So we use a little bit of algebra instead. Computations proceed at maximum speed so that no one in the audience can follow what is happening.

Consider a family of 2-planes $\pi_h : \frac{1}{2}\sigma_3 + \sigma_1 = h$. Look for values of h where the intersection of π_h with P_ℓ has a point with multiplicity greater than 1. In other words, we look for those values (h, ℓ) for which polynomial

$$P(\sigma_1, \sigma_2) = \sigma_2^2 + \ell^2 - 2(h - \sigma_1)(1 - \sigma_1^2), \quad |\sigma_1| \leq 1,$$

in (σ_1, σ_2) has a zero of multiplicity greater than 1 and σ_1 lies in $[-1, 1]$. (The polynomial P is obtained by eliminating σ_3 from the defining equation of P_ℓ using $\sigma_3 = 2(h - \sigma_1)$. This is equivalent to $\sigma_2 = 0$ and finding those values of (h, ℓ) where the cubic polynomial

$$p(\sigma_1) = (h - \sigma_1)(1 - \sigma_1^2) - \tfrac{1}{2}\,\ell^2, \tag{1.3.7}$$

in σ_1 has a zero of multiplicity greater than 1 in $[-1, 1]$. Let $s \in [-1, 1]$ be a zero of p of multiplicity at least 2 and let $t \in \mathbf{R}$ be zero of multiplicity at least 1. Then necessarily

$$\begin{aligned} p(\sigma_1) &= \sigma_1^3 - h\sigma_1^2 - \sigma_1 + h - \tfrac{1}{2}\,\ell^2 = (\sigma_1 - s)^2(\sigma_1 - t) \\ &= \sigma_1^3 - (2s + t)\sigma_1^2 + s(s + 2t)\sigma_1 - s^2 t. \end{aligned}$$

Comparing coefficients of powers of σ_1 gives

$$2s + t = h, \;\; s(s + 2t) = -1, \;\text{ and }\; -s^2 t = h - \tfrac{1}{2}\,\ell^2.$$

Solving the above equations for $\{h, \ell\}$ gives

$$\begin{aligned} h &= \tfrac{1}{2}\,(3s^2 - 1)/s \\ \ell^2 &= -(1 - s^2)^2/s, \end{aligned} \tag{1.3.8}$$

where $s \in [-1,0) \cup \{1\}$. The first two equations in (1.3.8) give a parametrization of the *discriminant locus* Δ of p. When s varies between -1 and 0, the parametrization traces out two 1-smooth branches of the discriminant locus Δ, which join together when $s=-1$ and form an angle. When $s=1$, $(h,\ell)=(1,0)$ is an *isolated* point of the discriminant locus Δ. Thus 1 is a critical value of the reduced Hamiltonian H_1 on the reduced space P_0 corresponding to the critical point $(1,0,0)$, which is a singular point of P_0, see figure 1.3.2.

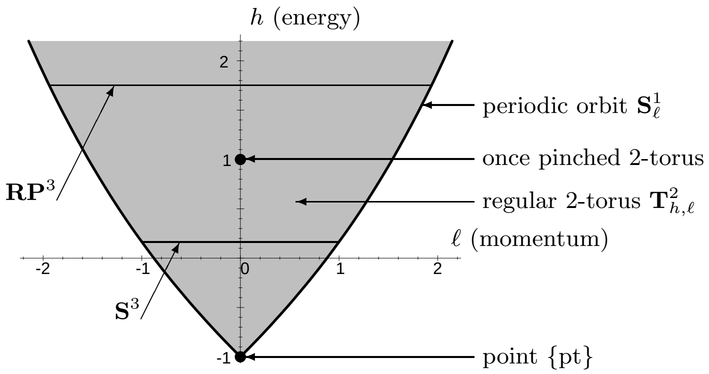

Fig. 1.3.2. Image and fibers of the energy-momentum map $\mathcal{EM}$ of the spherical pendulum.

Energy-momentum map $\mathcal{EM}$. The energy momentum map of the spherical pendulum is

$$\mathcal{EM} : T\mathbf{S}^2 \to \mathbf{R}^2 : p \mapsto (H(p), L(p)).$$

The region bounded by the black curves in figure 1.3.2 is the image of $\mathcal{EM}$. Its set of regular values is the grey shaded region; the black curves are the singular values of $\mathcal{EM}$ (= critical values of H_ℓ) together with the big dots, which mark the critical values $(1,0)$ and $(-1,0)$. Recall that critical values of H_ℓ are the same as critical values of $H\big|_{L^{-1}(\ell)}$ which in turn are the same as critical values of the energy-momentum map $\mathcal{EM}$.

1.3.5 Reconstruction

What is the topology of individual fibers $\mathcal{EM}^{-1}(h,\ell)$ of the energy-momentum map?

As S. Smale used to say: "whatever you do, don't lose geometry."

To determine the topology of fibers look at the projection of P_ℓ on the $\{\sigma_2 = 0\}$ plane. Remember that each regular point of P_ℓ lifts to a circle $\mathbf{S}^1$ and each singular point (of P_0) lifts to a point.

Regular fibers. If (h, ℓ) is a regular value of $\mathcal{EM}$, then the fiber $\mathcal{EM}^{-1}(h, \ell)$ is a smooth 2-torus. (The Liouville–Arnol'd theorem only shows that a *connected* component of $\mathcal{EM}^{-1}(h, \ell)$ is a 2-torus). To verify this, note that figure 1.3.3 shows that the h-level set of the reduced Hamiltonian H_ℓ on the reduced space P_ℓ is a circle C. Each point on C under the reduction map π lifts to a single $\mathbf{S}^1$ orbit of the S^1-action (1.3.5). Thus the lift of the circle C is the product $\mathbf{S}^1 \times \mathbf{S}^1$, which is the 2-torus $\mathcal{EM}^{-1}(h, \ell)$. Regular level sets of the reduced Hamiltonian H_0

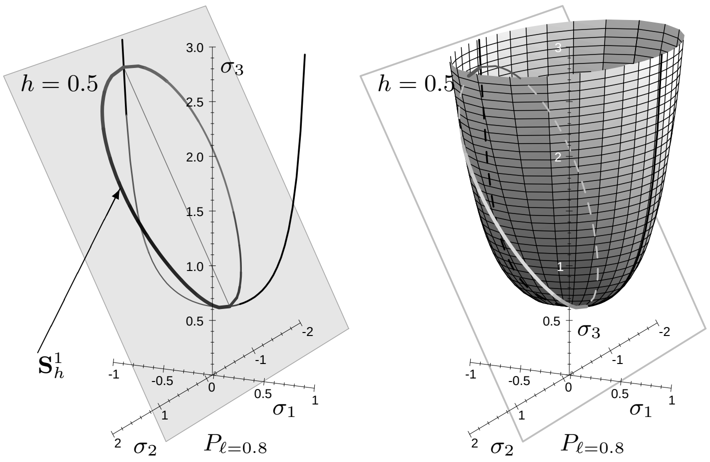

Fig. 1.3.3. h-level sets of H_ℓ on the regular reduced phase space P_l.

on the singular reduced phase space P_0 are also circles which lift to 2-tori (see figure 1.3.4). Dynamically, there are two different types of regular level sets: those *below* the critical energy $h = 1$ and those *above*. The image under the tangent bundle projection $\tau : T\mathbf{S}^2 \to \mathbf{S}^2 : (x, y) \mapsto x$ of an integral curve of the spherical pendulum on $\mathcal{EM}^{-1}(h, \ell)$, when (h, ℓ) is a regular value of $\mathcal{EM}$, is shown in figure 1.3.5.

Energy levels. How do regular tori fit together? The level $H^{-1}(h)$ is $\mathbf{RP}^3$ when $h > 1$ and $\mathbf{S}^3$ when $-1 < h < 1$. In more detail, using the solid ball model of SO(3), we see that SO(3) ($\simeq \mathbf{RP}^3$) is the union of two solid 2-tori, which are in turn the union of 2-tori with core a circle.

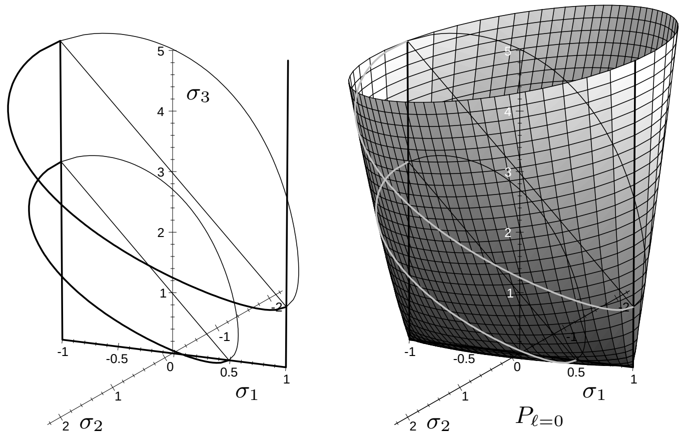

Fig. 1.3.4. Regular h-level sets of H_ℓ on the singular reduced phase space P_0.

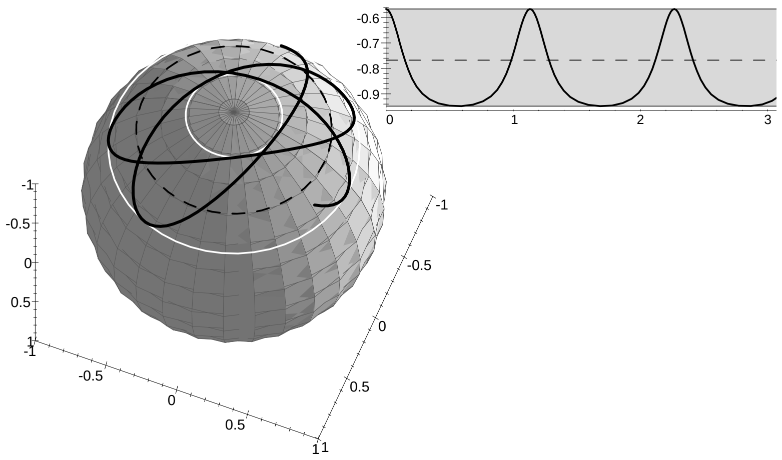

Fig. 1.3.5. Integral curve of the spherical pendulum on the configuration space $\mathbf{S}^2$ (view from the bottom, cf. figure 1.2.3) corresponding to the regular h-level set of H_ℓ. White circles indicate maximum and minimum elevation x_3^+ and x_3^-. The insert (top right) demonstrates the rotation angle $\theta > \pi$ by showing elevation $x_3(t)$ as function of longitude $\varphi(t)/\pi$. In this example $\ell = 0.3$, $h = -0.5$, rotation angle θ equals 1.1327π, and the period of $x_3(t)$ is 3.3453.

This describes the foliation of $H^{-1}(h)$ by level sets of L when $h > 1$. When $-1 < h < 1$, the foliation is the same as that given by the Hopf fibration.

Singular fibers. For critical values $(h, \ell \neq 0)$ of $\mathcal{EM}$, which form the boundary of the discriminant locus Δ, the h-level set of the reduced Hamiltonian H_ℓ is a point on P_l (see figure 1.3.6). The reconstructed fiber $\mathcal{EM}^{-1}(h, \ell)$ is a periodic orbit of the Hamiltonian vector field X_H which is also an orbit of the S^1-action (1.3.5). In other words, it is a *relative equilibrium* of X_H. On the singular reduced phase space P_0

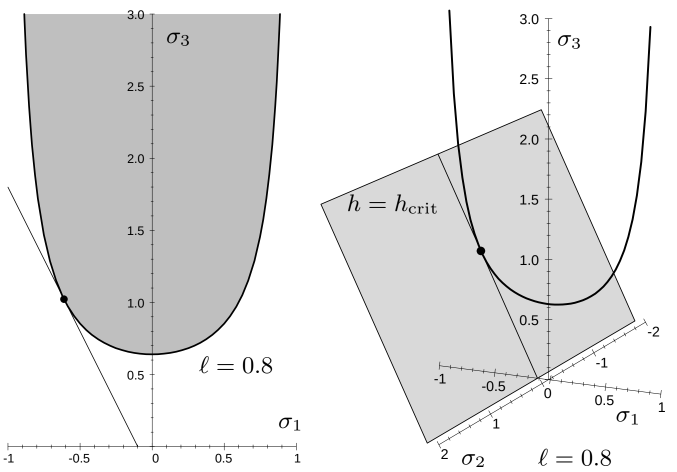

Fig. 1.3.6. Singular h-level sets of H_ℓ (relative equilibria) on the regular reduced phase space.

we have two kinds of critical slices (see figure 1.3.7). The level $h = -1$ is a point $(\sigma_1, \sigma_2, \sigma_3) = (-1, 0, 0)$ and the level $h = 1$ is a circle with one singular point $(\sigma_1, \sigma_2, \sigma_3) = (1, 0, 0)$. The point $\sigma = (-1, 0, 0)$ on P_0 corresponds to the stable equilibrium point $(0, 0, -1, 0, 0, 0)$ in $T\mathbf{S}^2$ of the spherical pendulum, because $h = -1$ is an absolute minimum energy. $\mathcal{EM}^{-1}(-1, 0)$ is, of course, a point. The point $\sigma = (1, 0, 0)$ in P_0 corresponds to the unstable equilibrium point $(0, 0, 1, 0, 0, 0)$ in $T\mathbf{S}^2$. Because this equilbrium point is a fixed point of the S^1 action (1.3.5), it lifts to a point in $T\mathbf{S}^2$. The rest of the points on $H_0^{-1}(1)$ lift to $\mathbf{S}^1$ orbits. From this it follows that $\mathcal{EM}^{-1}(1, 0)$ is a once pinched 2-torus (see figure 1.3.6.2 on page 69). This once pinched 2-torus is a homoclinic connection of the stable and unstable manifolds of the hyperbolic equilibrum of X_H at $(0, 0, 1, 0, 0, 0) \in T\mathbf{S}^2$.

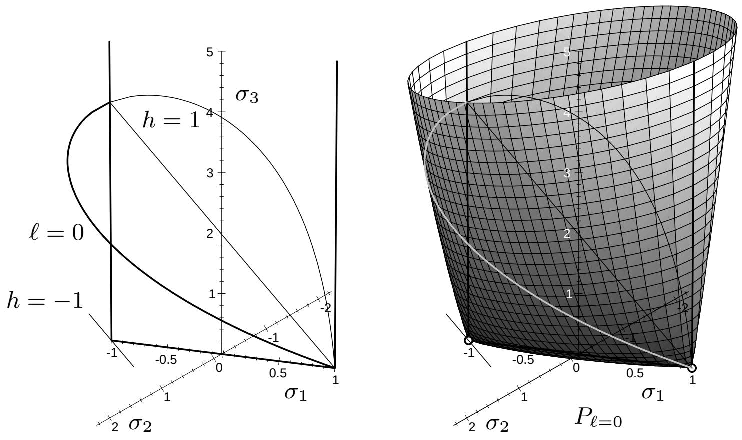

Fig. 1.3.7. Two singular h-level sets of H_ℓ on the singular reduced phase space P_0. The $h = 0$ level set lifts to the point (stable equilibrium), the $h = 1$ level set lifts to the pinched torus $\mathcal{EM}^{-1}(1, 0)$.

1.3.6 Monodromy

What we want to do now is to describe how the 2-torus fibers $\mathcal{EM}^{-1}(h, \ell)$ fit together as (h, ℓ) runs over a parameterized subset of the set of regular values of $\mathcal{EM}$. Now suppose that this set of regular values is a small open punctured disc $\mathbf{D}^* = \mathbf{D} - \{(h, \ell)_{\mathrm{crit}}\}$, which lies in the image of $\mathcal{EM}$. In other words, the critical value $(h, \ell)_{\mathrm{crit}}$ is *isolated*. Let Γ be a circle $\mathbf{S}^1 \subseteq \mathbf{D}^*$, which cannot be contracted to a point in $\mathbf{D}^*$, that is, $\mathbf{S}^1$ goes around the puncture $(h, \ell)_{\mathrm{crit}}$ as shown below

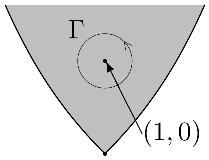

What is the topology of the 2-torus bundle $\Pi : \mathcal{EM}^{-1}(\Gamma) \to \Gamma$ over the circle Γ? (Recall the reconstruction of energy momentum level sets for regular values (h, ℓ)). Answer: The bundle Π is *non-trivial*. In other words, topologically $\mathcal{EM}^{-1}(\Gamma)$ is *not* a product $\mathbf{S}^1 \times \mathbf{T}^2$.

Monodromy map. How do we describe the topology of the 2-torus bundle Π over the circle Γ? Take the circle Γ and cut it at a point $\mathrm{pt} = (h, \ell)$.

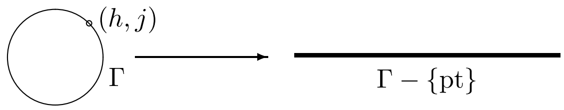

The resulting 2-torus bundle over the interval $\Gamma - \{\mathrm{pt}\}$ is *trivial* because the interval is can be contracted to a point. To obtain $\mathcal{EM}^{-1}(\Gamma)$ we glue the two tori over the end points of $\Gamma - \{\mathrm{pt}\}$ together. This is tricky business.

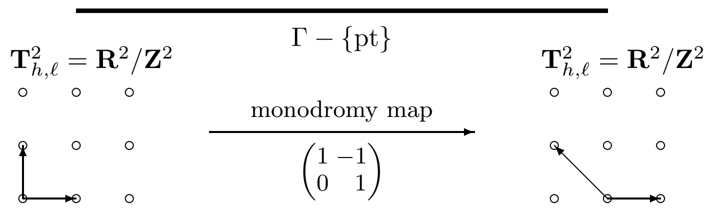

The map which identifies these tori is called the *monodromy map.* How do we glue the end 2-tori together? Since the tori of a Liouville integrable system are affine, such a 2-torus is $\mathbf{R}^2/\mathbf{Z}^2$, which is the 2-plane with points whose coordinates both differ by an integer being identified. The map which identifies the end tori is given by a 2×2 matrix M with integer entries having determinant 1, since M preserves $\mathbf{Z}^2$. If M is not conjugate by an integer 2×2 matrix with determinant 1 to the identity matrix, as in the figure above, then the bundle Π is nontrivial. When this is the case we say that the integrable system has monodromy.

Consequences. You may say – so what if the system has monodromy? Wait a minute. If the Liouville integrable Hamiltonian system with two degrees of freedom has monodromy, it *does not* have globally defined action-angle coordintes.

1.3.6.1 Analytical description of mondromy. Rotation angle

To compute monodromy analytically we need to use the *rotation angle* $\Theta_{(h,\ell)}$ of the flow of the Hamiltonian vector field X_H on a smooth 2-torus $\mathcal{EM}^{-1}(h,\ell)$, where (h,ℓ) is a regular value of $\mathcal{EM}$. The X_H and X_L on $\mathcal{EM}^{-1}(h,\ell)$ are linearly independent. The flow $\varphi^L_{t''}$ of X_L is periodic on the torus $\mathbf{T}^2_{(h,\ell)}$. We define the rotation angle $\Theta_{(h,\ell)}$ so that for *any* initial condition p

$$\varphi^L_{\Theta_{(h,\ell)}}(p) = \varphi^H_T(p),$$

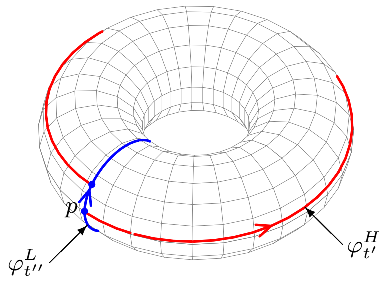

Fig. 1.3.8. Flow of two linearly independent vector fields on the torus $\mathbf{T}^2_{(h,\ell)}$ and definition of the rotation angle.

where T is the period of the flow $\varphi_t^{H_\ell}$ of the reduced vector field X_{H_ℓ} on $H_\ell^{-1}(h)$, see figure 1.3.8. The vector field $T(h,\ell)X_H + \Theta_{(h,\ell)}X_L$ has periodic flow on $T^2_{(h,\ell)}$. Projecting the tangent bundle $T\mathbf{S}^2$ on the configuration space $\mathbf{S}^2$ we can define $\Theta_{(h,\ell)}$ as the angle by which the pendulum turns about axis x_3 during the period of oscillation in x_3 (height)[1], see figure 1.3.5.

A standard classical argument shows that

$$\Theta_{(h,\ell)} = 2\sqrt{2}\ell \int_{\sigma_1^-}^{\sigma_1^+} \frac{d\sigma_1}{(1-\sigma_1^2)\sqrt{p(\sigma_1)}},$$

where p is the polynomial (1.3.7) and $\sigma_1^\pm$ are its real zeroes in $[-1,1]$ with $\sigma_1^- \leq \sigma_1^+$. The function $\Theta_{(h,\ell)}$ is a *multivalued* real analytic function on the set of regular values of $\mathcal{EM}$, for more details see [5]. When we let (h,ℓ) run over the curve Γ, the value of $\Theta_{(h,\ell)/2\pi}$ does not return to its original value. Instead it decreases by 1. Hence the variation of the lattice spanned by periodic Hamiltonian vector fields X_L and $X_{T(h,\ell)H+\Theta_{(h,\ell)}L}$ on $\mathcal{EM}^{-1}(h,\ell)$ corresponding to the local actions is $\left(\begin{smallmatrix}1 & -1\\ 0 & 1\end{smallmatrix}\right)$.

1.3.6.2 Geometric monodromy theorem

We now state the geometric monodromy theorem, which allows us to compute the monodromy using only geometry. Consider a two degree of freedom Liouville integrable Hamiltonian system with phase space $(\mathcal{M},\omega)$, which is a 4-dimensional symplectic manifold and Poisson com-

[1] Rotation angle equals π in the planar pendulum limit $\varphi^L \equiv 0$. For all regular (h,ℓ) $\pi < \Theta_{(h,\ell)} < 2\pi$, see chapter IV.6.3 of [5].

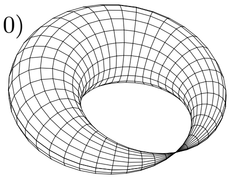

Fig. 1.3.9. A once pinched 2-torus.

muting integrals (F_1, F_2). Suppose that the integral map

$$\mathcal{I} : \mathcal{M} \to \mathbf{R}^2 : p \mapsto (F_1(p), F_2(p)).$$

has an isolated critical value of $(0,0)$ and that $\mathbf{D}^* = \mathbf{D} - \{(0,0)\}$ is contained its set of regular values. Suppose that for every c in $\mathbf{D}^*$ the preimage $\mathcal{I}^{-1}(c)$ is a smooth 2-torus, while $\mathcal{I}^{-1}(0,0)$ is a 2-torus which is once pinched at the point x. In other words, x is the only singular point of $\mathcal{I}^{-1}(0,0)$ and is a hyperbolic equilibrium point of X_{F_1}, that is, the linearization of X_{F_1} at x has two nonreal complex eigenvalues with positive real part and two nonreal complex eigenvalues with negative real part. Moreover, the whole of $\mathcal{I}^{-1}(0,0)$ is a homoclinic connection of the stable and unstable manifolds of x. If Γ is a smooth positively oriented circle in $\mathbf{D}^*$, then the 2-torus bundle $\mathcal{I}^{-1}(\Gamma)$ has monodromy $\left(\begin{smallmatrix} 1 & -1 \\ 0 & 1 \end{smallmatrix}\right)$.

If the singular fiber $\mathcal{I}^{-1}(0,0)$ is a k-pinched 2-torus, that is, is a heteroclinic k-cycle, then the monodromy is $\left(\begin{smallmatrix} 1 & -k \\ 0 & 1 \end{smallmatrix}\right)$.

1.C Comments on lecture IV

The concept of monodromy for two degree of freedom integrable Hamiltonian systems was first formulated by Duistermaat [15]. The spherical pendulum was historically the first example of a system with monodromy [15, 6]. It is discussed at length in chapt. IV of [5].

Reduction of the S^1 symmetry in the spherical pendulum is an example of *singular reduction* using invariants which was pioneered by Cushman. In his lecture Cushman relies on the simple elegant method of qualitative analysis (of functions defined on algebraic varieties, such as reduced Hamiltonians H defined on singular reduced phase spaces P) which can be called the "method of slices". Having both P and h-level sets of H described as surfaces in an ambient space with invariant polynomial coordinates, he studies the topology of their intersections D_h

which form a continuous one-parameter family. Critical sections $D_{h_{\rm crit}}$ have special topology and are isolated in this family, the values $h_{\rm crit}$ are critical values of the function H on P. A similar method (for functions defined on orbit spaces) was independently used by Zhilinskií (see section 5.6.1 of [26], appendix A in [27], and [36]).

The presentation of the spherical pendulum gives a convincing illustration of Cushman's leitmotiv "no polar coordinates", that is, of an analysis based on polynomial invariants. The reader who is still (uh) not converted to the faith should certainly enjoy drawing a picture of the singular reduced phase space P_0 in polar (cylindrical) coordinates.

Initially monodromy was uncovered analytically in terms of local angle-action variables and the variation of the period lattice [5]. In this approach the monodromy matrix was calculated directly after an explicit relation between the different local angle action variable charts was established. The geometric monodromy theorem was formulated later in [10]. According to this theorem and the results of [25] and [43] we can determine whether the system has monodromy and even find the monodromy matrix on the basis of the geometric reconstruction of the fibers of the energy-momentum map $\mathcal{EM}$.

All figures in this section were prepared from numerical computations.

1.C.1 Discrete symmetries

The spherical pendulum has a number of discrete symmetries in addition to the S^1 symmetry discussed in the lecture. To find these symmetries we consider operations which leave invariant the unconstrained Hamiltonian $\widetilde{H}$ *and* the phase space $T\mathbf{S}^2$. In this way we see that our system is invariant with respect to any reflection σ_v in a plane containing the e_3 axis, for example,

$$(x_1, x_2, x_3, y_1, y_2, y_3) \mapsto (x_1, -x_2, x_3, y_1, -y_2, y_3).$$

The resulting symmetry group has two classes of conjugate elements: one which contain rotations (S^1 symmetry) and the other the reflection σ_v. In the Schoenflies classification this group is called $C_{\infty v}$. The action of $C_{\infty v}$ on $T\mathbf{S}^2$ is symplectic. The S^1-invariant polynomials $\sigma_1, \ldots, \sigma_6$ are invariant under a larger group $C_{\infty v}$. When the action of $C_{\infty v}$ is reduced, its orbit space is $T\mathbf{S}^2/C_{\infty v}$.

The full symmetry group of the spherical pendulum is $C_{\infty v} \times \mathbf{Z}_2$. The nontrivial operation of the order two group $\mathbf{Z}_2 = \{\pm 1\}$ is the anti-symplectic symmetry $(x, y) \to (x, -y)$, which is sometimes called *time* *reversal*. After reduction this symmetry induces a nontrivial symmetry on $\mathbf{R}^4$ defined by

$$\mathbf{Z}_2 \times \mathbf{R}^4 \to \mathbf{R}^4 : (-1, (\sigma_1, \sigma_2, \sigma_3, \sigma_6)) \mapsto (\sigma_1, -\sigma_2, \sigma_3, -\sigma_6).$$

This has two important consequences:

(i) Points on $T\mathbf{S}^2$ with $L = \ell \neq 0$ which differ by the direction of rotation about axis e_3 are *equivalent*. Therefore it suffices to study only the case $\ell \geq 0$.
(ii) The reduced phase space P_ℓ can be "flattened" into the *fully reduced phase space* $P_\ell/\mathbf{Z}_2$ which is a projection of P_ℓ onto the plane with coordinates (σ_1, σ_3). The use of $P_\ell/\mathbf{Z}_2$ makes the geometric analysis of the level sets of $H_\ell = \frac{1}{2}\sigma_3 + \sigma_1$ particularly simple.

1.C.2 Geometric analysis on $P_\ell/\mathbf{Z}_2$

Analysis of the level sets of H_ℓ on P_ℓ can be done using level sets of H_ℓ on $P_\ell/\mathbf{Z}_2$ for $\ell \geq 0$. The h-level set of H_ℓ is an intersection of the line

$$\sigma_3 = 2(h - \sigma_1)$$

and the region of the coordinate plane (σ_1, σ_3) defined by the inequality

$$\sigma_3 \geq \ell^2/(1 - \sigma_1^2).$$

Note that on the boundary of $P_\ell/\mathbf{Z}_2$ the value of σ_2 is 0, while the value of H_ℓ is

$$H_\ell = \tfrac{1}{2}\sigma_3 + \sigma_1 = \frac{\ell^2}{2(1 - \sigma_1^2)} + \sigma_1.$$

Regular level sets of H_ℓ on $P_\ell/\mathbf{Z}_2$ are closed intervals. Its critical level sets are points (see figures in the lecture) on the boundary of $P_\ell/\mathbf{Z}_2$. To find the critical set for $\ell > 0$ we find those values of σ_1 where the slope of the boundary of $P_\ell/\mathbf{Z}_2$ equals that of the h-level set, that is,

$$\ell^2 \frac{d}{d\sigma_1}(1 - \sigma_1^2)^{-1} = -2, \quad \sigma_1 < 0.$$

Solving the above equation for ℓ gives

$$\ell = \pm(1 - s^2)/\sqrt{s}, \quad \text{where } s = -\sigma_1.$$

This yields the parametrization

$$\big(\ell(s), h(\ell(s), s)\big) = \left(\pm\frac{1 - s^2}{\sqrt{s}}, \frac{1 - s^2}{2\,s} - s\right)$$

of the discriminant locus Δ used in the lecture.

1.C.3 Quantum monodromy

Quantum mechanics provides a very clear interpretation of monodromy [8] which we think is worth mentioning here. We recall that in the quantized spherical pendulum it is the energy h and momentum ℓ of the classical system which are quantized. According to the Einstein-Brilluoin-Kramers (EBK) quantization principle, we should find regular tori $\mathbf{T}_{h,\ell}$ for which the actions are an integer value times an overall scale factor $2\pi\hbar$.

For the spherical pendulum the action ℓ, which corresponds to the S^1 symmetry, is quantized so that

$$\frac{\ell}{2\pi\hbar} = 0, 1, 2, \dots \ .$$

The action corresponding to the second vector field on $\mathbf{T}_{h,\ell}$ with periodic flow should be computed locally in (h, ℓ) and then quantized. The result of such computation is shown in figure 1.C.1, which was kindly provided to us by Igor Kozin [23]. Note that the value of $\hbar$ was "adjusted" so that there are enough quantum states in the region near the isolated critical value $(h, \ell) = (1, 0)$.

All quantum states (EBK tori) form a two-dimensional lattice of points in the image of the $\mathcal{EM}$ map (inside the discriminant locus). We can choose many regular one-dimensional sequences of nodes starting locally at any given node in this lattice; the distance between the neighbors in such sequences is a "quantum", and the distance between the last state and the border of the classical locus (measured along the direction of the sequence) is half of this quantum. In other words, we can define local quantum numbers which correspond to local action variables.

Boris Zhilinskií proposed to make manifest that the monodromy of the quantum system is a defect of the lattice formed by quantum states in the image of the $\mathcal{EM}$-map. This improved the original picture of Cushman and Duistermaat [8] so that anyone who sees one of Boris' pictures (including Cushman and Duistermaat) immediately begins to play around and try to "perfect" it. Therefore we call such a picture as figure 1.C.1 a *Zhilinskií diagram.*

We begin Zhilinskií's diagram (figure 1.C.1) by drawing an "elementary cell", which is a small quadrangle defined by one choice of local quantum numbers. We then propogate this cell along the contour Γ.

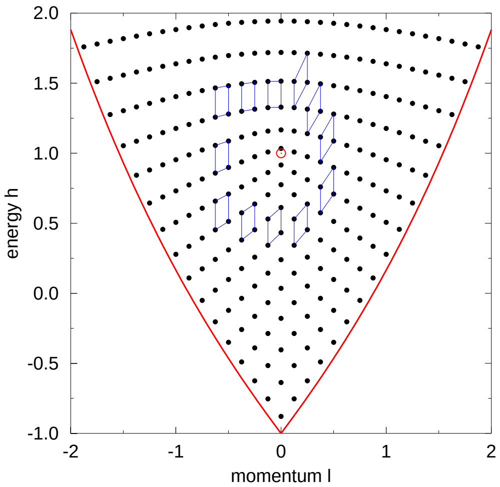

Fig. 1.C.1. Image of the classical and quantum $\mathcal{EM}$ map of the spherical pendulum. Hollow circle shows the isolated critical value, black circles represent quantum levels (= EBK tori). The family of quadrilaterals (= Zhilinskií's diagram) shows how local quantum numbers (= local action variables) are chosen along the circle Γ.

At each sufficiently small step along Γ, the choice of the new neighboring cell preserves the same choice of the quantum numbers and thus is unambiguous. However, after making the whole circuit of Γ, the cell does not come to itself because a global choice of quantum numbers is impossible. The map from the original cell to the final cell is of course the monodromy map. More precisely, the matrix which gives the transformation of the cell is the inverse transpose of the classical monodromy matrix. A rigorous mathematical formulation of quantum monodromy was given by Vu Ngoc in [39]; relation between quantum and classical monodromy matrices is also discussed in the appendix of [17].

If you like playing with little puzzles as much as Boris does [44], here are a couple of provocative conjectures which can be formulated on the basis of the Zhilinskií diagrams similar to the one in figure 1.C.1.

(i) The "sign conjecture" states that the monodromy matrix is $\left(\begin{smallmatrix} 1 & -k \\ 0 & 1 \end{smallmatrix}\right)$ where k is always a *positive* integer. Indeed, try changing the direction of your contour Γ or try flipping the lattice in figure 1.C.1 any way you can imagine (help yourself with scissors and glue, if you like). The monodromy transformation will always be $\left(\begin{smallmatrix} 1 & -k \\ 0 & 1 \end{smallmatrix}\right)$.

(ii) The "additivity conjecture" states that monodromies of several isolated critical values of the $\mathcal{EM}$-map, which all lie in the interior of the closure of a connected component of the set of regular values, can *only add up*. In other words, the distortion of the original elementary cell can only increase. For example, the monodromy matrix computed along a contour which encircles two isolated critical values with monodromy matrices $\left(\begin{smallmatrix} 1 & -k' \\ 0 & 1 \end{smallmatrix}\right)$ and $\left(\begin{smallmatrix} 1 & -k'' \\ 0 & 1 \end{smallmatrix}\right)$, respectively, should be $\left(\begin{smallmatrix} 1 & -k'-k'' \\ 0 & 1 \end{smallmatrix}\right)$.

Both of these conjectures have been recently proved by Cushman and Vu Ngoc [12]. They should help in the study of bifurcations of pinched tori associated to isolated critical values.

Among many examples of quantum systems with monodromy which have been found since 1980, we can add the textbook system of two (or more) coupled angular momenta [36]. It has also been suggested in [35] that nonintegrable systems with most of their KAM tori remaining intact can also have monodromy. This conjecture has been recently proven in [32]. In particular, the hydrogen atom in perpendicular electric and magnetic fields [35], an atomic realization of a particular perturbation of the Kepler system, has monodromy. Monodromy has been recently found in many molecular systems, notably in H_2^+ [41], a molecular realization of the two-center Kepler system, in floppy triatomic molecules, such as LiCN/CNLi [17], which are distant relatives of the spherical pendulum, and in Fermi resonant molecular elastic pendula, such as CO_2 [13]. See [17] for a brief review.

1.C.4 Finding monodromy by deformation argument

Monodromy is a global topological property of an integrable fibration. Thus regular fibers (tori) lying far away from the singularity, which is at the origin of monodromy (such as the pinched torus), continue to fit together in the way prescribed by the monodromy of the fibration. Furthermore, in a sufficiently small neighbourhood a small local continuous deformation, which changes qualitatively only the singularity, does not change the monodromy of the fibration. The far away tori will fit together in the same fashion as for the undeformed fibration. This simple deformation argument allows to find monodromy of many systems.

For example, consider a "quadratic spherical pendulum", which is obtained by a generic quadratic deformation $V_{a,b} = \frac{1}{2}ax_3^2 + bx_3$ of the original linear potential $V_{0,1} = x_3 = \sigma_1$ of the spherical pendulum. By analyzing the corresponding continuously deformed reduced system (an exercise which the reader is invited to do following the approach in sec. 1.3.4) we find that deformed system differs qualitatively from the original spherical pendulum only when $|a| > |b|$. Neglecting overall energy scaling, we can distinguish three robust deformations $V_{0,1}$, $V_{-1,\epsilon}$, and $V_{1,\epsilon}$ (here $0 < |\epsilon| < 1$), two special systems with $V_{\pm1,0}$, and two transitional systems with $V_{\pm1,1}$.

As shown in fig. 1.C.2, the $\mathcal{EM}$ map of the $V_{1,\epsilon}$ system has *two* isolated critical values at $\ell = 0$ which correspond to two pinched tori. The continuous deformation $V_{1,\epsilon} \to V_{1,0}$ merges these tori into one doubly pinched torus. The degenerate system $V_{1,0}$ was studied in [2] where it was shown to have monodromy $\left(\begin{smallmatrix}1 & -2\\ 0 & 1\end{smallmatrix}\right)$. This analysis was extended in [12] to $V_{1,\epsilon}$ where the authors show that the $V_{1,\epsilon}$ system also has monodromy 2 for the contour Γ which encircles both critical values. This assertion follows from a deformation argument for sufficiently small ϵ. A different continuous deformation $V_{1,\epsilon} \to V_{0,1}$ merges one of the critical values into the lower boundary of the image of $\mathcal{EM}$, while the other becomes the isolated critical value of the $V_{0,1}$. It follows that monodromy for a contour which goes around this remaining isolated critical value is 1. Replacing ϵ by $-\epsilon$, we see that monodromy for a contour around any of the two isolated critical values of the $V_{1,\epsilon}$ system is 1.

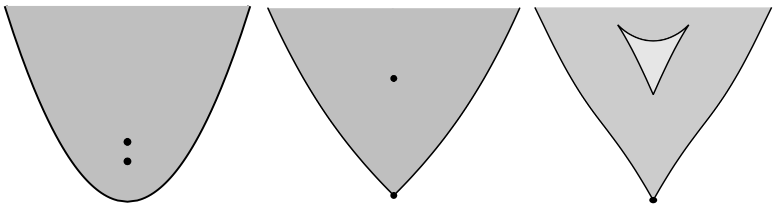

Fig. 1.C.2. Image of the $\mathcal{EM}$ map of the spherical pendulum (center) the deformed quadratic spherical pendulum of the $V_{1,\epsilon}$ kind (left) and of the $V_{-1,\epsilon}$ kind (right, cf. [17] and [41]).

The $V_{-1,\epsilon}$ case was analyzed recently in [17] as a model of triatomic floppy molecules. The image of the $\mathcal{EM}$ map has two leaves A and B (fig. 1.C.2, right). The "main" leaf A is unbounded from above and has a small cut $\mathcal{C}$ along the top edge of the curvalinear triangle B. The second "small" leaf B is glued to A along $\mathcal{C}$. The $\mathcal{EM}$ map is two-valued on $\mathcal{EM}^{-1}(B \setminus C)$. This system has *nonlocal monodromy* which we can observe for a contour $\Gamma \subset A$ which goes around $\mathcal{C}$. The continuous deformation $V_{-1,\epsilon} \to V_{0,1}$ shrinks B (and the cut $\mathcal{C}$) to a point, which becomes the isolated critical point of $V_{0,1}$. In the full space, the union of singular fibers which form $\mathcal{EM}^{-1}(\mathcal{C})$ shrinks to a pinch torus. Since this deformation does not involve the regular tori in $\mathcal{EM}^{-1}(\Gamma)$, monodromy of the $V_{-1,\epsilon}$ system along Γ is 1.

The transitional case $V_{1,1}$ corresponds to the moment of the bifurcation of the lower equilibrium of the system. When we move continuously in the parameter space so that $V_{0,1} \to V_{1,1} \to V_{1,\epsilon}$ (that is, going from center to left in fig. 1.C.2) the initially stable equilibrium detaches from the two families of relative equilibria and becomes an isolated focus-focus point whose stable and unstable manifolds connect and form a pinched torus. It has been proven in [16] that this is a supercritical Hamiltonian Hopf bifrucation.

The case $V_{-1,1}$ corresponds to the moment of the subcritical Hamiltonian Hopf bifurcation of the upper equilibrium of the system [16]. When $V_{0,1} \to V_{-1,1} \to V_{-1,\epsilon}$ (going from center to right in fig. 1.C.2) this initially isolated unstable equilibrium becomes stable (lower vertex of leaf B) and new families of relative equilibria are born (the rest of the boundary ∂B). In sec. 1.D Cushman shows that the monodromy of the $V_{-1,1}$ system is the same as that of the original spherical pendulum $V_{0,1}$. Of course we can now anticipate this result from our deformation argument, but we invite the reader to appreciate the hard way of computing directly the monodromy of $V_{-1,1}$.

1.D Homework problem. Monodromy about a degenerately pinched 2-torus

This appendix is contributed entirely by Cushman after a question by Boris Zhilinskií and Dmitrií Sadovskií at the end of his lecture on the spherical pendulum. This question turned into an interesting homework problem for the lecturer.

1.D.1 Introduction

In this section we construct a two degree of freedom Liouville integrable Hamiltonian system on the tangent bundle $T\mathbf{S}^2$ of the 2-sphere $\mathbf{S}^2$ whose energy momentum map $\mathcal{EM}$ has the following properties.

(i) $(0,0)$ is an isolated critical value, that is, there is an open disc $\mathbf{D}$ in $\mathbf{R}^2$ containing $(0,0)$ such that $\mathbf{D}^* = \mathbf{D} \setminus \{(0,0)\}$ consists of regular values of $\mathcal{EM}$ and $\mathbf{D}^*$ lies in its image.

(ii) For every $(h,\ell) \in \mathbf{D}^*$ the (h,ℓ)-level set

$$\mathcal{EM}^{-1}(h,\ell) = \{p \in T\mathbf{S}^2 \,\big|\, \mathcal{EM}(p) = (h,\ell)\}$$

is a smooth 2-dimensional torus $T^2_{h,\ell}$.

(iii) The singular fiber $\mathcal{EM}^{-1}(0,0)$ is an immersed 2-dimensional submanifold of $T\mathbf{S}^2$ which is smooth except at two pinch points $p_\pm$ where it has a self intersection. At p_- the pinch is transverse, that is, the tangent spaces to $\mathcal{EM}^{-1}(0,0)$ at p_- are transverse; whereas at p_+ the pinch is degenerate because the tangent spaces are *not* transverse.

Our calculations show that the global monodromy of the smooth 2-torus bundle $\mathcal{EM}^{-1}(\Gamma) \to \Gamma$ over a smooth positively oriented circle Γ in $\mathbf{D}^*$, which has winding number 1 about $(0,0)$ is $\left(\begin{smallmatrix} 1 & -2 \\ 0 & 1 \end{smallmatrix}\right)$. For more backgound on monodromy in Liouville integrable Hamiltonian systems see [15] or [5]. Our calculations show that the local monodromy around the degenerate pinch point p_+ is $\left(\begin{smallmatrix} 1 & -1 \\ 0 & 1 \end{smallmatrix}\right)$, which is the *same* as the local monodromy about the transversal pinch point p_-. This result is well known if both pinch points are transverse, see [43, 10].

To determine the local monodromy around p_+, we find the variation of the rotation angle of the flow of the Hamiltonian vector field on $T^2_{h,\ell}$ as (h,ℓ) traces out the curve Γ. This uses residues and follows closely the idea of the calculation of the local monodromy for the spherical pendulum given in Chapt. V of [5].

1.D.2 A model system

Consider the following model Hamiltonian system. On $T\mathbf{R}^3$ with coordinates (x,y) and symplectic form $\widetilde{\omega} = \sum_{i=1}^3 \mathrm{d}x_i \wedge \mathrm{d}y_i$ let

$$\widetilde{H}(x,y) = \tfrac{1}{2}\langle y,y\rangle + V(x_3), \tag{1.D.1}$$

be the unconstrained Hamiltonian. Here $\langle\,,\,\rangle$ is the Euclidean metric on $\mathbf{R}^3$. Constrain the Hamiltonian system $(\widetilde{H}, T\mathbf{R}^3, \widetilde{\omega})$ so that the motion takes place on the tangent bundle

$$T\mathbf{S}^2 = \{(x,y) \in T\mathbf{R}^2 \mid \langle x,x\rangle = 1,\ \ \langle x,y\rangle = 0\}$$

of the 2-sphere $\mathbf{S}^2$. The model problem we consider is the constrained system $(H, T\mathbf{S}^2, \omega)$, where $H = \widetilde{H}|T\mathbf{S}^2$ and $\omega = \widetilde{\omega}|T\mathbf{S}^2$. This system has an S^1 symmetry

$$S^1 \times T\mathbf{S}^2 \to T\mathbf{S}^2 : (t,(x,y)) \mapsto (R_t x, R_t y), \tag{1.D.2}$$

where $R_t = \left(\begin{smallmatrix} \cos t & -\sin t & 0 \\ \sin t & \cos t & 0 \\ 0 & 0 & 1 \end{smallmatrix}\right)$, whose momentum is

$$L : T\mathbf{S}^2 \to T\mathbf{S}^2 : (x,y) \mapsto x_1 y_2 - x_2 y_1. \tag{1.D.3}$$

Since the S^1 symmetry preserves the Hamiltonian H, the function L is an integral of the Hamiltonian vector field X_H. In other words, the functions H and L Poisson commute, that is, $\{H, L\} = 0$. Thus $(H, T\mathbf{S}^2, \omega)$ is Liouville integrable.

To remove the S^1 symmetry we apply singular reduction [5], which uses invariant theory. First we note that the algebra of S^1-invariant polynomials on $T\mathbf{S}^2$ is generated by

$$\begin{aligned} \rho_1 &= x_3 & \rho_3 &= y_1^2 + y_2^2 + y_3^2 & \rho_5 &= x_1 y_1 + x_2 y_2 \\ \rho_2 &= y_3 & \rho_4 &= x_1^2 + x_2^2 & \rho_6 &= x_1 y_2 - x_2 y_1 \end{aligned} \tag{1.D.4}$$

subject to the relations

$$\begin{aligned} \rho_5^2 + \rho_6^2 &= \rho_4(\rho_3 - \rho_2^2), \quad \rho_4 \geq 0,\ \rho_3 \geq \rho_2^2 \\ \rho_1^2 + \rho_4 &= 1 \\ \rho_1\rho_2 + \rho_5 &= 0. \end{aligned} \tag{1.D.5}$$

The above relations (1.D.5) define the space $T\mathbf{S}^2/S^1$ of S^1-orbits on $T\mathbf{S}^2$. The singular reduced space $P_\ell = L^{-1}(\ell)/S^1$ is the space of S^1-orbits on the ℓ-level set of the momentum L and is defined by equation (1.D.5) together with the relation $\rho_6 = \ell$. Eliminating ρ_4, ρ_5, and ρ_6 from these equations, we find that P_ℓ is the semialgebraic variety in $\mathbf{R}^3$ (with coordinates (ρ_1, ρ_2, ρ_3))

$$\rho_2^2 + \ell^2 = \rho_3(1 - \rho_1^2), \quad |\rho_1| \leq 1,\ \rho_3 \geq 0. \tag{1.D.6}$$

Since the Hamiltonian is invariant under the S^1 symmetry (1.D.2), it induces the reduced Hamiltonian

$$H_\ell : P_\ell \subseteq \mathbf{R}^3 \to \mathbf{R} : \rho = (\rho_1, \rho_2, \rho_3) \mapsto \tfrac{1}{2}\,\rho_3 + V(\rho_1). \tag{1.D.7}$$

1.D.3 A special case

We now look at the special case of the model problem when

$$V(x_3) = -(1 - x_3)^2.$$

Then the reduced Hamiltonian on the reduced space P_ℓ (1.D.6) is

$$H_\ell(\rho) = \tfrac{1}{2}\,\rho_3 - (1 - \rho_1)^2. \tag{1.D.8}$$

Its 0-level set on P_ℓ when $\ell = 0$ is illustrated in figure 1.D.1. After reconstruction $H_0^{-1}(0)$ becomes a 2-torus in the 0-level set of the momentum L with a nontransverse pinch point at $p_+ = (0, 0, 1, 0, 0, 0)$. To see this recall that over each smooth point of $H_0^{-1}(0)$ (that is, except for $\rho = (1,0,0)$) the fiber of the S^1-reduction map

$$\pi : L^{-1}(0) \subseteq T\mathbf{S}^2 \to P_0 \subseteq \mathbf{R}^3 : (x,y) \mapsto (\rho_1(x,y), \rho_2(x,y), \rho_3(x,y)) \tag{1.D.9}$$

is a unique circular orbit of the S^1 symmetry (1.D.2); whereas the fiber over the point $(1,0,0)$ is the point p_+, since it is a fixed point of (1.D.2). The pinch point p_+ is nontransverse because the 0-level set of the reduced Hamiltonian H_0 has second order contact with the reduced space P_0 at $(1,0,0)$.

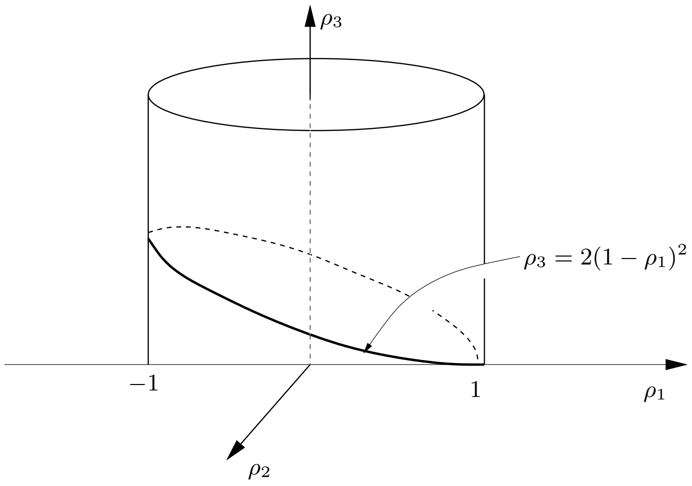

Fig. 1.D.1. The 0-level set of the reduced Hamiltonian $H_0(\rho) = \frac{1}{2}\rho_3 - (1-\rho_1)^2$ on the reduced space $P_0 : \rho_2^2 = \rho_3(1-\rho_1^2), \quad |\rho_1| \le 1, \ \rho_3 \ge 0$.

Before we compute the local monodromy around p_+ we need to show that $(0,0)$ is an isolated critical value of the energy momentum mapping

$$\mathcal{EM} : T\mathbf{S}^2 \to \mathbf{R}^2 : (x,y) \mapsto (\tfrac{1}{2}(y_1^2+y_2^2+y_3^2) - (1-x_3)^2, x_1y_2 - x_2y_1).$$

This is equivalent to showing that $(h,\ell) = (0,0)$ is an isolated point of the discriminant locus Δ of the polynomial

$$Q(\rho_1,\rho_2) = -\rho_2^2 + 2(h + (1-\rho_1)^2)(1-\rho_1^2) - \ell^2.$$

In other words, Δ is the set of $(h,\ell) \in \mathbf{R}^2$ where Q has a multiple root in $\{(\rho_1,\rho_2) \in \mathbf{R}^2 \mid |\rho_1| \le 1, \ \rho_2 \ge 0\}$. Thus $(h,\ell) \in \Delta$ if and only if

$\rho_2 = 0$ and

$$P_{h,\ell}(\rho_1) = 2(h + (1-\rho_1)^2)(1-\rho_1^2) - \ell^2 \tag{1.D.10}$$

has a multiple root in $[-1,1]$. A straightforward calculation shows that Δ is parmetrized by

$$\left\{ \begin{array}{rcl} h & = & -\dfrac{(r-1)^2(2r+1)}{r} \\ \ell^2 & = & 2\,\dfrac{(r-1)^3(r+1)^2}{r}, \end{array} \right. \tag{1.D.11}$$

where $r \in [-1,0) \cup \{1\}$. Hence $(0,0)$ (which corresponds to $r=1$) is an isolated point of Δ.

Thus we may choose a disc $\mathbf{D}$ in $\mathbf{R}^2$ containing $(0,0)$, which does not intersect Δ and lies in the image of $\mathcal{EM}$. Every $(h,\ell) \in \mathbf{D}^*$ is a regular value of $\mathcal{EM}$. For each $(h,\ell) \in \mathbf{D}^*$, the h-level set of the reduced Hamiltonian H_ℓ on P_ℓ is a smooth $\mathbf{S}^1$. Hence after reconstruction, the (h,ℓ)-level set of $\mathcal{EM}$ is a smooth 2-torus $T^2_{h,\ell}$.

We now turn to analyzing the rotation angle. Let $\mathcal{R}$ be the set of regular values of $\mathcal{EM}$ which lie in its image. For every $(h,\ell) \in \mathcal{R}$, the rotation angle of the flow of the Hamiltonian vector field X_H on the 2-torus $T^2_{h,\ell}$ is

$$\theta(h,\ell) = 2\ell \int_{x_-}^{x_+} \frac{dx}{(1-x^2)\sqrt{P_{h,\ell}(x)}}, \tag{1.D.12}$$

where $x_\pm = x_\pm(h,\ell)$ are simple zeroes of $P_{h,\ell}$ (1.D.10) in $[-1,1]$.

The following lemma is the key fact needed to compute the local monodromy of the 2-torus bundle $\mathcal{EM}^{-1}(\Gamma) \to \Gamma$ about p_+.

Lemma. Suppose that $\ell > 0$. Then

$$\lim_{\ell \to 0^+} \theta(h,\ell) = \left\{ \begin{array}{rl} \pi, & \text{if } h < 0 \\ 2\pi, & \text{if } h > 0. \end{array} \right. \tag{1.D.13}$$

Proof. We use complex analysis.
CASE 1. $h < 0$.

Consider the extended complex plane with cuts as indicated in figure 1.D.2 To see that the polynomial $P_{h,0}$ has exactly two simple roots $x_\pm$ in $(-1,1)$ when ℓ is small, first note that $P_{h,0}$ has four simple real roots ± 1 and $s_\pm = 1 \pm \sqrt{-h}$. Since $P_{h,\ell}(\pm 1) = -\ell^2$ and $P_{h,0}(0) =$

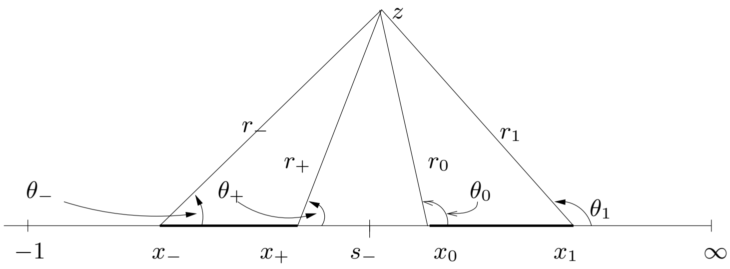

Fig. 1.D.2. The extended complex plane is cut at $[x_-, x_+]$ and $[x_0, x_1]$.

$2(h+1) - \ell^2$ is positive when $|h|$ and ℓ are small, $P_{h,\ell}$ has two simple roots $x_\pm$ in $(-1,1)$ and two simple roots x_0, x_1 outside of $[-1,1]$.

Consider the extended complex plane with cuts as indicated in figure 1.D.2. Write $z - x_\pm = r_\pm \mathrm{e}^{i\,\theta_\pm}$ and $z - x_{0,1} = r_{0,1}\mathrm{e}^{i\,\theta_{0,1}}$. Then

$$P_{h,\ell}(z) = -2(z - x_-)(z - x_+)(z - x_0)(z - x_1).$$

Define

$$\sqrt{P_{h,\ell}(z)} = i\,\sqrt{|P_{h,\ell}(z)|}\,\mathrm{e}^{i(\theta_- + \theta_+ + \theta_0 + \theta_1)/2}.$$

On the upper part of the cut $[x_-, x_+]$ the sign of $\sqrt{P_{h,\ell}(z)}$ is $+$, because $i\,\mathrm{e}^{(0+\pi+\pi+\pi)/2} = i(-i) = 1$. Now $z \mapsto \sqrt{P_{h,\ell}(z)}$ is a single valued holomorphic function on the cut extended complex plane, because it is single valued on a loop around each cut. Note that

$$\sqrt{P_{h,\ell}(-1)} = i\,\sqrt{|-\ell^2|}\,\mathrm{e}^{i(\pi+\pi+\pi+\pi)/2} = i\,\ell.$$

Consider the contours in figure 1.D.4a The contour C is homologous to $C' + C''$. Hence

$$\int_C \omega = \int_{C'} \omega + \int_{C''} \omega.$$

Here

$$\omega = \frac{1}{(1-z^2)\sqrt{P_{h,\ell}(z)}}$$

is a meromorphic 1-form on the cut extended complex plane, which has first order poles at $z = \pm 1$ and is holomorphic elsewhere. When the

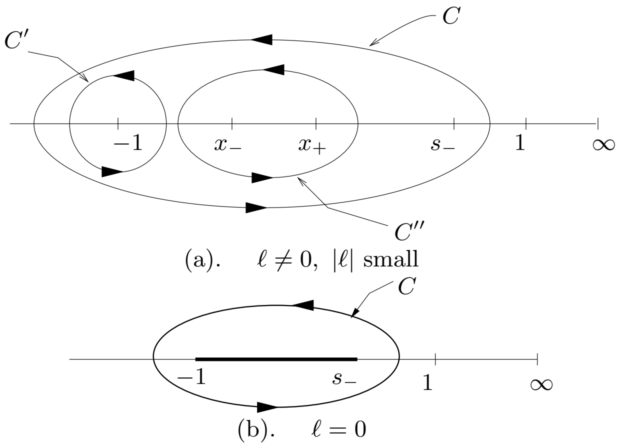

Fig. 1.D.3. Contours on the extended complex plane when $h < 0$.

contour C'' shrinks to the cut $[x_-, x_+]$ by Cauchy's theorem we obtain

$$\begin{aligned} \ell \int_{C''} \omega &= 2\ell \int_{x_+}^{x_-} \frac{dx}{(1-x^2)\sqrt{P_{h,\ell}(x)}} = -2\ell \int_{x_-}^{x_+} \frac{dx}{(1-x^2)\sqrt{P_{h,\ell}(x)}} \\ &= -\theta(h,\ell). \end{aligned}$$

By the residue theorem we find

$$\begin{aligned} \ell \int_{C'} \omega &= 2\pi i \ell \operatorname*{Res}_{z=-1} \omega = 2\pi i \ell \lim_{z \to -1} \frac{z+1}{(1-z)(1+z)\sqrt{P_{h,\ell}(z)}} \\ &= 2\pi i \ell \frac{1}{2\sqrt{P_{h,\ell}(-1)}} = 2\pi i \ell \frac{1}{2i\ell} = \pi. \end{aligned}$$

We now show that

$$\lim_{\ell \to 0^+} (\ell \int_C \omega) = 0.$$

Thinking of $(h,\ell) \in \mathcal{R}$ as complex variables in $\mathcal{R}^{\mathbf{C}}$, the function $(h,\ell) \to \int_C \omega$ is holomorphic on $\mathcal{R}^{\mathbf{C}}$. Since the contour C does not depend of ℓ,

$$\lim_{\ell \to 0^+} \int_C \omega = \int_C \lim_{\ell \to 0^+} \omega = \int_C \widetilde{\omega},$$

where

$$\widetilde{\omega} = \frac{dz}{(1-z^2)\sqrt{2(h+(1-z)^2)(1-z^2)}}.$$

$\widetilde{\omega}$ is meromorphic in the extended complex plane as cut in figure 1.D.3b with poles only at $z = \pm 1$. At $z = -1$, the 1-form $\widetilde{\omega}$ has a second order pole with zero residue. To see this, let $u^2 = 1 - z$. Then

$$\widetilde{\omega} = \frac{-2u\,du}{u^2(2-u^2)\sqrt{2(h+u^4)u^2(2-u^2)}} = \left(\frac{-1}{2\sqrt{h}}\,\frac{1}{u^2} + \mathrm{O}(1)\right)\,du.$$

At $z = s_- = 1 - \sqrt{-h}$ the 1-form $\widetilde{\omega}$ is holomorphic, because s_- is a simple zero of $P_{h,0}$, which is not equal to ± 1. Hence by the residue theorem

$$\int_C \widetilde{\omega} = 2\pi i \operatorname*{Res}_{z=-1}\,\widetilde{\omega} = 0.$$

Consequently,

$$\lim_{\ell\to 0^+}(\ell\int_C \omega) = \lim_{\ell\to 0^+}(\ell\int_C \widetilde{\omega}) = 0.$$

Taking the limit as $\ell \to 0^+$ of both sides of the equation

$$\ell\int_C \omega = \ell\int_{C'}\omega + \int_{C''}\omega = \pi - \theta(h,\ell)$$

gives

$$\lim_{\ell\to 0^+}\theta(h,\ell) = \pi,$$

when $h < 0$. This proves case 1 of the lemma.

CASE 2. $h > 0$.

The polynomial $P_{h,0}$ has four simple complex roots: ± 1, $1 \pm i\sqrt{h}$. It is positive when $x \in (-1,1)$ and negative elsewhere. When $|\ell|$ is small and positive, the polynomial $P_{h,\ell}$ has four simple complex roots: $x_\pm$, x_0, x_1 with $x_\pm \in (-1,1)$ and x_1 is the complex conjugate of x_0. The extended complex plane is cut along the real axis between x_- and x_+ and along a semicircle lying to the right of the line $\mathrm{Re}\,x = 1$ of radius $\frac{1}{2}\,|x_0 - x_1|$ with center at $\mathrm{Re}\,x_0 = 1 + \mathrm{O}(|\ell|)$, see figure 1.D.4

Consider the extended complex plane with cuts as indicated in figure 1.D.4. As in case 1 write $z - x_\pm = r_\pm \mathrm{e}^{i\,\theta_\pm}$, $z - x_{0,1} = r_{0,1}\mathrm{e}^{i\,\theta_{0,1}}$ and

$$P_{h,\ell}(z) = -2(z-x_-)(z-x_+)(z-x_0)(z-x_1).$$

Define

$$\sqrt{P_{h,\ell}(z)} = i\,\sqrt{|P_{h,\ell}(z)|}\,\mathrm{e}^{i\,(\theta_- + \theta_+ + \theta_0 + \theta_1)/2}.$$

From the fact that $\theta_0 + \theta_1 = 2\pi$ when z is real and less than 1, it follows that the sign of $\sqrt{P_{h,\ell}(z)}$ on the upper part of the cut $[x_-, x_+]$ is + (because $i\mathrm{e}^{(0+\pi+2\pi)/2} = i(-i) = 1$). Since the square root is single

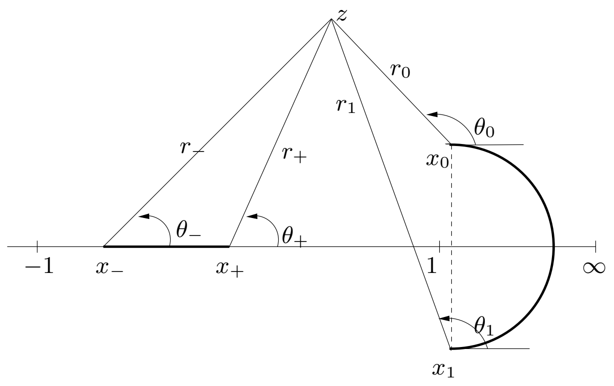

Fig. 1.D.4. Contours on the cut extended complex plane when $h > 0$.

valued along a loop about each cut, it is holomorphic on the extended cut complex plane. Note that

$$\sqrt{P_{h,\ell}(-1)} = i\sqrt{|-\ell^2|}\, \mathrm{e}^{i(\pi+\pi+2\pi)/2} = i\,\ell$$

and

$$\sqrt{P_{h,\ell}(1)} = i\sqrt{|-\ell^2|}\, \mathrm{e}^{i(0+0+2\pi)/2} = -i\,\ell.$$

Consider figure 1.D.5a Then $\widetilde{C}$ is homologous to $C + \widetilde{C}' + \widetilde{C}''$. When the contour C shrinks to the cut $[x_-, x_+]$, by Cauchy's theorem we obtain

$$\begin{aligned}\ell \int_C \omega &= 2\ell \int_{x_+}^{x_-} \frac{dx}{(1-x^2)\sqrt{P_{h,\ell}(x)}} = -2\ell \int_{x_-}^{x_+} \frac{dx}{(1-x^2)\sqrt{P_{h,\ell}(x)}} \\ &= -\theta(h,\ell).\end{aligned}$$

By the residue theorem, we have

$$\begin{aligned}\ell \int_{\widetilde{C}'} \omega &= 2\pi i\ell \operatorname*{Res}_{z=-1} \omega = 2\pi i\ell \lim_{z\to -1} (z+1) \frac{1}{(1-z)(1+z)\sqrt{P_{h,\ell}(z)}} \\ &= 2\pi i\,\ell \frac{1}{2\sqrt{P_{h,\ell}(-1)}} = 2\pi i\,\ell \frac{1}{(2i\ell)} = \pi.\end{aligned}$$

and

$$\begin{aligned}\ell \int_{\widetilde{C}''} \omega &= 2\pi i\ell \operatorname*{Res}_{z=1} \omega = 2\pi i\ell \lim_{z\to 1} (z-1) \frac{1}{(1-z)(1+z)\sqrt{P_{h,\ell}(z)}} \\ &= 2\pi i\ell \frac{1}{-2\sqrt{P_{h,\ell}(1)}} = -2\pi i\ell \frac{1}{(-2i\ell)} = \pi.\end{aligned}$$

Hence

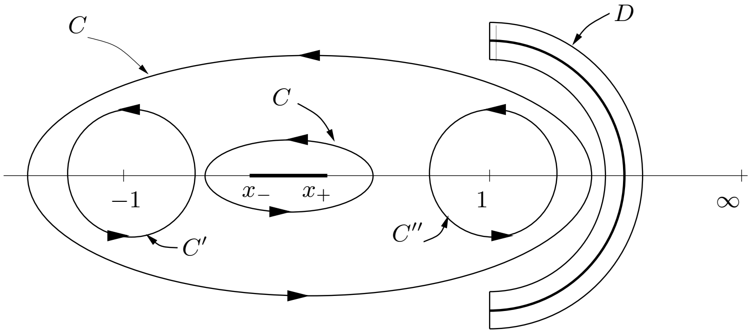

(a). $\ell \neq 0$, $|\ell| \leq \ell_0$, ℓ_0 small, when $h > 0$.

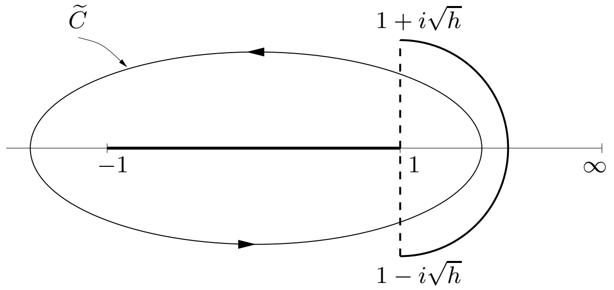

(b). $\ell = 0$ when $h > 0$

Fig. 1.D.5. Contours on the extended complex plane when $h > 0$. The contour $\widetilde{C}$ in figure 1.D.5a semicircular cut from x_0 to x_1 ranges when $|\ell| \leq \ell_0$.

$$\begin{aligned} \ell \int_{\widetilde{C}} \omega &= \ell \int_C \omega + \ell \int_{\widetilde{C}'} \omega + \ell \int_{\widetilde{C}''} \omega \\ &= -\theta(h,\ell) + \ell\pi + \ell\pi \;=\; -\theta(h,\ell) + 2\pi. \qquad (1.D.14) \end{aligned}$$

When $\ell = 0$ the contour $\widetilde{C}$ has not changed but the cut has, see fig. 1.D.5b. As in case 1 an argument shows that $\widetilde{\omega} = \lim_{\ell \to 0^+} \omega$ is meromorphic on the cut complex plane with a second order pole at ± 1. Since $\int_{\widetilde{C}} \omega$ is a continuous function of h and ℓ when $|\ell| \leq \ell_0$ with ℓ_0 small and the contour $\widetilde{C}$ does not depend on ℓ, it follows that

$$\lim_{\ell \to 0^+} (\ell \int_C \omega) = \lim_{\ell \to 0^+} (\ell \int_C \widetilde{\omega}) \;=\; 0.$$

Taking the limit as $\ell \to 0^+$ of both sides of equation (1.D.14) gives

$$0 = \lim_{\ell \to 0^+} \theta(h, \ell).$$

This proves case 2 of the lemma. $\square$

From the lemma and the fact that $\theta(h, -\ell) = -\theta(h, \ell)$ when $\ell \neq 0$ we conclude that the variation of θ is -2π along the positively oriented piecewise smooth curve γ, which is a rectangle in the (h, ℓ) plane, containing $(0,0)$ in the interior of the domain it bounds, with sides parallel to the axes and the sides parallel to the ℓ axis small, see figure 1.D.6.

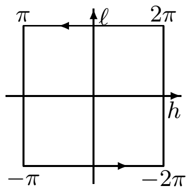

Fig. 1.D.6. The contour γ.

Since the variation of θ depends only on the homotopy class of the curve γ in the set $\mathcal{R}$ of regular values of the energy momentum mapping, it is the equal to the variation along the curve Γ which lies in the punctured disc $\mathbf{D}^*$. Thus the variation in the period lattice associated to the 2-torus bundle $\mathcal{EM}^{-1}(\Gamma) \to \Gamma$ is $\left(\begin{smallmatrix} 0 & -1 \\ 0 & 0 \end{smallmatrix}\right)$ as Γ is traversed once in the counterclockwise fashion. Hence the local monodromy of the bundle $\mathcal{EM}^{-1}(\Gamma) \to \Gamma$ is $\left(\begin{smallmatrix} 1 & -1 \\ 0 & 1 \end{smallmatrix}\right)$.

1.D.4 An example of a degenerate heteroclinic cycle

A doubly pinched 2-torus bundle with a transversal pinch at $p_- = (0,0,-1,0,0,0) \in T\mathbf{S}^2$ and a degenerate pinch at $p_+ = (0,0,1,0,0,0)$ is realized by taking the special case of the model problem with $V(x_3) = (x_3 - 1)^2(x_3 + 1)$. Note that $\mathcal{EM}(p_-) = \mathcal{EM}(p_+) = (0,0)$ is an isolated critical value and consider a positively oriented closed curve Γ in the set of regular values of the $\mathcal{EM}$ map having winding number 1 about $(0,0)$. By calculation in the preceding section the local monodromy about p_+ is $\left(\begin{smallmatrix} 1 & -1 \\ 0 & 1 \end{smallmatrix}\right)$. The local monodromy about p_- is $\left(\begin{smallmatrix} 1 & -1 \\ 0 & 1 \end{smallmatrix}\right)$. The global monodromy is the composition of the local monodromies. Hence the monodromy of the 2-torus bundle $\mathcal{EM}^{-1}(\Gamma) \to \Gamma$ is $\left(\begin{smallmatrix} 1 & -2 \\ 0 & 1 \end{smallmatrix}\right)$.

Bibliography

[1] L. Bates and R. Cushman, The rotation number and the herpolhode angle in Euler's top, preprint University of Calgary, September 2003; to appear in ZAMP.

[2] L. Bates and M. Zou, Degeneration of Hamiltonian monodromy cycles, Nonlinearity **6** (1993) 313–335.

[3] R. C. Churchill, M. Kummer, and D. L. Rod, On averaging, reduction and symmetry in Hamiltonian systems, J. Diff. Eqns. **71** (1983) 359–414.

[4] C. Cotter, Ph.D. Thesis, University of California at Santa Cruz, 1985.

[5] R. Cushman and L. Bates, *Global aspects of classical integrable systems*, Birkhauser, Basel, 1997.

[6] R. H. Cushman, Geometry of the energy-momentum mapping of the spherical pendulum, Centrum voor Wiskunde en Informatica Newsletter **1** (1983) 4–18.

[7] R. H. Cushman, Geometry of the bifurcations of the Henon-Heiles family, Proc. R. Soc. London A **382** (1982) 361–371.

[8] R. Cushman and J. J. Duistermaat, The quantum mechanical spherical pendulum, Bull. Am. Math. Soc. **19** (1988) 475–79.

[9] R. Cushman and D. L. Rod, Reduction of the semisimple 1:1 resonance, Physica D **6** (1982) 105–112.

[10] R. Cushman and J. J. Duistermaat, Non-Hamiltonian monodromy, J. Diff. Equations **172** (2001) 42–58.

[11] R. Cushman, The geometry of perturbation theory, in: *Deterministic Chaos and General Relativity*, ed. D. Hobill *et al*, p. 89–101, Plenum Press, New York, 1994.

[12] R. Cushman and S. Vũ Ngọc, The sign of the monodromy for Liouville integrable systems, Ann. Inst. H. Poincaré **3** (2002) 883–894.

[13] R. H. Cushman, H. R. Dullin, A. Giacobbe, D. D. Holm, M. Joyeux, P. Lynch, D. A. Sadovskií, and B. I. Zhilinskií, CO_2 molecule as a quantum realization of the 1:1:2 resonant swing-spring with monodromy, Phys. Rev. Lett. accepted in May (2004).

[14] G. Darboux, *Cours de Méchanique*, 1886.

[15] J. J. Duistermaat, On global action angle coordinates, Comm. Pure Appl. Math. **33** (1980) 687–706.

[16] K. Efstathiou, *Metamorphoses of Hamiltonian systems*, Ph.D. thesis, Université du Littoral, Dunkerque, 2004.

[17] K. Efstathiou, M. Joyeux, and D. A. Sadovskií, Global bending quantum number and the absence of monodromy in the HCN↔CNH molecule, Phys. Rev. A **69**(3) (2004) 032504-1–15.

[18] N. Fulton, J. Tennyson, D. A. Sadovskií, and B. I. Zhilinskií, Nonlinear normal modes and local bending vibrations of H_3^+ and D_3^+, J. Chem. Phys. **99** (1993) 906–918.

[19] H. Goldstein, *Classical Mechanics*, Addison Wesley, Reading MA, 1951.

[20] M. Hamermesh, *Group theory and its application to physical problems* Addison Wesley, Reading, MA, 1994.

[21] W. G. Harter and C. W. Patterson, Rotational energy surfaces and high-J eigenvalue structure of polyatomic molecules, J. Chem. Phys. **80** (1984) 4241–4261.

[22] M. Hénon and C. Heiles, The applicability of the third integral of motion: Some numberical experiments, Astronom. J. **69** (1964) 73–79.

[23] I. N. Kozin and R. M. Roberts, Monodromy in the spectrum of a rigid symmetric top molecule in an electric field, preprint, Warwick 2000; J. Chem. Phys. **118** (2003) 10523-10533.

[24] M. L. Lecornu, Sur l'herpolhodie, Bull. Soc. Math. France **XXXIV** (1906) 40–41.

[25] V. Matveev, Integrable Hamiltonian systems with two degrees of freedom. Topological structure of saturated neighborhoods of saddle-saddle and focus points, Mat. Sb. **187** (1996) 29–58.

[26] L. Michel and B. I. Zhilinskií, Symmetry, invariants, topology: Basic tools, Phys. Rep. **341** (2001) 11–84.

[27] L. Michel and B. I. Zhilinskií, Rydberg states of atoms and molecules: Basic group-theoretical and topological analysis, Phys. Rep. **341** (2001) 173–264.

[28] J. Marsden, R. Montgomery, and T. Ratiu, *Reduction, symmetry, and phases in mechanics*, Mem. Amer. Math Soc. **88**, Providence, RI, 1990.

[29] J. Montaldi, R. M. Roberts, and I. Stewart, Periodic solutions near equilibria of symmetric Hamiltonian systems, Phil. Trans. R. Soc. London Ser. A, **325** (1988) 237–293.

[30] I. Newton, *Philosophiae Naturalis Principia Mathematica*, London 1687 = English translation: *The Principia: Mathematical Principles of Natural Philosophy*, translated by B.I. Cohen and A. Whitman, University of California Press, Berkeley, 1999.

[31] L. Poinsot, *Théorie Nouvelle de la Rotation des Corps*, Paris, 1834.

[32] Bob Rink, A Cantor set of tori with monodromy near a focus-focus singularity, Nonlinearity **17** (2004) 347–356.

[33] D. L. Rod and R. C. Churchill, A guide to the Hénon-Heiles Hamiltonian, in: *Singularities and Dynamical Systems*, ed. S.N. Pnevatikos, pp. 385–395, Elsevier, New York, 1985.

[34] E. J. Routh, *Advanced Dynamics of a system of rigid bodies*, 6^{th} ed., MacMillian, London, 1905; reprint Dover, New York, 1955.

[35] D. A. Sadovskií and R. H. Cushman, Monodromy in the hydrogen atom in crossed fields, Physica D **142** (2000) 166–96.

[36] D. A. Sadovskií and B. I. Zhilinskií, Monodromy, diabolic points, and angular momentum coupling, Phys. Lett. A **256**(4) (1999) 235–44.

[37] G. Schwarz, Smooth functions invariant under the action of a compact Lie group, Topology **14** (1975) 63–68.

[38] J. Schwinger, On angular momentum, in: *Quantum theory of angular momentum*, eds. L. C. Biedenharn and H. V. Dam, p.229–279, Academic Press, New York, 1975.

[39] S. Vũ Ngọc, Quantum monodromy in integrable systems, Commun. Math. Phys. **203** (1999) 465–479.

[40] S. Vũ Ngọc, *Systèmes integrables semiclassiques: du local au global*, thèse d'habilitation, Institut Fourier, Grenoble, 2003.

[41] H. Waalkens, A. Junge, and H. R. Dullin, Quantum monodromy in simple molecules, J. Phys. A. Math. Gen. **36** (2003) L307–L314.

[42] E. T. Whittaker, *Analytical dynamics of particles and rigid bodies*, 4^{th} ed., Cambridge University Press, Cambridge, UK, 1937.

[43] N. Tien Zung, A note on focus-focus singularities, Differential Geom. Appl. **7** (1997) 123–130.

[44] B. I. Zhilinskií, Hamiltonian monodromy as lattice defect, arXiv:quant-ph/0303181 (2003).